Republic of Iraq
Ministry of Higher Education & Scientific Research
University of Babylon
College of Science
Department of Chemistry

The Biochemical Role of Xanthine Oxidase on severity of Ferroptosis in Patients with Beta Thalassemia Major in Babylon Governorate

A Thesis
Submitted to the Council of the College of Science، University of Babylon in Partial Fulfillment of the Requirements for the Degree of Master of Science in Chemistry

by

Ahlam Majid Azeez Mehdi

B.Sc. University of Babylon

2008-2009

Supervised by

Prof. Dr. Mahmoud Hussein Hadwan

1444 A.H **2022 A.D**

بِسْمِ ٱللَّهِ ٱلرَّحْمَٰنِ ٱلرَّحِيمِ

((يَرْفَعِ اللَّهُ الَّذِينَ آمَنُوا مِنْكُمْ وَالَّذِينَ أُوتُوا الْعِلْمَ دَرَجَاتٍ وَاللَّهُ بِمَا تَعْمَلُونَ خَبِيرٌ))

المجادلة:[11]

صدق الله العلي العظيم

CERTIFICATION

I certify that this thesis entitled (**The Biochemical Role of Xanthine Oxidase on severity of Ferroptosis in Patients with Beta Thalassemia Major in Babylon Governorate)** is prepared under my supervision at the Department of chemistry/ College of Sciences / University of Babylon, in partial requirements for the Degree of Master of Science in Biochemistry and this work has never been published anywhere.

Signature:

Name: **Dr. Mahmoud Hussein Hadwan**

Title: Professor

Address: Department of Biochemistry -College of Sciences - University of Babylon

Date: / / 2022

In the view of the available recommendation, I forward this thesis for debate by the Examination Committee.

Signature:

Name: **Dr. Abbas Jassim Atiyah**

Title: Professor

Address: Head of Department of Chemistry-College of Sciences-University of Babylon

Date: / /2022

DEDICATION

To Humansty Saver

To my parents

For raising me to believe that anything was possible.

To my husband

For making everything possible.

And to my brothers , sisters and sons to support me.

Ahlam

ACKNOWLEDGEMENTS

First of all, my great thanks and appreciation to God for granting me health and strength to facilitate my studies and completion.

My thanks, appreciation and gratitude to my great supervisor of Prof. Dr. Mahmoud Hussein Hadwan for their assistance, support, supervision and encouragement.

I would like to thank the Deanship of the Faculty of Science, University of Babylon, for providing the necessary facilities.

My sincere thanks to the head and staff of the department of chemistry, Faculty of Science, University of Babylon for their assistance in this work.

I want to thanks my friends who have helped me on this stage.

Finally, I want thanks to everyone who helped me .

Ahlam

Summary

Thalassemia is linked to a number of major health issues, including cancer, Bone deformities, splenomegaly, Slow growth rates, and heart problems. Thalassemia is caused by mutations in the DNA of cells responsible for producing hemoglobin , a substance in red blood cells that carries oxygen throughout the body. The mutations associated with thalassemia are passed from parents to children. β-thalassemia major is the most critical form that need immediate medical treatment. because of ineffective erythropoiesis. As a result, frequent blood transfusions become critical for life. An inevitable consequence of chronic transfusions is the accumulation of iron. Iron is generally coupled to transferrin and transported to the bone marrow and tissue, where it is received via the transferrin receptor and stored as ferritin.

Excess iron saturates the binding capacity of transferrin and the non-transferrin-bound iron (NTBI) functions as a catalyst in the generation of reactive oxygen species (ROS). The overproduction of ROS causes oxidative stress in individuals with thalassemia major, resulting in protein oxidation and tissue damage through lipid peroxidation. Protein carbonyls are used to assess increased protein oxidation, while malondialdehyde (MDA), a sensitive biomarker of tissue damage, is used to assess enhanced lipid oxidation

In the year 2021-2022, the study was conducted at the University of Babylon. Blood samples were collected From the Thalassemia Center at the Children's Hospital of Babylon.

The current study was carried out on the following two groups:

Group I: 150 Control

Group II: 150 patients

This study deals :-

1. The individuals' total oxidant status (TOS) and total antioxidant status (TAS) levels were assessed. Thalassemia had significantly higher serum concentrations of total oxidants species than Control. While patients serum total antioxidant capacity was considerably lower than that of Control. These findings point to oxidative stress and a patients oxidant defense mechanism being compromised.
2. The concentration of lipid peroxidation in the sera of control and patients was investigated. The current study's findings show a substantial rise ($p < 0.05$) in Malondialdehyde concentration in all study patients, as compared to the control group . Many free radicals and other highly reactive compounds have been found in patients. Increased concentrations of these reactive molecules in tissues would cause lipid peroxidation, resulting in the release of compounds such as MDA, which was detected as one of the lipid oxidation products.
3. The current study describes a simple spectrophotometric protocol for Modified CUPRAC method for assessment of XOI and demonstrates its reproducibility, accuracy, and precision. Result of this study refers to significant decrease ($p < 0.05$) in xanthine oxidase inhibitor concentration in all group of study patients with β- thalassemia major and comparable to healthy control persons .
4. The xanthine oxidase activity level is studied, and the results of the study indicate a significant increase ($p < 0.05$) in xanthine oxidase activity concentration in all group of study patients with β- thalassemia major and comparable to healthy control persons [3.8811 U\ L] in patients with β- thalassemia major increased significantly to be [4.7115 U\ L].

5. The extent of the effect of β- thalassemia major on the activity of xanthine oxidase has been reached, as well as the development of a new method for measuring enzyme activity, and comparing it with the usual methods.

Table of Contents

List of Figures

List of tables

List of Abbreviation

Abbreviation	Details
ALT	Alanine amino transferase
ALD	Alcoholic Liver Disease
CAT	Catalase
CKD	Chronic Kidney Disease
d-ROMs	derived -Reactive oxygen metabolites compounds
DILI	Drug-Induced Liver Injury
ELISA	Enzyme-Linked Immunosorbent Assay
FAS	Ferrous ammonium sulfate
FAD	Flavin Adenine Dinucleotide
GSH	Glutathione
GGC	γ-glutamylcysteine
GCL	γ-glutamylcysteine ligase
GSS	Glutathione synthetase
GPX	Glutathione peroxidase
GPX4	Glutathione peroxidase4
GR	Glutathione reductase
GSSG	Glutathione disulfide
GST	Glutathione S-transferase
Hb	Hemoglobin
HbF	Hemoglobin Fetal
HbA	Hemoglobin Adult
HIV	Human Immunodeficiency Viruses
Hp	Haptoglobin
Hx	Hemopexin
HO-1	Heme Oxygenase-1
$HO^{\bullet}$	Hydroxyl radical
$HO_2^{\bullet}$	Hydroperoxyl radical
H_2O_2	Hydrogen peroxide
HOCl	Hypochloric acid
HCV	Hepatitis C Virus infection
HCC	Hepato Cellular Carcinoma
LPO	Lipid peroxidation
$LOO^{\bullet}$	Lipid peroxyl radical
LOOH	Lipid peroxide

MDA	Malondialdehyde
NBT	Nitro Blue Tetrazolium
$NO^{\bullet}$	Nitric oxide radical
$NO_2^{\bullet}$	Nitrogen dioxide radical
NADPH	Nicotinamide adenine dinucleotide phosphate
NASH	Non-Alcoholic SteatoHepatitis
NOS	Nitric oxide synthase
$O_2^{\bullet-}$	Superoxide Radical
O_3	Ozone
$ONOO^-$	Peroxynitrite
OD	Optical Density
PCD	Programmed Cell Death
RBC	Red Blood Cell
$RO_2^{\bullet}$	Peroxyl radical
ROS	Reactive Oxygen Species
$RO^{\bullet}$	Alkoxyl radical
RNS	Reactive Nitrogen Species
RES	ReticuloEndothelial System
SCD	Sickle cell disease
SSA	SulfoSalicylic Acid
TAC	Total Antioxidant Capacity
TAS	Total Antioxidant Status
TBA	Thiobarbituric Acid
TBARS	Thiobarbituric acid-reacting
TCA	Trichloroacetic Acid
TOS	Total oxidants status
UA	Uric Acid
XO	Xanthine Oxidase
XOR	Xanthine Oxidoreductase
XDH	Xanthine Dehydrogenase
X	Xanthine

Chapter One

Introduction

1.Introduction :

1.1. Human hemoglobins

Human hemoglobins are a group of proteins that are present in erythrocytes. Multiple forms of hemoglobin are produced at different stages of development, resulting in variability. [1-2].

1.1.1 Hemoglobin's structure

All human hemoglobins are tetrameric, having two different globin polypeptide chain pairs (2α, 2β) and a tetrameric structure. A single heme molecule connects each globin chain **Figure 1-1**. During the formative stages of human development, a variety of hemoglobins are created [3].

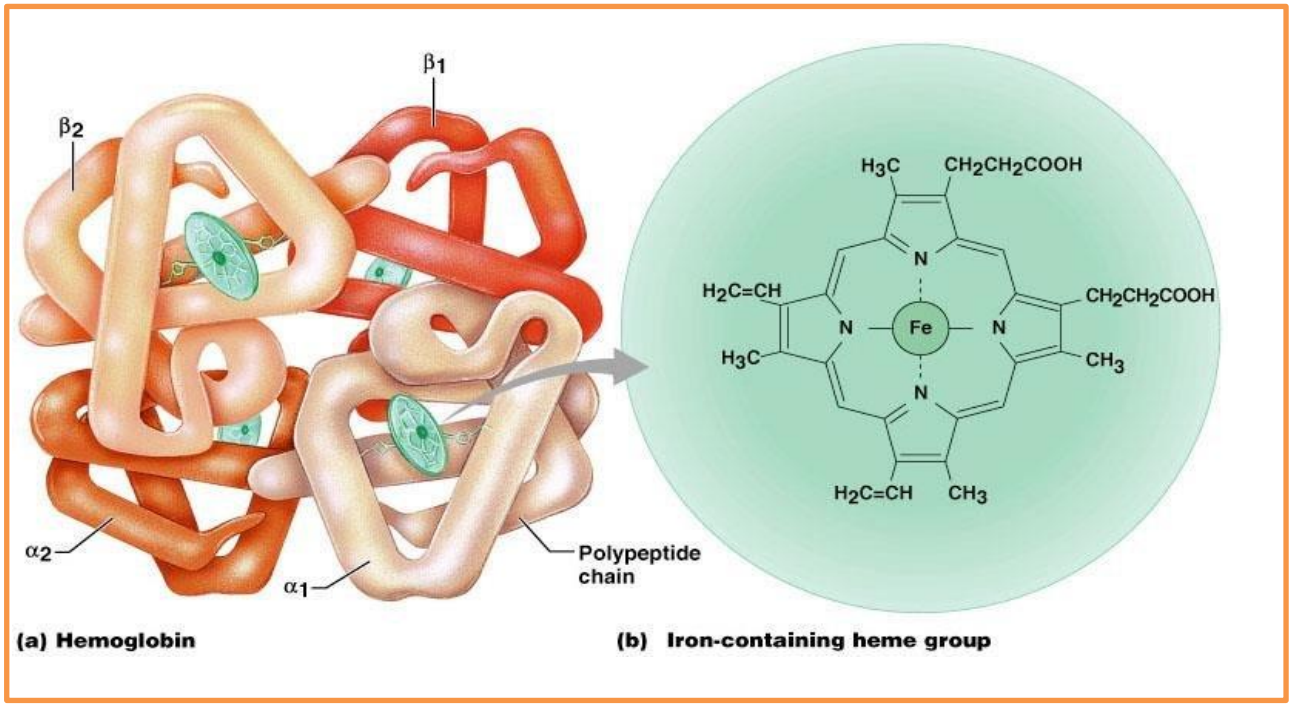

Figure 1-1 :a: The Three Dimensional Structure of Hemoglobin Tetramer, b: The Chemical Structure of Heme [3].

Table: (1-1) Hemoglobin in various forms at various stages of human development.

Developmental stages	Normal	BHFS
Embryonic	Hb Gower I ($\zeta_2\varepsilon_2$) Hb Gower II ($\alpha_2\varepsilon_2$) Hb Portland I ($\zeta_2\gamma_2$)	Hb Gower I ($\zeta_2\varepsilon_2$) Hb Portland I ($\zeta_2\gamma_2$)
Fetal	Hb F ($\alpha_2\gamma_2$)	Hb Bart's (γ_4) Hb Portland I ($\zeta_2\gamma_2$)
Postnatal/Adult	Hb A ($\alpha_2\beta_2$) Hb A_2 ($\alpha_2\delta_2$)	Hb H (β_4) Hb Portland II ($\zeta_2\ \beta_2$)

1.1.2. Thalassemia

Thalassemia is a group of Mediterranean-derived hereditary autosomal recessive blood disorders. A genetic defect causes thalassemia, which is caused by a modification or removal that causes a reduced speed of production or no synthesis of one of the hemoglobin chains. This might lead to the formation of abnormal hemoglobin molecules, causing in anemia, the typical presenting sign of thalassemia [4].

Thalassemia is characterized by a variety of alterations that result in aberrant globin gene expression, resulting in the absence or reduction of globin chain synthesis [5]. Based on which globin chain is generated in smaller proportions, they are divided into the following categories:

1- A decreased or absent β-globin chain is a symptom of thalassemia.

2- A decreased or absent α-globin chain is a symptom of thalassemia.

3. A decreased or absent δβ-globin chain is a symptom of thalassemia.

4. A thalassemia is characterized by a γδβ-globin chain that is either decreased or lacking.

Quantitative hemoglobin disorder encompasses all kinds of thalassemia. Only α-thalassemia and β-thalassemia are prevalent enough to cause health problems. [6].

1.1.2.1. α-thalassemia: Deletions in the α-globin gene group cause one or both α-globin genes at each locus to lose their function, resulting in an excess of β-globin chains. The illness α-thalassemia is a life-threatening condition that affects a vast number of people. As a consequence, there are four α-globin genes, each of which requires several mutations to produce a clinical outcome. Furthermore, β-thalassemia α-globin chains are less likely than unpaired α-globin chains to precipitate [4-5].

1.1.2.2. β-thalassemia: Since it is so public and frequently results in stark anemia, it is the most dangerous of the thalassemia diseases [6]. A lack of or absenteeism of β-globin chain construction effects in an over an abundance of globin chains. β-thalassemia is frequently characterized as a stark kind of sickness because it produces stark anemia in both homozygous and compound heterozygous phases [7-8].

1.1.3. Clinical classification of β-thalassemia

According on the strictness of the symptoms, beta-thalassemia may be divided into three groups:

1.1.3.1. β-thalassemia minor: Is the clinically asymptomatic β-thalassemia transporter condition, which occurs from heterozygosis for β-thalassemia and is characterised by particular hematological characteristics [7].

1.1.3.2. β-thalassemia intermedia: It's a group of illnesses related to thalassemia that vary in severity from asymptomatic carriers to severe transfusion-dependent situations [8].

1.1.3.3. β-thalassemia major: β-thalassemia major is a severe transfusion-dependent anemia also known as Cooley's anemia or Mediterranean anemia. It's a mendelian disease that strikes individuals all over the world [9]. It's a recessive mendelian illness that affects individuals all over the globe, and it may be homozygous or compound heterozygous. Because γ-globin chain synthesis is regular and HbF (α2γ2) production is sufficient, patients with β-thalassemia major have a nearly normal hematological profile at natal. As a result, when these children need to change their fetal RBCs with cells that contain primarily HbA (fetal to adult Hb changeover), there is a shortfall of β-globin synthesis (α2β2). Because the fundamental shift from HbF to HbA occurs at this period, the most severe types of β-thalassemia develop in the first year of life [10-11].

Table (1-2): Types of thalassemia and clinical features.

	CLINICAL FEATURES	LABORATORY FEATURES
THALASSEMIA MAJOR	▪ Anemia ▪ Hepatosplenomegaly ▪ Growth failure	▪ Hb : < 7 g/dL ▪ HbF : > 90% ▪ HbA2: normal or high ▪ HbA : usually absent
THALASSEMIA INTERMEDIA	▪ Milder anemia ▪ Thalassemia facies ▪ Hepatosplenomegaly	▪ Hb : < 8-10 g/dL ▪ HbF : > 10% ▪ HbA2: 4-9%, if > 10% suggests HbE ▪ HbA : 5-90%
β THALASSEMIA TRAIT	▪ Normal to mild anemia ▪ No organomegaly	▪ Hb : < 10 g/dL ▪ MCH : < 27 pg ▪ HbF : > 2.5-5% ▪ HbA2: 4-9%, if >20% suggests HbE trait ▪ HbA : > 90%

1.2. Antioxidant and ROS

"Any material that slows, stops, or eliminates oxidative destruction to a target molecule" is how antioxidants are definite. [12-13] by Gutteridge and Halliwell. Antioxidants are definite as "any chemical that sifts (ROS) directly or indirectly to update antioxidant resistances or suppress ROS generation," according to Khlebnikov et al. [14]. "Oxidation" is a chemical reaction that causes electrons to be removed and the oxidant state to increase. The manufacture of free radicals, which are unsteady atoms, and the loss of electrons in molecules are the outcomes of oxidation. These are extremely reactive and contain unpaired electrons, allowing chain reactions to occur, destabilizing other compounds that create free radicals.

These free radicals, also known as reactive oxygen species (ROS), disrupt the body's homeostasis, causing oxidative stress, cell death, and tissue damage. ROS include superoxide ($O_2^{-\cdot}$), hydroxyl ($HO^{\cdot}$), peroxyl ($RO_2^{\cdot-}$), hydroperoxyl ($HO_2^{\cdot}$), alcoxyl ($RO^{\cdot}$), nitric oxide ($NO^{\cdot}$), nitrogen dioxide ($NO_2^{\cdot}$), lipid peroxyl ($LOO^{\cdot}$), non-radical hydrogen peroxide (H_2O_2), hypochloric acid (HOCl), ozone (O_3), and lipid peroxide (LOOH) [15-16]. **Figure 1-2** shows how free radicals create oxidative stress.

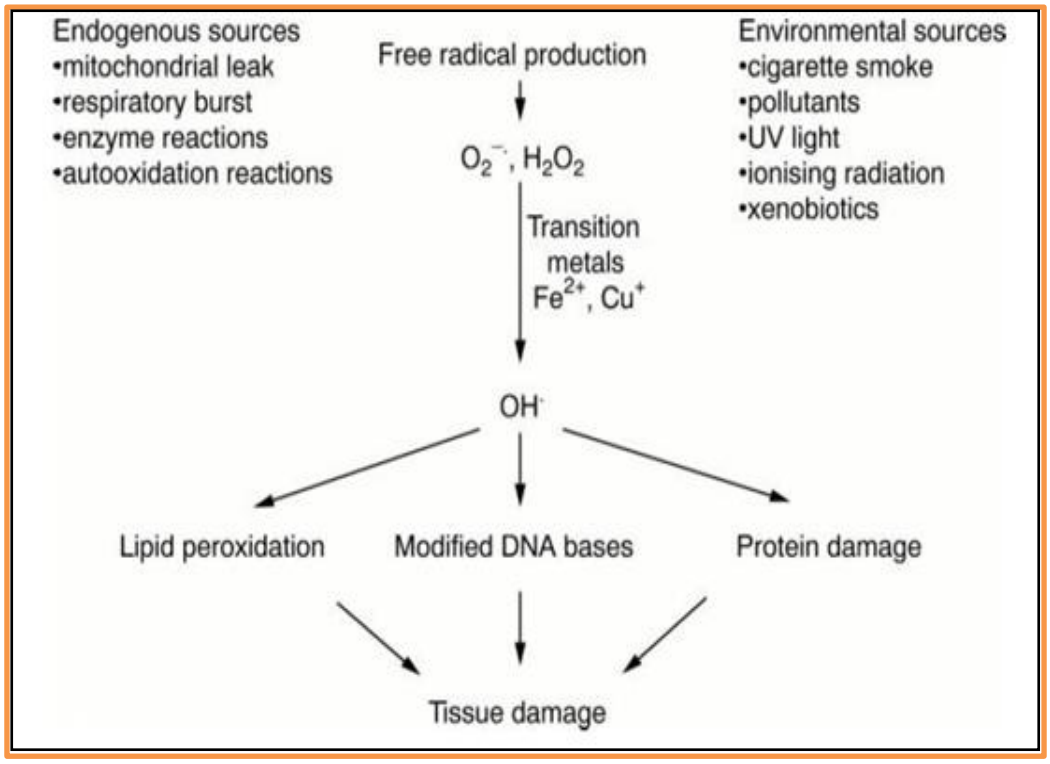

Figure 1-2: Free Radical; Production and Effect [16].

Antioxidants may prevent or repair reactive oxygen cell damage by preventing or delaying the initiation or replication of the oxidative chain reaction, depending on the balance between ROS and the availability of antioxidants in the cell's microenvironment [17-19].

Free radical sifting, action reduction, pro-oxidant complexing, lipid peroxyl radical sifting, and single oxygen reduction are some of the processes that antioxidants are thought to function by. Shielding oxidants are antioxidants that act as free radical oxidation inhibitors. Single-oxygen quenchers, reduction agents that convert hydroperoxides to stable compounds, metal chelators that convert pro-oxidant metals (iron and copper derivatives) to stable products, and pro-oxidant enzyme inhibitors (lipoxygenases) that prevent the formation of free lipid radicals are all examples of chain-breaking antioxidants [20-21].

1.2.1.Classification of Antioxidants

Antioxidants were divided into two categories: enzymatic and non-enzymatic antioxidants **Figure 1-3.**

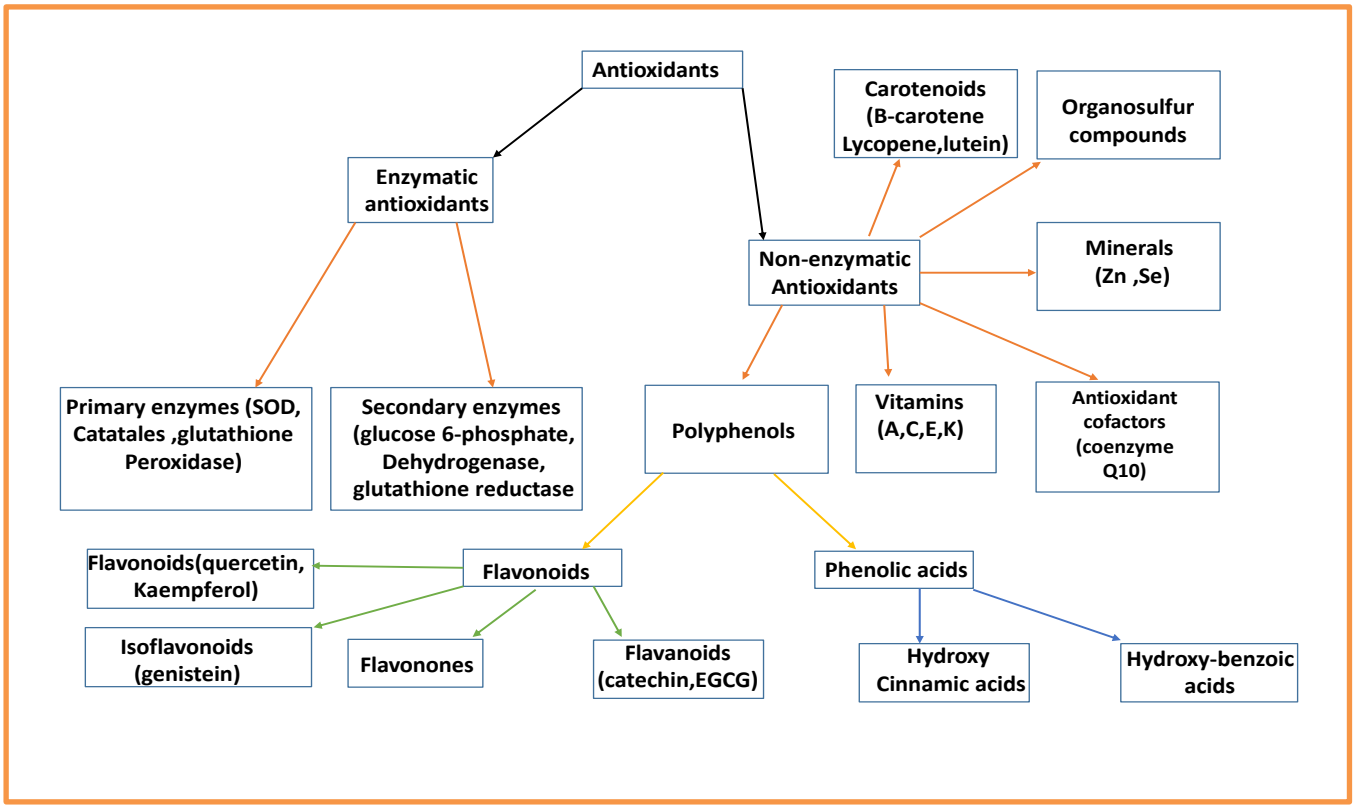

Figure1-3: Classification of Antioxidants [22].

1.2.1.1.Enzymatic Antioxidants

Primary and secondary defenses are the two types of enzymatic antioxidants. (SOD), which transforms superoxide into hydrogen peroxide as a catalase substrate [22]. Hydrogen peroxide is converted to water and molecular oxygen by catalase (CAT). The secondary enzymatic shield system includes GSH reductase and glucose-6-phosphate dehydrogenase. GSH reductase converts oxidized glutathione to depleted glutathione, allowing more free radicals to be replenished and killed.

Glucose-6-phosphate replenishes the anabolic coenzyme nicotinamide adenine dinucleotide phosphate (NADPH), resulting in a confined environment [23- 24].

1.2.1.1.1.Superoxide Dismutase (SOD) (EC 1.15.1.1)

Superoxide Dismutases are antioxidant enzymes that catalyze superoxide radical dismutation into hydrogen peroxide and oxygen. SOD may shield cells from tissue injury induced by inflammatory processes and neutrophil-produced superoxide.

1.2.1.1.2.Catalase (CAT) (EC 1.11.1.21)

The principal antioxidant enzyme found is catalase, which catalyzes the two-phase change of H_2O_2 to H_2O and O_2 with the help of an iron or manganese cofactor. One hydrogen peroxide molecule oxidizes its cofactor, which is then aided by the associated oxygen being transported to a second substrate molecule.

$$\text{Catalase-Fe}^{3+} + H_2O_2 \longrightarrow \text{Compound I}$$

$$\text{Compound I} + H_2O_2 \longrightarrow \text{Catalase-Fe}^{3+} + H_2O + O_2$$

A heme collection and a NADPH molecule are found in each of catalase's four protein subunits [25].

1.2.1.1.3.Glutathione Enzymes

Glutathione transferases, glutathione peroxidases, glutathione reductase and glutathione are all part of the glutathione mechanism. The selenium-containing enzyme glutathione peroxidase catalyzes the breakdown of hydrogen peroxide and organic hydroperoxides. The lipid peroxide action of glutathione S-transferases is high. The liver has a high concentration of these enzymes. Glutathione peroxidases are enzymes

that stimulate the oxidation of glutathione. Hydro peroxides, for example H_2O_2 and lipid hydro peroxides, action as substrates for these enzymes [26].

$$ROOH + 2\,GSH \longrightarrow GSSG + H_2O + ROH$$

1.2.1.2.Non-Enzymatic Antioxidants

Compounds containing organosulfur (allium and allium sulfur), coenzyme (Q10), vitamins (A, C, E, and K), nitrogen compounds (uric acid), minerals (Zn and Se), peptides (glutathione), and polyphenols are among the non-enzymatic antioxidants (flavonoids and phenolic acid).

1.2.1.2.1.Vitamin A

Vitamin A is a carotenoid generated in the liver as a consequence of β-carotene degradation. It has antioxidant properties because it has the potential to attach to peroxyl radicals before they cause lipid peroxidation Vitamin A, among other things, protects the face, hair, and internal organs. [27- 28].

1.2.1.2.2.Coenzyme (Q10)

CoenzymeQ10 is hypothesized to operate by avoiding lipid peroxyle radical formation. It neutralizes radicals even after they have created. Vitamin E regeneration is an essential function of this coenzyme. Vitamin E regeneration is more probable with this method than with ascorbate (vitamin C). This co enzyme may be current in every cell and membrane and is required for cell respiration and other metabolic processes [29].

1.2.1.2.3.Uric Acid

Uric acid is the Human purine nucleotide metabolism end product 90% of uric acid is reabsorbed by the body after renal purification, showing that it plays important functions inside the body. Uric acid is a strong seeker of singlet oxygen and hydroxyl radicals, and it protects erythrocytes against peroxidation-induced lysis. It has also been shown to prevent oxo-heme oxidant overproduction caused by hemoglobin-peroxide interactions [30].

1.2.1.2.4.Glutathione

Glutathione is a tripeptide that provides an electron or a hydrogen atom to protect cells from free radicals. It is also necessary for the recovery of a variety of antioxidants, including ascorbate [31]. The endogenous antioxidant system, on the other hand, is inadequate, and people must rely on dietary antioxidants to lower free radical levels [32].

1.2.1.2.5.Vitamin C

Vitamin C and vitamin E are known by their generic names of ascorbic acid and tocopherols, respectively. Ascorbic acid is broken down into two antioxidant compounds: L-ascorbic acid and L-dehydroascorbic acid. The gastrointestinal system processes these two compounds, which may be enzymatically interchanged in *vivo*. Radical anion, H_2O_2, $HO^{\cdot}$, singlet oxygen, and $NO^{\cdot}$ are all scavenged by ascorbic acid [33].

1.2.1.2.6.Vitamin E

Vitmin E is the only lipid-soluble, chain-breaking antioxidant found in plasma, red blood cells, and tissues, and it assists in lipid structure protection. especially membranes. By converting phenolic hydrogen to peroxyl radicals, which subsequently form tocopheroxyl radicals, which,

although being radicals, are non-reactive and incapable of initiating the oxidative chain reaction, this prevents lipid peroxidation. Four tocopherols and four tocotrienols make up vitamin E [34].

1.2.1.2.7.Vitamin K

K1 and K2 are the two natural isoforms of this vitamin. Vitamin K is a family of fat-soluble chemicals that are required for the change of protein-bound glutamates in a variety of target proteins to γ-carboxyglutamates after translation. The antioxidant action of several vitamins is attributed to their 1, 4- naphthoquinone content [35].

1.2.1.2.8.Flavonoids

Flavonoids are a collection of compounds with a skeleton of diphenyl propane (C6C3C6). Flavonols, flavanols, anthocyanins, isoflavonoids, flavanones, and flavones are all examples of flavonoids.. Flavanones and flavones are often found together in fruits and are linked by certain enzymes., whereas flavones and flavonols are not linked by specific enzymes and are seldom found together.Plants that are high in flavanone lack anthocyanins as well. The phenolic hydroxyl groups coupled to ring complexes in flavonoids provide antioxidant activity. Among other things, they may act as reducing agents, superoxide radical scavengers, hydrogen donors, single oxygen quenchers, and metal chelators.. They increase uric acid levels and low molecular weight molecules, activate antioxidant enzymes and limit oxidation [36-37].

1.2.1.2.9.Phenolic Acids

Hydroxy cinnamic and hydroxybenzoic acids are made from phenolic acids. Gallic acid, a kind of phenolic acid found in gallnuts, sumac, tea leaves, oak bark, and other plants, is one of the most

researched and promising hydroxybenzoic compounds, whereas cinnamic acid is the predecessor of all hydroxyl cinnamic acid. They may be found in plant products as well as as esters and glycosides on rare instances. They operate as scavengers and chelators of free radicals, particularly hydroxyl and peroxyl radicals, superoxide anions, and peroxynitrites [38-39].

1.2.1.2.10.Carotenoids

Plants and microbes create carotenoids, which are natural colors. Carotenes with distinctive end-groups like lycopene and -carotene, as well as xanthophyll-known oxygenated carotenoids like zeaxanthin and lutein, are two types of carotenoid hydrocarbons. The solvent is interacted with in a series of rotational and vibrational exchanges., singlet oxygen quenching causes excited carotenoids to lose the newly obtained energy, allowing more radical species to quench themselves [40].

1.2.1.2.11.Minerals

Minerals are present in trace amounts in animals and account for just a tiny fraction of dietary antioxidants, but they play a crucial role in their metabolism. Selenium and zinc are two minerals that have antioxidant properties. In the human body, selenium may be found in both organic (selenocysteine and selenomethionine) and inorganic (selenite and selenate) forms. It does not directly battle free radicals, but it is a required component of the majority of antioxidant enzymes (metalloenzymes, glutathione peroxidase, and thioredoxin reductase), without which it is ineffective [41].

1.2.2.Antioxidants: Health and Diseases

Reactive Oxygen Species (ROS) is assumed to be the cause of a number of human illnesses, including neurological disorders, mortality, stroke, and a range of other conditions. Antioxidants are supposed to guard beside the harmful properties of reactive oxygen species (ROS) and, as a result, can heal oxidative stress-related illnesses **Figure 1-4** . An antioxidant methodology to illness therapy has promise since most diseases are mediated by ROS; there has also been a huge increase in oxidative stressors with the fast growth of civilization, industrialisation, and overpopulation. Antioxidant and scavenger-containing products have been shown to protect against ROS-induced illnesses in epidemiological investigations [42].

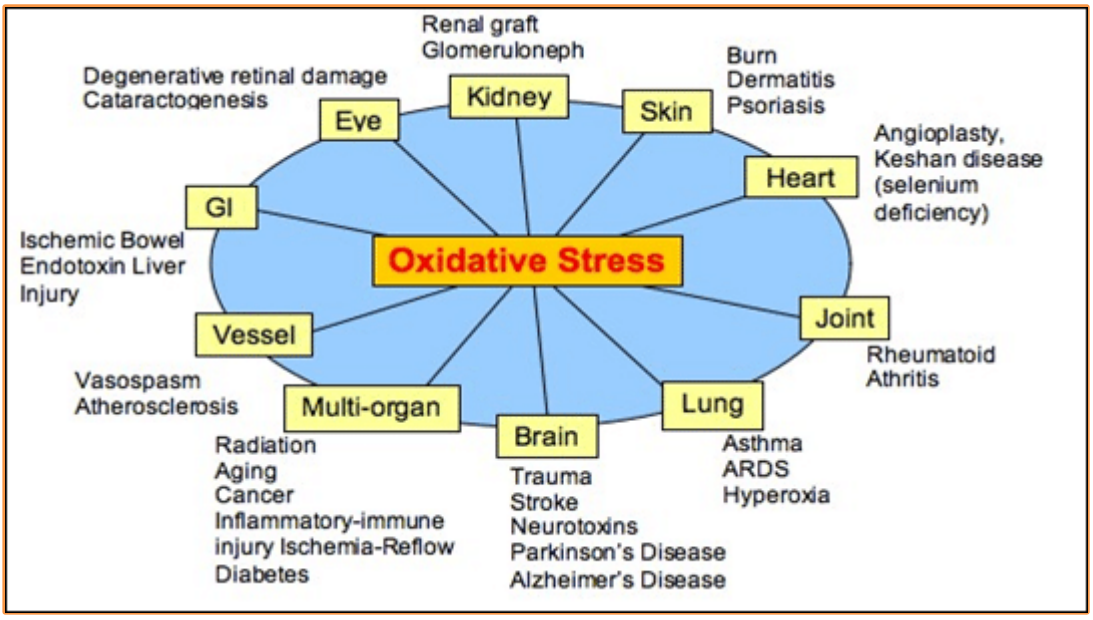

Figure 1-4: Oxidative stress-induced diseases in human [42].

Hemolytic illnesses associated to excess circulating free heme include thalassemia, sickle cell disease (SCD), sepsis, malaria , and cardiac bypass [43-45]. When reduced heme (Fe^{2+} to Fe^{3+}) is oxidized, heme and hemoglobin (Hb) may be released into the circulation from red blood cells (RBCs) [44-46]. Heme and Hb are scavenged and removed in

plasma under normal physiologic circumstances, or sequestered and transferred to organs such as the liver for breakdown [44-46]. On the other hand, severe hemolysis causes circulating heme to surpass the sifting and poverty pathways, resulting in huge levels of extracellular free heme, which may cause intravascular cell and tissue damage[44-46].

Hemoglobin (Hb) is guided to macrophages by haptoglobin (Hp) at low levels of hemolysis, when the complex is taken up by endocytosis and destroyed [44]. Hemopexin (Hx) binds able heme in the plasma, which is subsequently destroyed by the enzyme heme oxygenase-1 (HO-1) to iron, carbon monoxide, and biliverdin [43]. Hx concentrates heme in the spleen and liver, enabling it to flow through the endothelium, be endocytosed and destroyed by cellular HO-1, or be restructured for heme iron recycling [44-46]. Hx and HO-1, on the other hand, become saturated during acute hemolysis, causing oxidative injury to surrounding tissues owing to a reduction in heme breakdown and a corresponding increase in circulating free heme. [44].

Interaction of free heme with O_2, for example, may form superoxide ($O_2^{\bullet-}$), which can subsequently be utilized to enhance hydrogen peroxide (H_2O_2) levels by natural or enzymatic dismutation, in addition to hydroxyl radical ($HO^{\bullet}$) levels via peroxide(s) reactivity with transition metals, such as heme-iron (Fe). Increased levels of these reactive species cause lipid, protein, and DNA oxidation, resulting in cell and tissue damage, endothelial dysfunction, and vascular homeostasis [43-47]. While it is considered that the catalytically active Fe in heme, as well as "free Fe" formed from heme, is the major source of oxidants in hemolytic illness, later contributions from other sources play a key role in the advancement of this inflammatory process. Toll-like receptor 4 (TLR4) signing is activated by free heme, which leads to the stimulation

of pro-inflammatory pathways, including the extension of ROS stages from causes other than Fe-mediated activities **Figure 1-5** [44-48]. Reactive oxygen and nitrogen species (ROS and RNS) (e.g. nitric oxide ($NO^{\bullet}$), nitrogen dioxide ($NO_2^{\bullet}$), and peroxynitrite ($ONOO^-$)) are generated under a variety of clinical situations that often accompany hemolytic illnesses (e.g. ischemia-reperfusion damage and chronic inflammation) [49-51]. The mitochondrial electron transport chain, nicotinamide-adenine dinucleotide phosphate (NADPH) oxidases, uncoupled nitric oxide synthase (NOS), and xanthine oxidase (XO) are the main sources of $O_2^{\bullet-}$ [50]. One such mechanism is XO, which has been shown to be elevated in hemolytic disease [52]. XO produces oxidants by transferring electrons from purine oxidation to decrease O_2 univalently ($O_2^{\bullet-}$) or divalently (H_2O_2)[52]. Increased RNS synthesis might be due to the diffusion-limited interaction of XO-derived $O_2^{\bullet-}$ with $NO^{\bullet}$ to generate $ONOO^-$ [53], but higher rates of $O_2^{\bullet-}$ generation from the other sources discussed above could also play a role. Increased $ONOO^-$ levels have been associated to changes in cell signaling, a reduction in $NO^{\bullet-}$mediated vasodilation, and a loss of endothelial barrier integrity owing to lipid peroxidation in the membrane [54-55].

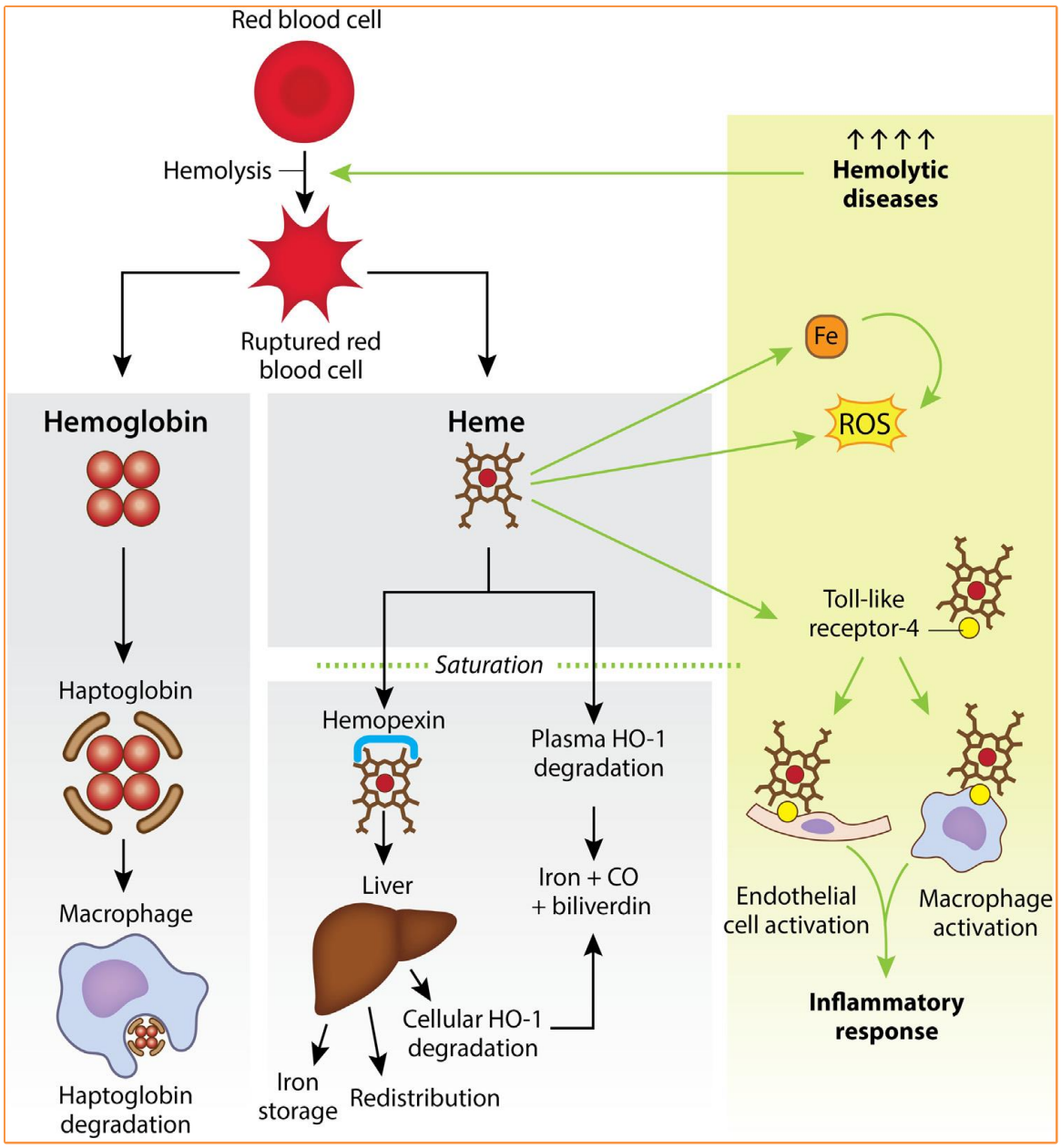

Figure 1-5: Hemolysis is the process of releasing hemoglobin (Hb) and heme from a red blood cell (RBC) [44].

1.3. Xanthine oxidase (XO, EC 1.1.3.22)

Human physiopathological conditions are often associated with reactive oxygen species (ROS) such as singlet oxygen, superoxide radical anions, hydrogen peroxide, and hydroxyl radicals [56]. A number of neurodegenerative disorders including brain and heart reperfusion damage, Alzheimer's dementia, atherosclerosis, and Parkinson's disease have been linked to oxidative stress, which is generated by an imbalance between antioxidant systems and oxidant production, including ROS [57], and the pathogenesis of inflammation, cancer, arthritis, and aging [57-58]. ROS are created in human tissues as a result of exposure to exogenous substances in the environment such as gamma rays, UV light, and x-rays, or during metal catalyzed reactions [59] and some endogenous metabolic activities involving bioenergetics electron transfer and redox enzymes [60].

Xanthine oxidase (XO), an enzyme that catalyzes conversion of hypoxanthine to xanthine and xanthine to uric acid, is another biological source of superoxide radicals. In both processes, superoxide anions and hydrogen peroxide are formed when molecular oxygen is reduced [61].

Polyphenols such as flavonoids have been shown to have antiallergenic, antiviral, anti-inflammatory, and vasodilating effects in several studies. Flavonoid antioxidant activities are associated with these pharmacological properties. Flavonoid protective properties are attributed to the ability to inhibit ROS generation by blocking specific enzymes or chelating transition metals implicated in free radical formation, scavenging radical species, particularly ROS, and increasing antioxidant defense regulation [62- 63].

Xanthine Oxidase (XO) is a complex molybdoflavoprotein that is primarily present in dehydrogenase form; only the oxidase form participates in production of considerable superoxide $O_2^{\bullet-}$ and hydrogen peroxide (H_2O_2). XO is a key biological $O_2^{\bullet-}$ producer associated with a number of disorders. XO is involved in ischemia and different forms of vascular damage, chronic heart failure, and inflammatory diseases [64]. XO is responsible for uric acid production; its presence at elevated concentrations may indicate increased oxidative stress and consequent risk. Gout is caused by high concentrations of uric acid in the blood, known as hyperuricemia [65]. The kidneys and gastrointestinal tract are responsible for final elimination [66]. Increases in serum uric acid, oxidative stress, endothelial dysfunction, and left ventricular dysfunction, all of which have been associated with the etiology of heart failure [67], may result from increased XO pathway activity [68- 69].

Inhibition of XO reduces tissue and vascular damage resulting from oxidative stress. Furthermore, it lowers uric acid concentration, a risk factor for development of all types of cardiovascular disease [70]. Xanthine oxidase inhibitors (XOIs) have demonstrated effectiveness in treatment of hepatitis, brain tumors, and gout [71-72]. XOIs may be effective in the treatment of a variety of other diseases [73- 74].

Researchers have provided many protocols to measure XO enzyme activity. The most common protocol is based on measuring the change in absorbance in the ultraviolet region by following the increase in absorbance at 295 nm caused by the formation of urate [75] or by the production of NAD(P)H [76]. Another protocol is based on measurement of the disappearance rate of xanthine at 270 nm [77]. Atlante *et al*. [78] described a fluorometric protocol to measure XO activity. As a consequence of pterine oxidation by the produced hydrogen peroxide, the

process was used to synthesize fluorescent isoxanthopterin from non-fluorescent pterine (Ex/Em: 345 nm/390 nm).

A novel protocol for assessing XO activity was developed using the oxidation of 2,2'-azino-di(3-ethylbenzthiazoline-6-sulphonate) (ABTS) by peroxidase and uricase [79]. After 10 min at 410 nm, the increase in absorbance of the oxidized form of ABTS was proportional to XO activity. Naoghare *et al*. [80] developed a high-throughput chip-based protocol using a photodiode array (PDA) microchip technique to examine the inhibitory effects of pharmacological analogs on XO. The test used the red light absorption properties of nitroblue tetrazolium (NBT) formazan, which is produced when NBT is reduced by free radicals.

Liu *et al*. [81] devised an ultrahigh-performance liquid chromatography and triple quadrupole mass spectrometry (UHPLC–TQ-MS) technique with improved accuracy and speed by adding WST-1 (2-(4-iodophenyl)-3-(4-nitrophenyl)- 5-(2,4-disulfophenyl)-2H-tetrazolium sodium salt) to the XO enzymatic reaction. Using digital automation, the methodology was applied to test the XO inhibitory properties of a range of herbal extracts and components from natural sources.

Özyürek *et al.* [82] used the cupric reducing antioxidant capacity (CUPRAC) spectrophotometric protocol to measure the XO-inhibitory activity of polyphenols (XOI–CUPRAC method). The method used direct measurements of hydrogen peroxide and uric acid production to assess XO with and without interference. The CUPRAC absorbance of the enzymatic reaction solution decreased in the presence of polyphenols owing to the reduction of Cu(II)–neocuproine reagent (Cu(II)–Nc) by the products of the xanthine–xanthine oxidase system, with the difference proportional to the XO inhibition ability of the investigated compound.

1.4. Ferroptosis

The presence of hepatocyte mortality in the liver is reflected in serum transaminases, which are the most extensively utilized hepatic function indicators [83]. Furthermore, these markers have prognostic importance in a variety of Chronic Liver Disease (CLD), including hepatitis C virus infection (HCV), alcoholic liver disease (ALD), non-alcoholic steatohepatitis (NASH), drug-induced liver injury (DILI), and hepatocellular carcinoma (HCC), which all involve persistent inflammation from any underlying cause. [84-85].Cell death is not just a reaction to various insults, but it may also be self-executed via a process known as programmed cell death (PCD).

Hepatocyte cell death includes apoptosis (a frequent kind of PCD), necrosis, pyroptosis, necroptosis, and autophagy. Various changes in the nucleus, cytoplasm, and other organelles such as lysosomes define different instruments of liver cell death. Regardless of the routes implicated, all of these methods lead to irreversible cellular malfunction and cell death [86-87]. Ferroptosis is a new kind of cell death that has just been discovered, with the feature of iron being involved in the formation of oxidative cell damage [88]. Animal models of cancer, renal damage, and neurological impairment have all been used to study ferroptosis [89-90].

Ferroptosis has been related to a range of chronic liver illnesses, including hemochromatosis, ALD, HCV, NASH, and HCC, as well as DILI. Liver damage has been associated to an imbalance in iron metabolism as well as ROS-induced lipid peroxidation in these disorders [91-92] **Figure 1-6 .**

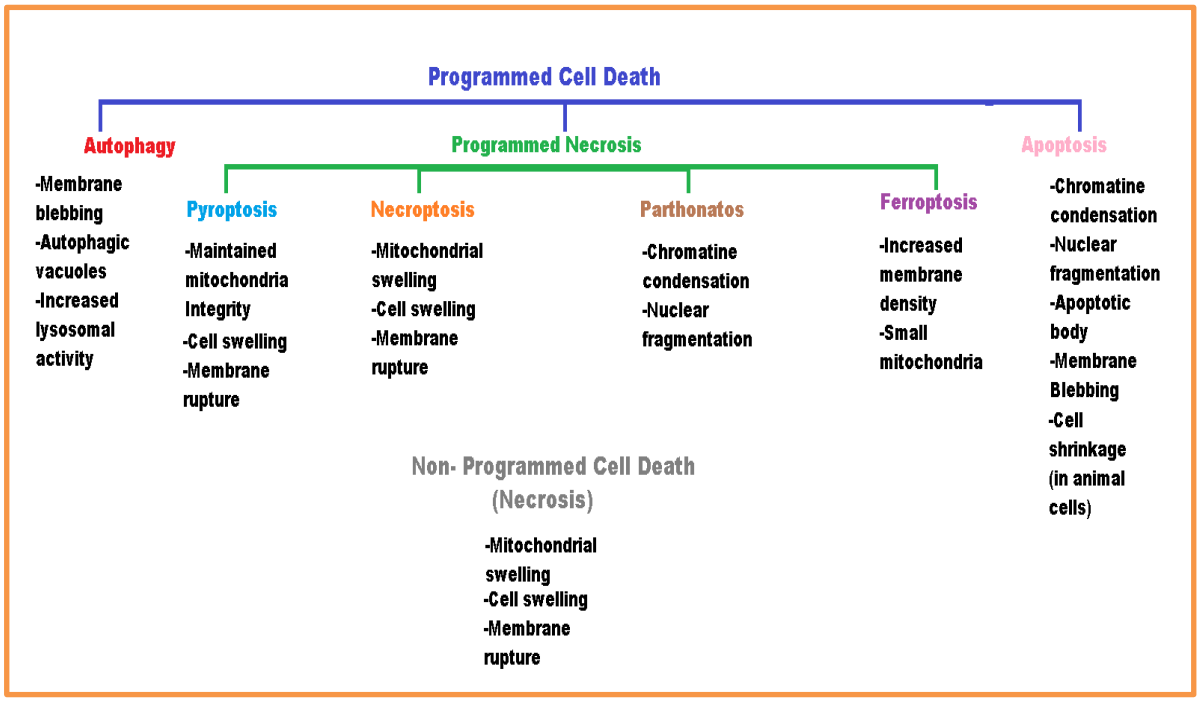

Figure 1-6:Characteristics of several forms of cell death [92].

1.5. A simple chemical sensor for quantifying xanthine oxidase inhibition activity

Free radicals are chemical species that are very reactive and often very unstable [93]. Many diseases have been associated with them, including inflammation, stroke, coronary artery disease, diabetes mellitus, rheumatism, liver disorders, Alzheimer's disease, renal failure, and cancer [94-96]. Free radicals are by-products of cellular metabolism that are continually produced by membrane enzymes, cytoplasmic proteins, peroxisomes, and mitochondrial and microsomal electron transport systems. In addition, tobacco smoke, ionizing radiation, and pollution are exogenous free radical sources [93].

A molybdoflavoprotein hydroxylase known as xanthine oxidoreductase can function as an oxidase or a reductase, although it primarily acts as an oxidase. It catalyzes the breakdown of hypoxanthine to xanthine and then to uric acid, creating superoxide and hydrogen peroxide (H_2O_2) [97]. It is a rate-limiting enzyme in nucleotide

metabolism. Xanthine oxidase (XO) is a significant source of free radicals that contribute to the oxidative breakdown of living tissue [98]. XO causes gout, a medicinal disorder characterized by hyperuricemia, which involves uric acid deposition in the joints and severe inflammation. Notably, 5%–30% of the general population have hyperuricemia, which is believed to be increasing worldwide and a significant risk factor for life-endangering diseases such as renal failure [99- 101].

XO inhibitors (XOIs) are biomolecules that inhibit the final stage of uric acid formation or uricosuric medications that promote urine excretion of uric acid, reducing plasma uric acid concentrations, and are often used to treat gout [102-103]. The only XOI used clinically to treat gout is allopurinol [104-105]. However, it has several adverse effects, including nephritis, allergic problems, and hepatitis . Therefore, identifying innovative XOIs to treat gout and other XO-activity-associated conditions with increased therapeutic efficacy and fewer adverse effects is urgently required [106].

Botanical components are gaining increasing attention in the continued search for novel medications or lead compounds for treating many diseases [107]. Natural compounds produced from conventional medicinal plant extracts have continuously offered an attractive prospect for creating novel therapeutic agents. Newman and Cragg [108] reported that globally, many novel biomolecules approved for use as medications between 1981 and 2006 were derived from or inspired by natural compounds. There are many XOIs in natural products, which could be made into therapeutic agents in the future [109-110]. However, the potential for establishing effective natural therapies for treating gout disorders is currently underdeveloped. Optimizing and screening effective

and safe XOIs would be an excellent strategy for controlling XO-dependent disorders [111].

Numerous methods have been developed to quantify XO enzyme activity. The most commonly used method involves monitoring the increase in absorbance at 295 nm caused by urate synthesis [112] or the production of the reduced form of nicotinamide adenine dinucleotide phosphate [76]. A different protocol is based on measuring xanthine's dissociation rate at 270 nm [77]. Atlante *et al*. [113] assessed XO activity using a fluorometric procedure that creates fluorescent isoxanthopterin from non-fluorescent pterine (Ex/Em: 345 nm/390 nm) via oxidation by the generated H_2O_2. A sensitive method for measuring XO activity was developed by Fried [114], using the reduction of nitroblue tetrazolium (NBT) salt as an electron acceptor and phenazine methosulfate, ethylenediaminetetraacetic acid, and gelatin to accelerate the reaction rate.

A novel sensor for quantifying XO activity used the oxidation of 2,2'-azino-di(3-ethylbenzothiazoline-6-sulfonate; ABTS) by uricase and peroxidase [79], where the increase in oxidized ABTS absorbance at 410 nm after 10 minutes is due to XO activity. Naoghare *et al*. [115] studied the inhibitory effects of pharmaceutical analogs on XO activity with a high-throughput chip-based protocol using a photodiode array microchip device. The NBT formazan created when free radicals reduce NBT was used in this assay due to its ability to absorb red light.

Liu *et al.* [116] developed an ultrahigh-performance liquid chromatography and triple quadrupole mass spectrometry method, showing improved accuracy and measurement speed. This protocol used 2-(4-iodophenyl)-3-(4-nitrophenyl)-5-(2,4-disulfophenyl)-2H-tetrazolium

as the substrate to assess H_2O_2 production. This digital automation method was used to investigate the XOI ability of various herbal extracts and natural components. Özyürek *et al*. [117] measured the XOI activity of polyphenols using a spectrophotometric cupric reducing antioxidant capacity (CUPRAC) method by quantifying XO activity with and without interference using direct measurements of H_2O_2 and uric acid generation. CUPRAC absorbance decreased in the presence of polyphenols due to the reduction of Cu(II)-neocuproine reagent by the xanthine-XO system products, with the difference proportional to the examined compound's XOI activity. Wu *et al*. [118] developed a capillary-electrophoresis-based XO immobilized enzyme microreactor to evaluate enzymatic reaction kinetics and screen flavonoid XOIs. A polydopamine/graphene oxide membrane to immobilize the enzyme on the capillary's inner wall.

This thesis presents method that describes a sensitive chemical sensor for measuring XOI activity. In this protocol, enzyme samples are incubated for 30 minutes at 37°C with a suitable xanthine concentration as the substrate before XO activity is quantified by directly measuring H_2O_2 generation using a 3,3′,5,5′-tetramethylbenzidine(TBM)-H_2O_2 system catalyzed by cupric ions (Cu^{2+}). XOI activity is quantified based on the difference in XO activity with and without the XOI. The chemical sensor produces optical signals that can be visually recognized or detected using a UV-visible spectrophotometer.

1.6. Aims of the study:

The study aims to show the correlation between xanthine oxidase enzyme activity and ferroptosis in patients with β-thalassemia major aged (5-15 years) via :

1. Measuring of blood parameters that relate with β-thalassemia, such as Hb, Iron and Ferritin.
2. Measuring Xanthine Oxidase Enzyme Activity and Trying to develop new methods for assessment of Xanthine Oxidase Activity and compared it with ordinary methods.
3. Assessment Total Antioxidant Capacity , Total Glutathione Concentration, Glutathione Peroxidase 4 concentration (ELISA),Total Vitamin E Concentration and Total Oxidant Status, lipid peroxidation .
4. Determination the Ferroptosis levels.

Chapter Two

MATERIALS AND METHODS

2.1. Material

2.1.1. Chemicals

All chemical and biochemical reagents were supplied from analytical grade and were purchased from standard chemical commercial providers, then consumed without any addition purification as shown in **Table (2-1):**

Chemicals	Purity %	Supplied company
1,3-Diethyl-2-thiobarbituricAcid (DETBA)	99.0	Sigma-Aldrich
AAPH(2,2′-azobis-2-methyl-propanimidamide,dihydrochloride)	99.0	Sigma-Aldrich
Absolute Ethanol	96.0	Fluka
Ammonium acetate (NH_4AC)	99.0	BDH
Copper (II) chloride $CuCL_2.2H_2O$	99.0	Sigma-Aldrich
Disodium hydrogen phosphate-Sodium phosphate dibasic	-----	Sigma-Aldrich
DTNB (Elman's reagent)	99.0	Sigma-Aldrich
Ethyl acetate	99.0	BDH
Ferric chloride hexahydrate	98.0	BDH
Ferrous ammonium sulfate (FAS) $(Fe(SO_4)(NH4)_2(SO_4)$)	99.0	BDH
Gallic acid	99.0	Sigma-Aldrich
Gelatine	99.0	BDH
Glycerol ($C_3H_8O_3$)	99.0	Sigma chemicals
Glutathione peroxidase 4 (kit) ELISA	-----	Bioassay

		technology laboratory
GSH (glutathione)	99.0	BDH
Hydrochloric acid (HCl)	99.0	BDH
Hypochloric acid HOCl	7%	Traditional
Hydrogen peroxide (H_2O_2)	98.0	Fluka
Hypoxanthine	99.0	Sigma-Aldrich
KH_2PO_4	99.0	Sigma chemicals
Na_2HPO_4	99.0	BDH
Neocuproine (Nc) 2,9-dimethyl-1,10-phenanthroline ($C_{14}H_{12}N_2$)	98.0	Sigma-Aldrich
n-propyl alcohol	99.0	BDH
O-dianisidine dihydrochloride ($C_{14}H_{16}N_2O_2$.2HCl)	95.0	Sigma
Peroxidase (horseradish)	Type I	Sigma-Aldrich
Pyrogallol red	99.0	Sigma-Aldrich
Phenazine metosulfate	99.0	Sigma-Aldrich
Sodium azide (NaN_3)	98.0	BDH
Sodium chloride (NaCl)	98.0	Sigma
Sodium dihydrogen phosphate monohydrate-Sodium phosphate monobasic monohydrate	-----	Sigma-Aldrich
Sodium dodecyl sulfate (SDS) $NaC_{12}H_{25}SO_4$	99.0	BDH
Sodium hydroxide NaOH	99.0	BDH
Sulfosalicylic acid	99.0	BDH
Sulfuric acid (H_2SO_4)	98.0	BDH

t-BOOH (70% solution in water)	98.0	Sigma
TCA (trichloro acetic acid) ($C_2HCl_3O_2$)	99.0	BDH
Trolox(6-hydroxy-2,5,7,8-tetramethylchroman-2-carboxylic acid)	97.0	Sigma-Aldrich
Uric acid	99.0	BDH
Uricase	Type I	Sigma-Aldrich
Vit E (α-Tocopherol)	99.0	BDH
Xanthine	98.0	Sigma
xanthine oxidase	Type I	Sigma-Aldrich
Xylene	99.0	BDH
xylenol orange ($C_{31}H_{32}N_2O_{13}S$)	98.0	Sigma chemicals
α,α‾ dipyridyl	99.0	BDH
Sodium acetate	99.0	BDH
Acetic acid (HAc)	99.0	BDH
2,2'-azino-di(3-ethylbenzthiazoline-6-sulphonate) (ABTS)	99.0	Sigma-Aldrich
3,3′,5,5′-tetramethylbenzidine (TMB)	99.0	Sigma-Aldrich

2.1.2. Table : (2-2) Instrument Analysis and Equipment

Instrument	Supplied company
pH meter	Jenway(Germany)
Sensitive balance	Stanton 461 AN(Germany)
Vortex mixer	Karlkole (Germany)
Water bath	Karlkole (Germany)
Shaker water bath	Tecam(England)

Oven	Hearson (England)
Magnetic stirrer	Gallin kamp (England)
Centrifuge	Heraeus (Germany)
Spectrofluorometer	Shimadzu 3101A
Spectrophotometer	Shimadzu 1800 spectrophotometer
UV-visible spectrophotometer	PG T80+, England
UV/visible Shimadzu spectrophotometer 1301A	Tokyo, Japan
Abbott C4000	USA
Auto Hematology Analyzer	model : BC_ 10 Germany
Microplate reader	BioTek (USA)

2.2. Methodologies

2.2.1. Collection of Blood and Serum Preparation

The vein on the front of the elbow or forearm is almost employed. The arm must be temperate to develop the circulation and distend the vein. The arm is extended, and a tourniquet is firmly applied (10-15) cm above the elbow. The skin over the vein will be sterilized with a small pad of cotton wool soaked with hapten. Disposable sterile needle fixed onto a disposable syringe is inserted into the vein. When the needle enters the vein the plunger of the syringe is slightly withdrawn. If blood appears, the tourniquet is released. When five ml of blood has been drawn into the needle was inserted, and the needle is withdrawn. This pad is firmly pressed on to until the bleeding stops. The needle is removed from the syringe and the blood was divided almost equally (1.0 ml) into 12x56mm K3-EDTA polypropylene tubes and in a Gel tubes without anticoagulant (

4.0 ml). The blood in the K3-EDTA tubes was used to perform a hemoglobin (Hb), while the blood in a gel tubes permitted to clot for 15 minutes; the clot shrinks, and serum can be taken by centrifuging for approximately 10 minutes at a relative centrifugal force (RCF) of 1500 RPM to 2000 RPM and used to determine Total Oxidant Status, Total Antioxidants Capacity, Lipid Peroxidation, Glutathione peroxidase 4 (ELISA kits), vitamin E, Xanthine Oxidase Activity, Ferritin, GSH and Iron.

2.2.2. Patients and Controls

A clinical study was performed in the Chemistry department during 2021 - 2022. In this study overall 300 patients (male) were divided to two comparison groups- Cases and Control and described as follows:

I- Cases included the patients diagnosed with β-thalassemia. Blood samples were drawn from the Patients From the Thalassemia Center at the Children's Hospital of Babylon.

II- Control included the healthy individuals from similar background and geographic area, having similar food habits and having no history of blood transfusion.

All participants were aged(5-15years).

2.3. Reactive Oxygen Metabolites Derived Compounds (d-ROMs) assay

2.3.1. Principle

Reactive oxygen metabolites (ROMs) assay were measured the ROOH and H_2O_2, although the exact ROS components that measured have not been described yet. This test was based on Fenton's reaction, which consists of indirect estimation of total ROOH in a solution test by monitoring N,N-dyethyl-paraphenyldiamine radical cation ($DEPPD^{\bullet}$) concentration. This radical cation originated from the diamine oxidation by $ROO^{\bullet}$ and $RO^{\bullet}$ that result from the reaction between peroxides present in the sample and the iron ions (Fe^{2+}, Fe^{3+}) released by the proteins in the acidic medium. Such radicals are then trapped by alchilamine present in the reaction medium [119].

The concentrations of these newly formed radicals ($DEPPD^{\bullet-}$), which have a pink color, were measured at 505 nm, and they were directly proportional to the peroxides present in the sample **Figure 2-1**.

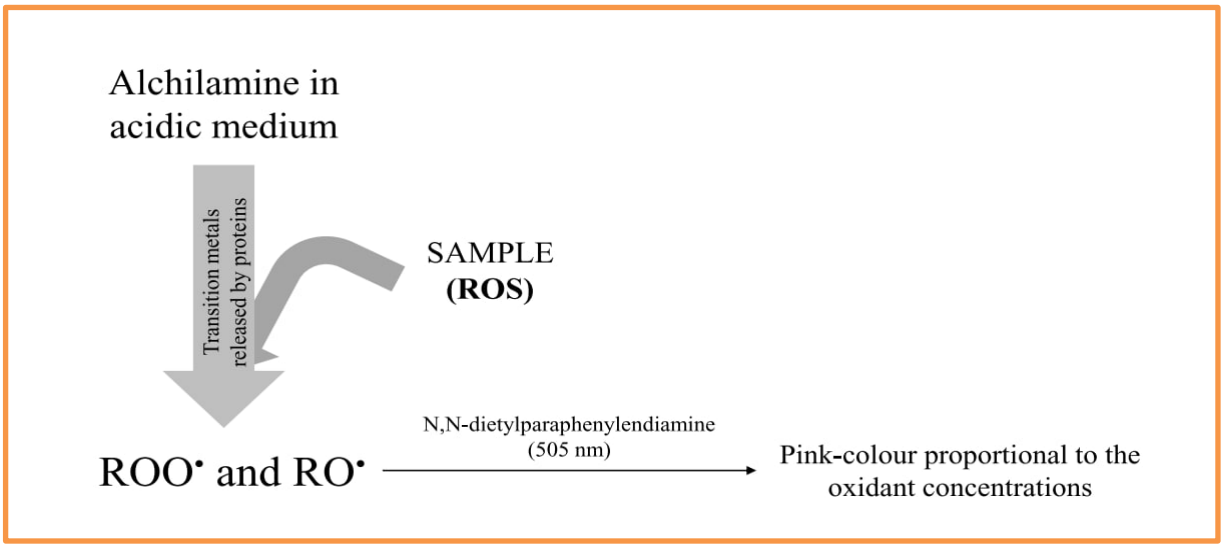

Figure 2-1 : An overview of reactive oxygen metabolites derived compounds (d-ROMs) reaction.

The concentrations of d-ROMs were stable in human serum samples when they were stored at 4 °C for 24 h and at − 80 °C for 3 months. However, the validity of this assay had been questioned. Previous studies demonstrated that d-ROMs, in a dose-response study, gave no response with H_2O_2, t-Bu-OOH and Cu-ROOH pure solutions. In addition, it had been shown that ceruloplasmin is a potential source of the signal detected by the test in serum, together with other compounds such as iron, albumin, and thiol.

2.3.2. Reagents

1. Iron(II) sulfate $FeSO_4$ (2.8 x 10^{-3} M in water): was prepared by dissolving 42.5342 milligrams in 100 ml distilled water.
2. N,N,N',N'-tetramethyl p-phenylenediamine (DEPPD (3.7 x 10^{-3} M) was prepared by dissolving 60.7725 milligrams of DEPPD in 100 ml of an acetate buffer solution. The final solution contains butylated hydroxytoluene (3.3 x 10^{-3} M; 72.7155 milligrams).
3. Hydrogen Peroxide (STD) a **(**100 µmol/L) daily standardized and newly diluted using a molar extinction coefficient of 43.6 M-1 cm-1 at 240 nm.

2.3.3. Procedure

	Blank	Standard	Sample
Distilled water	25 µl	-----	------
Serum	------	-----	25 µl
Hydrogen peroxide	------	25 µl	------
Fe^{2+} solution	1 ml	1 ml	1 ml
Test tubes was mixed by vortex, then add:			
$DEPPD^{\bullet}$ solution	250 µl	250 µl	250 µl

Every tube were gently after the addition, and let to stand at room temperature for 30 minute, then absorbance was read at 505 nm.

2.3.3. Calculation

Total oxidants status = $\frac{\text{Atest}}{\text{ASTD}} \times$ Conc. of STD

Conc. of STD= 100 µmol/L

2.4.1. Total Antioxidants Capacity Assay: The ORAC-Pyrogallol Red Assay

2.4.1.1 Principle:

The consumption of Pyrogallol Red (PGR) was evaluated from the progressive absorbance decrease measured at 540 nm in the thermostatted wells of a multimode microplate reader. The area under the curve (AUC) of these kinetic data was assessed by their integration up to a time such that (A/A0) reached a value of 0.2. All experiments were carried out in triplicate[120].

2.4.1.2.Reagents:

Pyrogallol Red (PGR) and antioxidants were easily oxidized; these solutions were prepared daily. 2,2′-azobis-2-methyl-propanimidamide,dihydrochloride (AAPH) solution was stable for at least 2 days; however it was also prepared daily. Phosphate buffer was stable for 2 weeks. Samples were analyzed immediately after opening.

1- Phosphate buffer solution (75 mM, pH 7.4)-A 10.65 g amount of disodium hydrogen phosphate was weighed into 1 L deionized water; 10.35 g sodium dihydrogen phosphate monohydrate was weighed into 1 L deionized water. Sodium dihydrogen phosphate monohydrate solution was added to the disodium hydrogen phosphate solution to reach a pH value of 7.4.

2- Pyrogallol Red (PGR) stock solution (64 μM)-A 4 mg amount of PGR was weighed and solubilized in 10 mL phosphate buffer solution. From this solution of 1 mM, an aliquot of 64 μL was taken and added to 936 μL phosphate buffer to obtain a 64 mM PGR solution. From the latter

solution, aliquots of 20 μL were taken and added to each well (final volume, 250 μL) to obtain a final PGR concentration of 5 μM.

3- 2,2′-azobis-2-methyl-propanimidamide,dihydrochloride (AAPH) (120 mM)-A 0.163 g amount was weighed and solubilized in 1 mL phosphate buffer. From this solution of 0.6 M, an aliquot of 200 μL was taken and added to 800 μL phosphate buffer to obtain a 120 mM AAPH solution. From the latter solution were taken aliquots of 21 μL and added to each well (final volume 250 μL) to obtain a final AAPH concentration of 10 mM.

2.4.1.3. Procedure:

1- Standards and sample antioxidants (50 μM) were prepared daily in phosphate buffer or ethanol as necessary for solubility.

2- Beverage samples should be diluted 20 times with phosphate buffer.

3- Microplate preparation: The reaction mixture (final volume 250 μL in 75 mM phosphate buffer, pH 7.4) containing PGR (20 μL, 5 μM final concentration), antioxidants (20 μL stock solutions), or diluted beverage samples (25 μL) were placed in the well of the microplate. Final volume was adjusted to 250 μL using phosphate buffer. This solution was preincubated for 30 min at 37°C. AAPH solution (21 μL, 10 mM final concentration), previously incubated at 37°C, is added to the microplate well.

2.4.1.4. Determination

The microplate was immediately placed in the reader, automatically shaken, and the absorption units (A) were registered every 30 s for 180 min. Collected absorbance values were plotted as (A/A0) as a function of the incubation time.

2.4.1.5. Calculations

The AUC for each plot of A/A0 is determined. AUC data were used to obtain ORAC values of beverages, according to equation 1.

$$ORAC = \frac{AUC - AUC^{0}}{AUC_{Trolox} - AUC^{0}} f\,[Trolox] \qquad (1)$$

In this equation AUC = area under the curve in the presence of the tested beverages, integrated between zero time and that corresponding to 80% of PGR consumption; AUC^{o} = area under the curve for the control (PGR plus AAPH in the absence of sample); AUC_{Trolox} = area under the curve in the presence of Trolox; f = dilution factor, equal to the ratio between the final volume of the solution (250 µL) and the added beverage volume; and Trolox = Trolox concentration (µM) **Figure 2-2**.

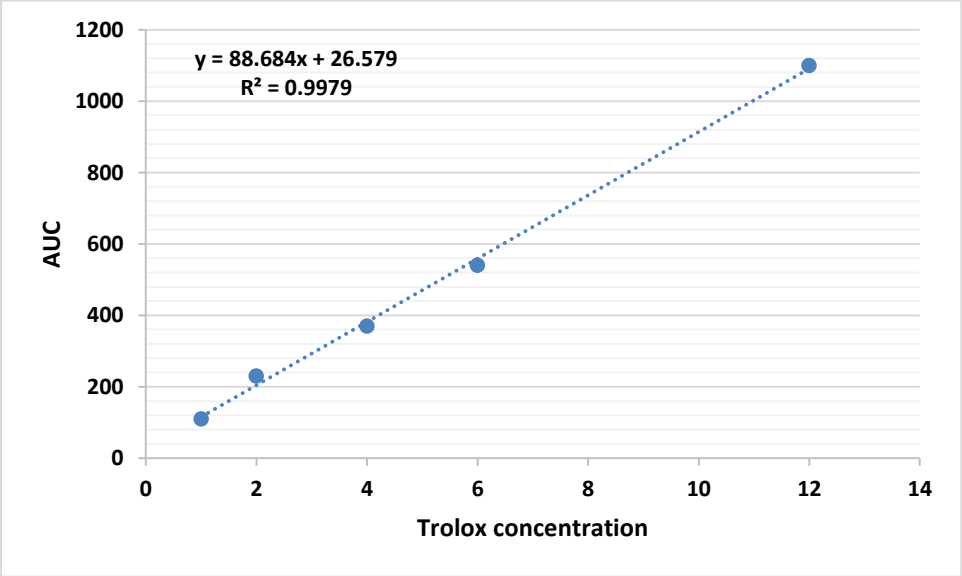

Figure 2-2 : ORAC Standard curve of Trolox (µmol/l).

2.5. Determination of Serum Lipid Peroxidation

2.5.1 principle

Lipid peroxidation in sera was evaluated by thiobarbituric acid reative substances (TBARS). TBARS test gives a basic, reproducible, and standardized tool for measuring lipid peroxidation in serum. The MDA-TBA adduct designed by the response of MDA and 1,3-Diethyl-2-thiobarbituric acid (DETBA) under high temperature (90-100°C) at acidic conditions was measured colorimetrically at 530-540 nm or fluorometrically at an excitation wavelength of 515 nm and an emission wavelength of 555 nm. This reaction had a much higher sensitivity when measured fluorometrically [121] as a **Figure 2-3** .

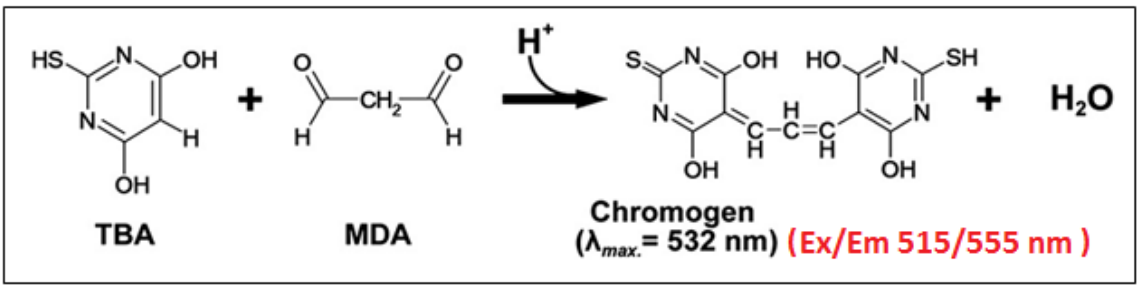

Figure 2-3: Scheme of the adduct MDA–$(TBA)_2$[121].

2.5.2. Reagents

1. 8.1% SDS
2. 0.25 mM HCl
3. 12.5 mM of 1,3-Diethyl-2-thiobarbituric Acid (DETBA) in a sodium phosphate buffer (0.125 M, pH 3.0) warmed to 50°C
4. 20 mM BHT
5. Ethyl acetate

2.5.3. Procedure:

1- A volume of 100 µl of serum was added to the test tube.

2-A volume of 200µL of 8.1% SDS, 1.5 mL of 0.25 mM HCl, 1.5 mL of 0.375 % of TBA, 50µL of 20 mM BHT, and 250µL of DDW were added to a test tube.

3-The sample was vortexed and heated in a 90 C water bath for 15 min, and then allowed to cool.

4- To extract the DETBA-MDA adduct, 4 ml of ethyl acetate was added, and the mixture was shaken vigorously. After centrifugation at 2000 rpm for 10 min at 20°C, the fluorescence intensity of the organic layer was measured at an excitation wavelength of 515 nm and emission wavelength of 555 nm (Ex 515 Em 555)·

Preparation of MDA stock solution

A solution was prepared with 22µl of 1,1,3,3-tetramethoxypropane added to 10 ml of H_2SO_4 (1%), and it was left to stand at room temperature for 2 h in a place protected from light to generate MDA from acid hydrolysis of the standard. Then, 10µl of the MDA stock solution were added to 3 ml of H_2SO_4 (1%). determined the concentration of the MDA stock solution by reading the absorbance at 245 nm in the spectrophotometer (ϵ 245nm=13700 $M^{-1}cm^{-1}$).

2.5.4. Calculation:

MDA Concentration = $\frac{\text{F test}}{\text{F STD}} \times \text{Conc. of STD}$

2.6. Determination of Serum Glutathione Peroxidase 4 (GPX4)

The kit is a sandwich enzyme immunoassay for in vitro quantitative measurement of GPX4 in human serum, plasma, tissue homogenates.

2.6.1. principle

This kit is an Enzyme - Linked Immunosorbent Assay (ELISA) . The plate has been pre - coated with Human GPX4 antibody . GPX4 present in the sample is added and binds to antibodies coated on the wells . And then biotinylated Human GPX4 Antibody is added and binds to GPX4 in the sample . Then Streptavidin - HRP is added and binds to the Biotinylated GPX4 antibody . After incubation unbound Streptavidin - HRP is washed away during a washing step . Substrate solution is then added and color develops in proportion to the amount of Human GPX4 . The reaction is terminated by addition of acidic stop solution and absorbance is measured at 450 nm .

2.6.2. Reagent preparation

1. All components of the kit and samples have been brought to room temperature (18-25C^{o}) before use.

2. Standard – The standard solution is prepared as shown in the table explain how to prepare standard solutions.

12ng/ml	Standard	120µl Original Standard + 120µl Standard
6ng/ml	Standard	120µl Standard No.5 + 120µl Standard
3ng/ml	Standard	120µl Standard No.4 + 120µl Standard
1.5ng/ml	Standard	120µl Standard No.3 + 120µl Standard
0.7ng/ml	Standard	120µl Standard No.2 + 120µl Standard

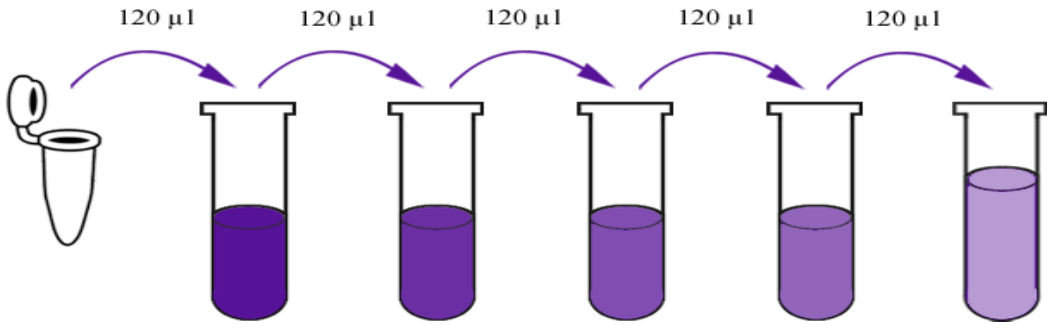

Standard Concentration	Standard No.5	Standard No.4	Standard No.3	Standard No.2	Standard No.1
24ng/ml	12ng/ml	6ng/ml	3ng/ml	1.5ng/ml	0.7ng/mL

3.Wash Buffer 20mLof Wash Buffer Concentrate 25x is dissolved into deionized or distilled water to yield 500 mLof 1x Wash Buffer.

2.6.3.Assay procedure

1. All reagents, standard solutions and samples were Prepared as instructed. Bring all reagents to room temperature before use. The assay is performed at room temperature.

2. A 50µl standard was added to standard well. Without add antibody to standard well because the standard solution contains biotinylated antibody.

3. A 40µl sample was added to sample wells and then add 10µl anti-GPX4 antibody to sample wells, then add 50µl streptavidin-HRP to sample wells and standard wells (Not blank control well). Incubate 60 minutes at 37°C.

4.The plate were washed 5 times with wash buffer. And Soak wells with at least 0.35 mL wash buffer for 30 seconds to 1 minute for each wash., overfilling wells with wash buffer. the plate has been filtered onto paper towels or other absorbent material.

5. A 50µl substrate solution has been added to each well and after we add 50µl substrate solution B to each well. Incubate plate covered with a new sealer for 10 minutes at 37°C in the dark.

6. A 50µl Stop Solution was added to each well, then the blue color changed into yellow immediately.

7. The optical density (OD value) was determined of each well immediately at 450 nm within 10 minutes after adding the stop solution.

2.6.4. Calculation of Result

A standard curve was constructed by plotting the average OD for each standard on the vertical (Y) axis against the concentration on the horizontal (X) axis and a best fit curve were drawn through the points on the graph. These calculations were performed with computer-based curve-fitting software and the best fit line were determined by regression analysis **Figure 2-4** .

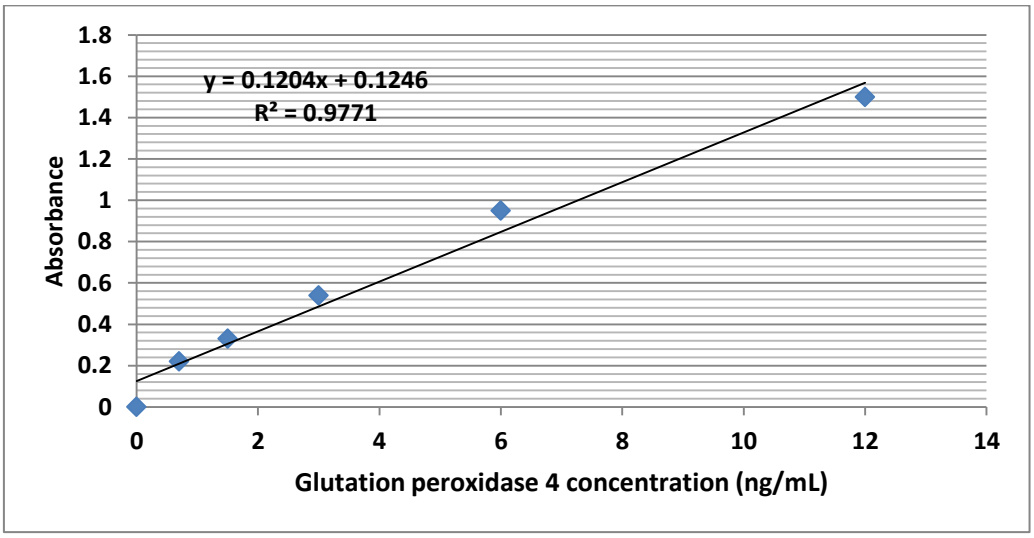

Figure 2-4 : Standard curve of Glutathione peroxidase 4 concentration.

2.7. Assay of total tocopherol (vitamin E) in serum

2.7.1. Principle:

Plasma total tocopherol was assayed by the method of Quaife et al. , It was involved the Emmerie- Engel color reaction with ferric chloride and α,α¯-dipyridyl to give a red color [122].

2.7.2. Reagents:

1. absolute ethanol.

2. α,α-dipyridyl : was prepared by dissolving 0.120 gm of α,α-dipyridyl in 100 ml of n-propyl alcohol.

3. Ferric chloride hexahydrate : was prepared by dissolving 0.120 gm of Ferric chloride hexahydrate in 100 ml of absolute ethanol. Keep this solution in a dark brown or red glass bottle.

4. α-tocopherol standard (1µmol/L) was prepared by dissolving 2.0 mg of α-tocopherol in 100 ml of absolute ethanol.

2.7.3. Procedure:

Reagents	Test	STD	Blank
Absolute ethanol	0.6 mL	0.6 mL	0.6 mL
Sample	0.3 mL	------	-------
D.W.	-----	------	0.3 mL
STD	-----	0.3 mL	-------
Xylene	0.6 mL	0.6 mL	0.6 mL
Mixed well and centrifuged for 10 min at 3000 rpm.			
xylene supernatant layer	0.1 mL	0.1 mL	0.1 mL
α,α-dipyridyl was added and vortexed	0.1 mL	0.1 mL	0.1 mL
The 0.2 mL of this mixture was then pipetted into a cuvette and the absorption was measured spectrophotometrically at 460 nm against deionized water.			

ferric chloride	0.05 mL	0.05 mL	0.05 mL
Mixed thoroughly and absorption was again read at 520 nm spectrophotometrically exactly 1.5 min after addition of ferric chloride.			

2.7.4. Calculation:

$$\text{Conc. of test} = \frac{(\text{A } 520 - 0.29\ \text{A } 460)\ \text{test}}{\text{A } 520\ \text{STD}} * \text{Conc. of STD}$$

2.8. Determination of Xanthine Oxidase Activity

2.8.1. Reagents

Substrate-buffer solution: To prepare 10 mmol/L hypoxanthine solution, 0.13611g of hypoxanthine was dissolved in 70 mL of 25 mmol/L NaOH solution, and 30 mL of 66.7 mmol/L KH_2PO_4 was added. This solution contains 20 mmol/L NaN_3, and has pH 7.9.

Reagent solution: By optimizing the conditions, a reagent solution with the following composition was made: 2 mmol/L ABTS, and 2 500 U/L POD in 1000 ml of 66.7 mmol/L phosphate buffer, pH 7.9. This solution is stable for more than 2 mth. Uricase (10 U/mg) was used undiluted.

2.8.2. Procedure for xanthine oxidase assay

Substrate-buffer solution (1.0 ml), 5 μL of uricase, and 50 μL of serum were mixed well and incubated 10 min at 30°C in a centrifuge tube. Add 1.0 ml of reagent solution, vortexed and immediately added 1.0 ml of 2 mol/L HClO,. Vortexed again and centrifuge for 5 min at 3 000 mm-‘. The absorbance of the clear supematant was read at 410 nm

against a blank (containing 1.0 mL of 66.7 mmol/L phosphate buffer with 20 mmol/L NaN_3, 5 μL uricase, 50 μL serum, 1.0 mL reagent solution, and 1.0 mL HClO,) prepared in the same way as the test. The final reaction product was stabled for 15 min [79].

2.8.3. Calculation

The xanthine oxidase catalytic activity was calculated as:

Activity = A_{410}nm *X* 79.9 on the basis of $ABTS_{ox}$ molar extinction coefficient which is 2550 m^2/mol .

2.9. Determination of Iron

In the present study serum iron was determined using a Microparticle Enzyme Immunoassay (MEIA) technology. For this purpose we used Abbott full automated Axsym immunoassay analyzer ferritin assay system (Abbott C4000,USA) was used **Figure 2-5.**

Figure 2-5: Abbott instrument.

2.10. Determination of Ferritin

In the present study serum ferritin was determined using a Microparticle Enzyme Immunoassay (MEIA) technology. For this

purpose we used Abbott full automated Axsym immunoassay analyzer ferritin assay system (Abbott C4000,USA) was used **Figure 2-5.**

2.11. Determination of Hb (Hemoglobin)

In the present study Hb was determined using Auto Hematology Analyzer (model : BC_ 10 Germany).

2.12. Xanthine Oxidase Inhibition Activity

2.12.1. Reagents

Phosphate buffer solution (pH 7.8, 0.1 M) was prepared by dissolving 13.61 g of monopotassium phosphate (KH_2PO_4 MW, 136.09 g/mol) and 3.62 g of sodium hydroxide (NaOH MW, 40.00 g/mol) in 800 ml of distilled water. The pH of the solution was adjusted using HCl or NaOH. The final volume was increased to 1 L with distilled water. Xanthine solution (10 mmol/l) was prepared by dissolving 0.1521 g of xanthine in 70 ml of sodium hydroxide (25 mmol/l) and 30 ml of KH_2PO_4 (66.7 mmol/l). Sodium azide (25 mg) was added. The final pH was adjusted to 7.8. Phosphate buffer solution was used to prepare standard hydrogen peroxide (2 mM) (pH 7.8, 100 mM). At 240 nm, a molar extinction value of 43.6 M^{-1} cm^{-1} was used to adjust the final concentration. Copper(II) chloride (100 mM) was prepared with 0.4262 g of $CuCl_2 \cdot 2H_2O$ dissolved in 250 ml of distilled water. Ammonium acetate buffer (NH_4Ac) (pH 7.0, 1.816 M) was prepared with 35 g of NH_4Ac dissolved in 250 ml of distilled water. Neocuproine (2,9-dimethyl-1,10-phenanthroline) (Nc) (7.5 mM) was prepared with 0.039 g of Nc dissolved in 25 ml of 96% ethanol. Fresh working reagent (CUPRAC reagent**)** was prepared by mixing volumes of the prepared reagents

Cu(II):Nc:NH_4Ac at a ratio of 1:1:2 (v/v/v). XO solution was prepared by diluting 3 $U.mg^{-1}$ solid of original XO suspension with PBS (pH 7.8, 100 mM) to a final concentration of 0.04 U mL^{-1}. The perchloric acid solution 3.2% (w/v) was prepared with 3.2 ml of perchloric acid dissolved in a suitable volume of distilled water in a 100-ml volumetric flask.

2.12.2. Procedure

2.12.2.1.Standard method for assessment of XOI

The XO activity was measured spectrophotometrically at 293 nm by detecting the production of uric acid. Potassium phosphate buffer (100 mM, pH 7.8), 75 mM xanthine, and 0.04 units of XO were used in the enzymatic reaction. The decrease in uric acid production at 293 nm was used to test the inhibition of XO activity with different inhibitors. The enzyme was preincubated for 5 min with the test chemical, which was dissolved in an appropriate buffer, before the reaction was started using xanthine. The herbal extract inhibition ratio was calculated using Eq. (1).

Inhibition ratio (%) = 100*[A_0-A)/ A_0] --- (1)

where A_0 and A are the absorbances of the system in the absence and presence of the inhibitor, respectively.

2.12.2.2. CUPRAC method for assessment of XOI

A mixture of 0.5 mL of 0.5 mM xanthine, 0.2 mL of antioxidant sample solution, 1.8 mL of 1:9 EtOH–PBS (pH 7.8) (v/v), and 0.2 mL of 0.04 U mg^{-1} XO was added to a test tube in this order. The mixture was incubated in a water bath at 37 °C for 30 min in a total volume of 2.7 mL. After 30 min, the reaction was terminated by vortexing for one minute with 0.1 mL of 3.2% perchloric acid solution.

Fresh CUPRAC reagent was added to 0.2 mL of the incubation solution in the following order: (V total = 1.0 mL) 0.2 mL Cu(II) + 0.2 mL Nc +

0.4 mL NH4Ac buffer + 0.2 mL incubation solution. The absorbance was measured after 30 min against a reagent blank, with and without an inhibitor. The average of three experiments was used for calculation.

The inhibition ratio (%) of the herbal extract was calculated using Eq. (2).

Inhibition ratio (%) = 100*[A_0-A)/ A_0] --- (2)

where A_0 and A are the CUPRAC absorbances of the enzymatic solution in the absence and presence of the inhibitor, respectively.

2.12.2.3. Modified CUPRAC method for assessment of XOI

The modified XOI–CUPRAC method is presented in **Table (2-3).**

Table (2-3): Details of modified XOI–CUPRAC method

Reagent	**Test (t_{30})**	**Test (t_0)**	**Control**	**Blank**
Xanthine	0.5 mL	0.5 mL	0.5 mL	0.5 mL
Antioxidant sample	0.2mL	0.2mL	-------	-------
1:9 EtOH–PBS mixture (pH 7.8) (v/v)	1.8mL	1.8mL	2.0 mL	2.2 mL
3.2% perchloric acid solution	------	0.1 mL	------	------
XO solution	0.2 mL	0.2 mL	0.2 mL	------
The test tubes were incubated at 37 ˚C for 30 min.				
Perchloric acid solution	0.1 mL	------	0.1 mL	0.1 mL
Following incubation, fresh CUPRAC reagent was added to 0.2 mL of incubation XOI solution as follows: (V total = 1.0 mL) 0.2 mL Cu(II) + 0.2 mL Nc + 0.4 mL NH_4Ac buffer + 0.2 mL incubation XOI solution. The absorbance was measured at 450 nm after 30 min against a reagent blank. The average of three experiments was used for calculation.				

The inhibition ratio of the herbal extract (%) was calculated using Eq. (3):

$$\mathbf{A_{corrected} = At_{30} - At_0 \text{ ---- (3)}}$$

$$\mathbf{\text{Inhibition ratio (\%)} = 100*[A_0\text{-}A_{corrected})/\ A_0] \text{ --- (4)}}$$

where A_0 is the absorbance of the control tube; At_0 and At_{30} are the absorbances of the test tube at t = 0 and t = 30 min, respectively.

2.12.2.4. Validation and reproducibility

The proposed method was evaluated using the UV method, as previously reported [75]. Three duplicates of five samples were examined

to determine intra- and inter-day precision and accuracy. The data was analyzed using GraphPad Prism v.8 software (San Diego, CA, USA).

2.13. Determination of total Glutathione concentration (GSH)

2.13.1. Principle

5,5̄ - Dithiobis (2-nitrob enzoic acid)(DTNB) is adi chromogen that is readily reduce by sulfhydry groupof GSH to produce an intensely yellow Compound. Reduce chromogen has maxmum absorbance at 412 nm and is directly proportional to GSH concentration [123] **Figure 2-6** show the reaction between GSH and DTNB(Elman's reagent)**.**

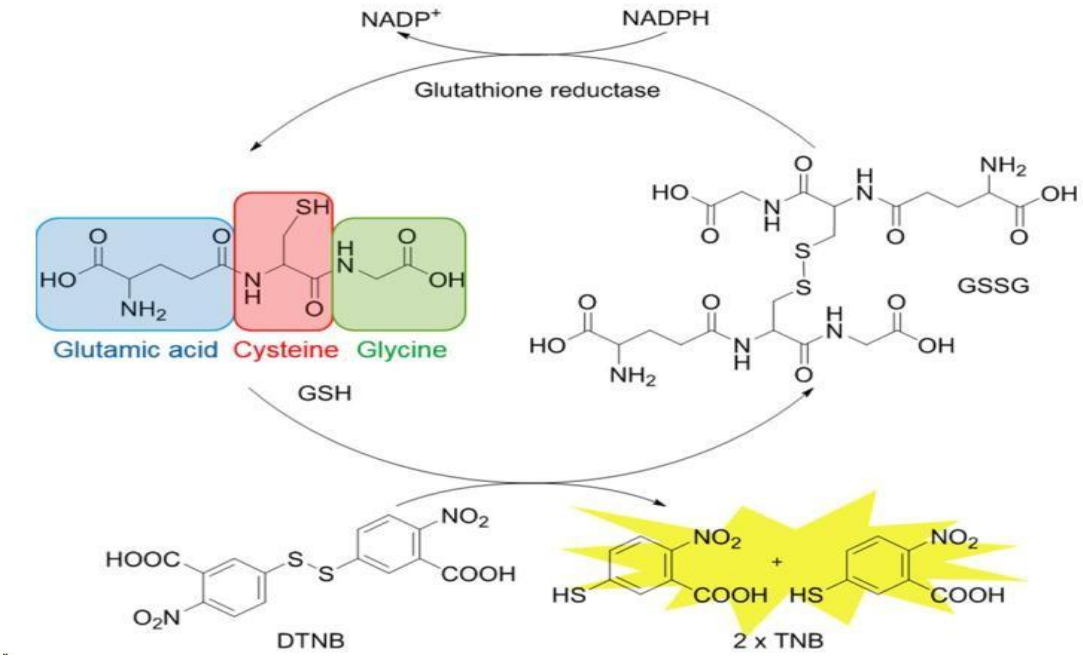

Figure 2-6: Reaction between GSH and DTNB(Elman's reagent)[123].

2.13.2. Preparation of Reagent

1- The precipitating solution. Trichloroacetic acid (TCA) 50% 50gm of TCA dissolved in a final volume of 100 ml of DDW.

2-Ethylene di amine tetra acetic acid- di sodium (EDTA-Na_2)(0.4M) 148.9gm of EDTA are dissolved in a final volume of 1 litter of DDW.

3-Tris-EDTA buffer (0.4) (pH = 8.9)

48.458 gm of tris is dissolved in 800 ml of DDW. 100 ml of (0.4M) EDTA solution are added and bring to a final volume of 1 liter with DDW. The pH adjusted to 8.9 by the addition of 1M of HCl.

4- DTNB reagent (0.01M)

0.099 gm of DTNB is dissolved in absolute methanol. And bring to a final volume of 25 ml (this reagent stable for at least 13 week at 4 ^{o}C).

5- GSH standard

Stock standard solution (0.001M) prepared by dissolving 0.0307 gm of a GSH in a final volume of 100 ml of (0.4M) EDTA solution. Dilution is made in EDTA solution to 2,5,10,20,30 and 40μM (this working standard solution should be prepared daily).

2.13.3. Procedure

Sample GSH was determined by using a modified procedure utilizing Ellman's reagent (DTNB), which is summarized as follows.

Duplicates of each standard and sample test tubes are prepared then pipette into test tubes.

Reagents	Sample µL	Reagent black µL	Standard µL
Sample	100	-----	-----
Standard	-----	----	100
DDW	800	900	800
TCA	100	100	100

Tubes are mixed in vortex mixture. Intermittently for 10-15 minutes, and Centrifuge for 15 minutes at 300 xg, then pipette into test tubes.

Reagents	Sample µL	Reagent blank µL	Standard µL
Supernatant	400	400	400
Tris EDTA buffer	800	800	800
DTNB reagent	20	20	20

Tubes are mixed in vortex mixture. The spectrophotometer adjusted with reagent blank to read zero absorbance at 412 nm, and the absorbance of standards and sample is read within five minutes of the addition of DTNB.

2.13.4. Calculation of Serum GSH

The concentration of GSH is obtained from the calibration curve in μM **Figure 2-7** .

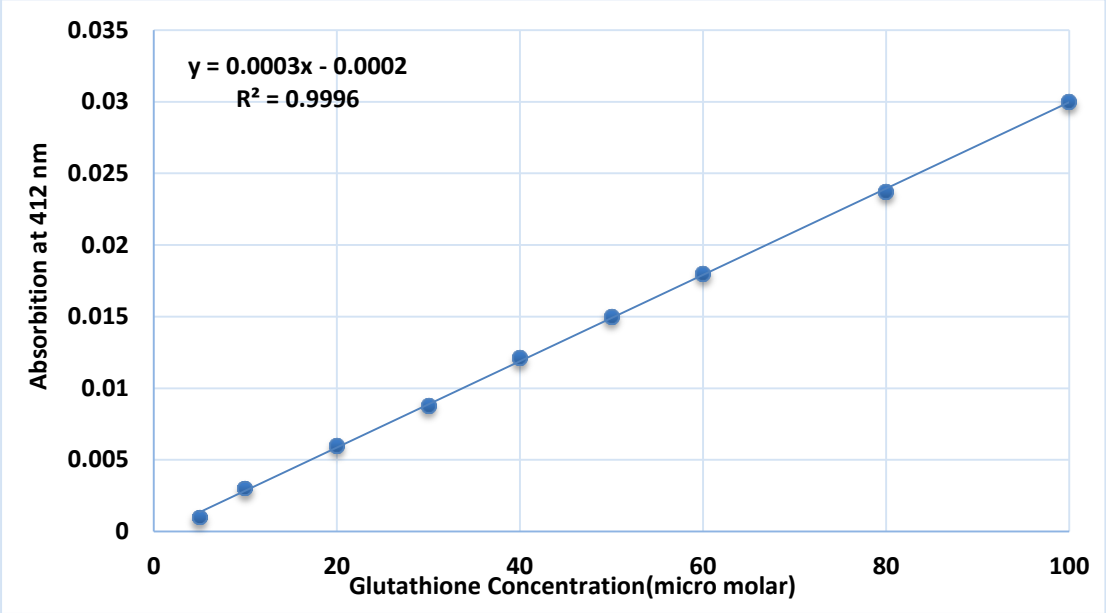

Figure 2-7 : Standard curve of glutathione concentration.

2.14. A simple chemical sensor for quantifying xanthine oxidase inhibition activity

2.14.1. Reagents

The 250 mM acetic acid-sodium acetate (HA/SA) buffer (pH. 2.6) comprised 2.8 mL of acetic acid and 0.26 g of sodium acetate dissolved in 100 mL distilled water. The 50 mM phosphate-buffered saline solution (PBS; pH 7.8) comprised 0.68 g of monopotassium phosphate (KH_2PO_4) and 0.18 g of sodium hydroxide (NaOH) dissolved in 100 mL of distilled water. The pH of all buffer solutions was adjusted using NaOH and HCl. The 10 mM xanthine solution (pH 7.8) comprised 0.1521 g of xanthine and 25 mg of sodium azide dissolved in 30 mL of 66.7 mM KH_2PO_4 and 70 mL of 25 mM sodium hydroxide. A 50 mM PBS (pH 7.8) solution was used to prepare a standard 2 mM H_2O_2 solution; a molar extinction value of 43.6 M^{-1} cm^{-1} was used to adjust the final concentration at 240

nm. The 10 mM copper(II) chloride solution comprised 0.147 g of cupric chloride dihydrate dissolved in 100 mL of distilled water. The fresh 6 mM TMB stock solution comprised 144.2 mg of TMB dissolved in a 50:50 (v/v) mixture of water and ethanol (EtOH). The 2 M sulfuric acid solution was prepared in a 100 mL volumetric flask by carefully and slowly adding 10.87 mL of sulfuric acid to 89.13 mL of distilled water. XO solution was composed of 3 $U.mg^{-1}$ of original XO suspension that dissolved in PBS (pH 7.8, 50 mM) to a final activity of 0.06 $U. mL^{-1}$. Perchloric acid solution 3.2% (w/v) was composed of 3.2 ml of perchloric acid and 96.8 ml of distilled water in a 100-ml volumetric flask. ABST reagent solution was prepared by mixing 2500 U/l peroxidase and 2 mmol/l ABTS in 1L of PBS (pH 7.8). Undiluted uricase (10 U/mg) was utilized directly.

2.14.2. Procedure

2.14.2.1. Standard methods for quantifying XOI activity

2.14.2.1.1. UV method

Uric acid generation was monitored spectrophotometrically at 293 nm to measure XO activity. The enzymatic reaction used 75 mM xanthine dissolved in PBS (pH 7.8) and 0.04 U of XO enzyme. The reduction in uric acid synthesis was used to measure the inhibition of XO activity by particular XOIs. Before initiating the reaction with xanthine, the enzyme was preincubated for 5 min with the PBS solution. The herbal extract inhibition ratio was calculated using Eq. (1).

2.14.2.1.2. ABTS method

First, 1.0 mL substrate-buffer solution, 25 µL of herbal extract sample solution, 25 µL of XO enzyme, and 5 µL of uricase were combined in a centrifuge tube and incubated for 10 minutes at 30°C. Next, 1 mL of ABTS solution was added, followed by 1 mL of 2 mol/L perchloric acid, and vortexed. Then, the solution was centrifuged at 3000

rpm for 5 minutes. Finally, the absorbance of the supernatant was measured at 410 nm. The herbal extract inhibition ratio was calculated using Eq. (1).

2.14.2.1.3. TMB methods for quantifying XOI activity

2.14.2.1.3.1.Cuvette spectrophotometric protocol

First, 0.5 mL of 75 mM xanthine, 0.2 mL of antioxidant sample solution, 1.8 mL of 1:9 EtOH-PBS (pH 7.8; v/v), and 0.2 mL of XO enzyme solution were added to a test tube in that order. Next, the mixture was incubated at 37°C for 30 minutes. Then, 1 mL of 250mM HA/SA buffer (pH. 2.6), 250 µL of Cu^{+2}, and 500 µL of TMB were added, in that order. The resulting solution was vortexed and incubated for 7 minutes at 60°C before being allowed to cool to room temperature. Finally, 500 µL of sulfuric acid was added.

2.14.2.1.3.2. Microplate protocol

A mixture containing 20 µL of 75 mM xanthine, 20 µL of antioxidant sample solution, 65 µL of 1:9 EtOH-PBS (pH 7.8; v/v), and 20 µL of XO enzyme solution was added to each well of a 96 well plate in that order. Next, the plate was incubated at 37 °C for 30 minutes in a water bath. Then, 40 µL of 250 mM HA/SA buffer (pH. 2,6), 20 µL of Cu^{+2}, and 40 µL of TMB were added, in that order. The plate was mixed and incubated at 60°C for 7 minutes before being allowed to cool to room temperature. Finally, 25 µL of sulfuric acid was added to each well, followed by thorough mixing.

2.14.3. Calculation

Eq. (1) was used to calculate the XO inhibition percentage ratio of the herbal extract (%):

$$\textbf{XO inhibition ratio (\%)} = 100 \times [(A_0 - A) / A_0], \qquad (1)$$

where A_0 and A are the reaction system absorbances without and with the inhibitor.

2.14.4. Optimization of TMB-XO assay

The optimization process used a second-order model to investigate the significance of the variables and their interactions to identify the optimal analysis response. The Response Surface Methodology (RSM) was subject to the Box-Behnken Design (BBD) to enhance the TMB-XO assay. The Chemoface software (v.1.5) [124] was used to predict the statistical parameters to design the TMB-XO assay experiments and enhance the system's performance. A 50 U L^{-1} XO solution was used to perform enzymatic reactions, manually prepared by mixing an appropriate amount of standard XO powder with 100 mL of PBS (pH 7.8). The resulting XO activity was adjusted to 50 U L^{-1} using the UV-based method [112]. The XO activity measured by the presented chemical sensor was the dependent variable, and the concentrations of TMB, Cu^{2+}, and incubation time were the independent variables **Table (2-4)**.

The constant rate equation was used to determine enzyme activity for a first-order reaction (k). A second-order polynomial equation (Eq. [2]) was used for mathematical modeling of the relationship between the dependent and independent variables.

$$Y = \beta_0 + \sum\beta_i X_i + \sum\beta_{ii} X_i^2 + \sum\beta_{ij} X_i X_j + \varepsilon, \quad (2)$$

where Y represents XO activity (the response variable), X_iX_j represents **independent variables (**TMB concentration, Cu^{+2} concentration, and incubation time), and β_0, β_i, β_{ii}, and β_{ij} are the coefficients of intercept, linear, quadratic, and interaction, respectively. ε represents random error.

Table (2-4): The BBD was used to optimize the XO activity assay. The independent factors were TMB concentration, Cu^{2+} concentration, and incubation time, while the dependent variable was the resulting XO activity.

Run	TMB concentration (mM)	Cu^{2+} concentration (mM)	Incubation time (min)	XO activity (U/L)
1	4	5	15	38
2	4	5	45	46
3	4	15	15	47
4	4	15	45	47
5	8	5	15	42
6	8	5	45	46
7	8	15	15	48
8	8	15	45	50
9	2.64	10	30	40
10	9.36	10	30	50
11	6	1.59	30	41
12	6	18.41	30	51
13	6	10	4.77	44
14	6	10	55.23	50
15	6	10	30	50
16	6	10	30	49
17	6	10	30	50

2.14.5. Signal stability

Diimine (dicatione) is the final product of the TMB-XO assay. We used 0.5 mM diimine to assess the stability of the colored end product by measuring its absorbance at 450 nm after 15 min, 30 min, 1 h, 2 h, 3 h, 4 h, 5 h, 1 day, and 2 days at 20°C.

2.14.6. Linearity and sensitivity

The presented method's sensitivity and linearity were evaluated using different XO activities (from 0.1 to 60 U L^{-1}). The linearity of this method was compared to the ABTS assay [79] using a web-based application for analytical protocol comparison and bias assessment [125].

The TMB-XO assay's sensitivity was calculated using limits of quantitation (LOQ) and detection (LOD) [126].

2.14.7. Selectivity, reproducibility, and accuracy

Four flasks containing PBS (pH 7.8) were used to prepare various interfering biomolecules to assess the accuracy of the TMB-XO assay. The first contained PBS (pH 7.8). The second contained 1 mM ribose, sucrose, and glucose. The third contained 1 mM lysine, glutamic acid, proline, and methionine. The fourth contained 3% bovine serum albumin.

The proposed method's intra- and inter-day repeatability were evaluated using various biological samples, and the findings are presented as relative standard deviations. A home blender was used to prepare five polyphenol-rich plant extracts. Fifty grams of fresh leaves were combined with 950 mL of PBS (pH 7.8), with the final volume adjusted to 1 L. A spectrophotometric method was used to calculate the total polyphenol content [127]. Each extract was prepared in various concentrations based on its polyphenol content. A suitable series of quercetin and catechin concentrations were used as standards.

2.14.8. Validation

The TMB-XO assay was compared against the UV method [112] using a Bland–Altman analysis and Passing–Bablok regression [128]. Statistical analyses were performed with the Qi Macros plug-in (Know Ware International, Denver, CO, USA) for Microsoft Excel 2020.

Chapter Three

RESULTS AND DISCUSSION

3.1. General and clinical characteristics

Table (3-1) The general and clinical features of the research groups. Red blood cell transfusions lower erythropoietic incentive and increase iron overload, resulting in a large hepcidin flat that restricts dietary iron absorption and macrophage iron freedom. Iron accumulation in Kupffer cells might result as a result of this [129]. Although the symptoms of iron overload take longer to show, they may be equally as severe as those observed in people with thalassemia major who rely on blood transfusions.

Table(3-1): The research groups' general and clinical characteristics.

Character	Patients	Controls	p-value
Age	9.5 ± 2.2	9.2 ± 1.29	0.91
Ferritin (ng/ml)	3337.0±1475	44.5±25.15	< 0.001
Hb (g /dL)	7.1±1.0	11.5±0.75	<0.01

The kind of beta-thalassemia determines the quantity of hemoglobin in the blood. HbA is lacking in beta0-thalassemia, a condition marked by a lack of beta globin chain production. HbF concentrations vary from 95 to 98 percent, whereas HbA2 concentrations range from 2 to 5%. The Hb form reveals HbA between 10% and 30%, HbF between 70 and 90%, and HbA2 between 2 and 5% in beta-thalassemia homozygotes with residual variable beta globin production or beta0/beta_ compound heterozygotes [130].

3.2. Xanthine Oxidase Activity

The activity of XO in the sera of individuals with β- thalassemia major was compared to that of healthy controls. The findings of this investigation revealed that XO levels are substantially higher in the experimental group than in the control group. XO is an enzyme that has

been found in a variety of mammalian tissues [131]. XO has been found in the liver, lungs, heart, colon, and capillary endothelial cells, according to studies [132]. When compared to bigger channels, endothelial cells in micro vascular systems are the most prolific source of the enzyme[133]. Because the enzymatic activity that transfers electrons from hypoxanthine to uric acid is connected with a decrease of O_2 to $O_2^{\cdot-}$, XO is thought to have a role in the pathophysiology of oxidant-induced microvascular changes and tissue damage [134].

Several studies have looked at thalassemia patients' oxidant and antioxidant levels [135]. However, most research have only looked at the stark and midway forms of thalassemia, and there are limited documents on the heterozygote profile [136]. Furthermore, the oxidative station of various β-thalassemia mutations has not been assessed, despite the fact that such an evaluation is critical because to the considerable genotypic and phenotypic variability of changed people [137]. Auto oxidation in β-thalassemia refers to the generation of superoxide radicals ($O_2^{\cdot-}$) and hydrogen peroxide (H_2O_2), which causes oxidative stress [138].

Oxidative stress is caused by a malfunction of the enzyme complicated in the synthesis of ROS, as well as a simple inequality between the creation and sifting of ROS. NAD(p)H oxidase failure, XO activation, and mitochondrial dysfunction are all underlying indications of oxidative stress, hence XO is an important therapeutic target [139]. The activity of xanthine oxidase in the research individuals is shown in **Table (3-2)**.

Table (3-2): Xanthine oxidase activity (U/L) in sera of patients with beta-thalassemia major and healthy control subjects.

Group	*n.*	Mean	Std. Deviation	Std. Error	Sign.
Control	150	3.88	0.88	0.07	---
Patients	150	4.71	1.38	0.11	0.005*

*: in comparison to group I (Healthy donors).

3.3. Total Oxidant and Total Antioxidant Levels

The total oxidant in the serum of individuals with β- thalassemia major was compared to that of healthy controls. The findings of this investigation revealed that total oxidant levels are considerably higher in the experimental group than in the control group.

The abundant enzyme superoxide dismutase transforms superoxide anion to H_2O_2 during metabolism. The enzymes catalase and peroxidase ordinarily convert H_2O_2 to harmless molecules. If there is free iron, it combines with H_2O_2 to create hydroxyl radicals, which are extremely reactive species that cause polymer depolymerization, DNA strand breaking, functional protein inactivation, and other problems [140]. **Table (3-3A)** shows the total oxidant levels of the research subjects.

Table (3-3 A): Total oxidant (µmol/L) in sera of patients with beta-thalassemia major and healthy control subjects.

Group	*n.*	Mean	Std. Deviation	Std. Error	Sign.
Control	150	4.56	1.98	0.16	---
Patients	150	5.98	2.26	0.18	0.023*

*: in comparison to group I (Healthy donors).

When compared to controls, patients had significantly reduced levels of Total Antioxidant Capacity TAC ($p<0.01$). In beta thalassemia major patients, iron overload and increased ROS generation may be linked to increased hemolysis. Antioxidants serve a crucial part in the body's defensive system, which protects it from free radicals while also stimulating their breakdown. TAC levels may be lower as a result of its use to counteract the effects of ROS and iron overload. As a result, the current research reveals changes in iron metabolism, as well as increased formation of oxygen free radicals and consequent antioxidant use[140]. **Table(3 -3B)** demonstrate In individuals with beta thalassemia major, the total antioxidant in their sera was compared to a healthy control group.

Table (3-3 B): Total antioxidant levels (µmol/L) in sera of patients with beta-thalassemia major and healthy control subjects.

Group	*n.*	Mean	Std. Deviation	Std. Error	Sign.
Control	150	949.77	103.09	8.42	---
Patients	150	700.32	100.25	8.19	0.01*

*: in comparison to group I (Healthy donors).

3.4. Vitamin E concentrations

In this investigation, there is a very significant reduction of serum vitamin E ($p<0.011$). Vitamin E is important for protecting cells from oxidative damage. Vitamin E's antioxidant activity is linked to its capacity to donate hydrogen to a highly reactive lipid peroxide intermediate, preventing hydrogen extraction from Poly Unsaturated

Fatty Acid PUFA. This helps to keep the self-perpetuating lipid peroxidation chain reaction at bay [141].

According to our findings, oxidative stress may be a substantial contributor to hemolysis in beta thalassemia major. Antioxidant therapy using specific antioxidants like vitamin E might be a viable strategy to combat oxidative stress[142]. **Table (3-4)** compares Vitamin E levels in the sera of β-thalassemia major patients to healthy controls.

Table(3-4): Vitamin E (mg/L) in sera of patients with beta- thalassemia major and healthy control subjects.

Group	*n.*	Mean	Std. Deviation	Std. Error	Sign.
Control	150	10.73	5.58	0.46	---
Patients	150	8.98	6.27	0.51	0.011*

*: in comparison to group I (Healthy donors).

3.5. Glutathione (GSH) concentrations

Glutathione depletion in patients with β-thalassemia major compared to healthy persons. The most common thiol-containing peptide found in the liver, spleen, kidneys, erythrocytes, and eye lens is reduced glutathione (γ-L-glutamyl-L-cysteinylglycine, GSH). Because of its high abundance in cells and great electron-donation potential through the sulfhydryl groups of cysteine residues, it is the principal molecule for cellular redox maintenance [143]. GSH gives reducing equivalents to free-radical scavenging enzymes such as glutathione peroxidase (GPx) and glutathione-S-transferase (GST) in response to oxidative stress, and transforms to its oxidized state (GSSG). This GSSG might be converted to GSH via a glutathione reductase (GR)-catalyzed mechanism. As a

consequence, a lower ratio of reduced to oxidized glutathione (GSH/GSSG) in cells might indicate more oxidative stress[144,145]. **Table (3-5)** compares glutathione levels in beta thalassemia major patients to healthy controls.

Table (3-5): Glutathione (µmol/L) in sera of patients with beta-thalassemia major and healthy control subjects.

Group	*n.*	Mean	Std. Deviation	Std. Error	Sign.
Control	150	23.18	5.08	0.46	---
Patients	150	18.74	4.75	0.19	0.01*

*: in comparison to group I (Healthy donors).

3.6. Malondialdehyde concentrations

β- thalassemia major patients had higher levels of oxidized lipids than healthy persons. Malondialdehyde (MDA), a lipid peroxidation product, is produced in additional in thalassemia, indicating that thalassemic erythrocytes contain substantial levels of membrane bound iron. MDA is a bifunctional reagent that has been shown to crosslink a variety of cell components, including membrane components. [146] The stiffness of thalassemic erythrocytes deformability is a primary predictor of anemia in thalassemia, which might explain why a cross-linked erythrocyte membrane is predicted to be inflexible. [147-148], resulting in a decrease in RBC deformability and an increase in RBC membrane rigidity [149-150]. The reticuloendothelial system (RES) relies heavily on lipid peroxidation to remove RBCs. It has been found to change the asymmetry of membrane phospholipids, which is a key factor in macrophage identification of RBCs [150-151]. Furthermore, RBCs with aberrant lipid distribution in *vitro* were phagocytosed four times faster

than control RBCs [152]. In **Table(3-6)**, malondialdehyde levels in sera of beta thalassemia major patients were compared to healthy controls.

Table (3-6): Malondialdehyde (µmol/L) in sera of patients with beta-thalassemia major and healthy control subjects.

Group	*n.*	Mean	Std. Deviation	Std. Error	Sign.
Control	150	2.89	0.92	0.08	---
Patients	150	3.96	1.05	0.09	0.01*

*: in comparison to group I (Healthy donors).

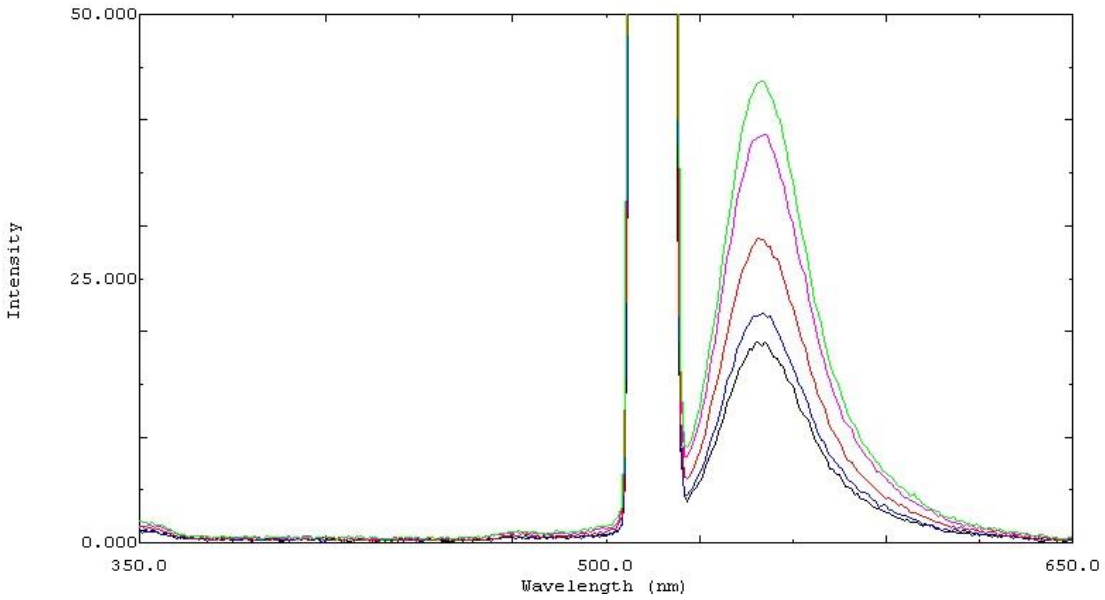

Figure 3-1 : Fluorescence of MDA

3.7. Modified CUPRAC method for assessment of XOI

This study presents a simple protocol for evaluating XOI activity using the CUPRAC method. The protocol depends on the reduction of ($Cu(Nc)_2^{2+}$) to a brightly colored Cu(I)-neocuproine complex ($Cu(Nc)_2^{+}$)

by XO products (uric acid and hydrogen peroxide); the resulting solution was measured by spectrophotometry at 450 nm. XO activity is related to the incremental absorbance. In **Figure 3-2**, the proposed assay is based on XO products used to measure XO activity.

The resulting CUPRAC complex ($Cu(Nc)_2^+$) produces a single peak at 450 nm. The absorbance was proportional to the concentration of uric acid and hydrogen peroxide formed as a result of XO activity **Figure 3-3**. The number of micromoles of uric acid or hydrogen peroxide generated per unit time represents one unit of XO enzyme.

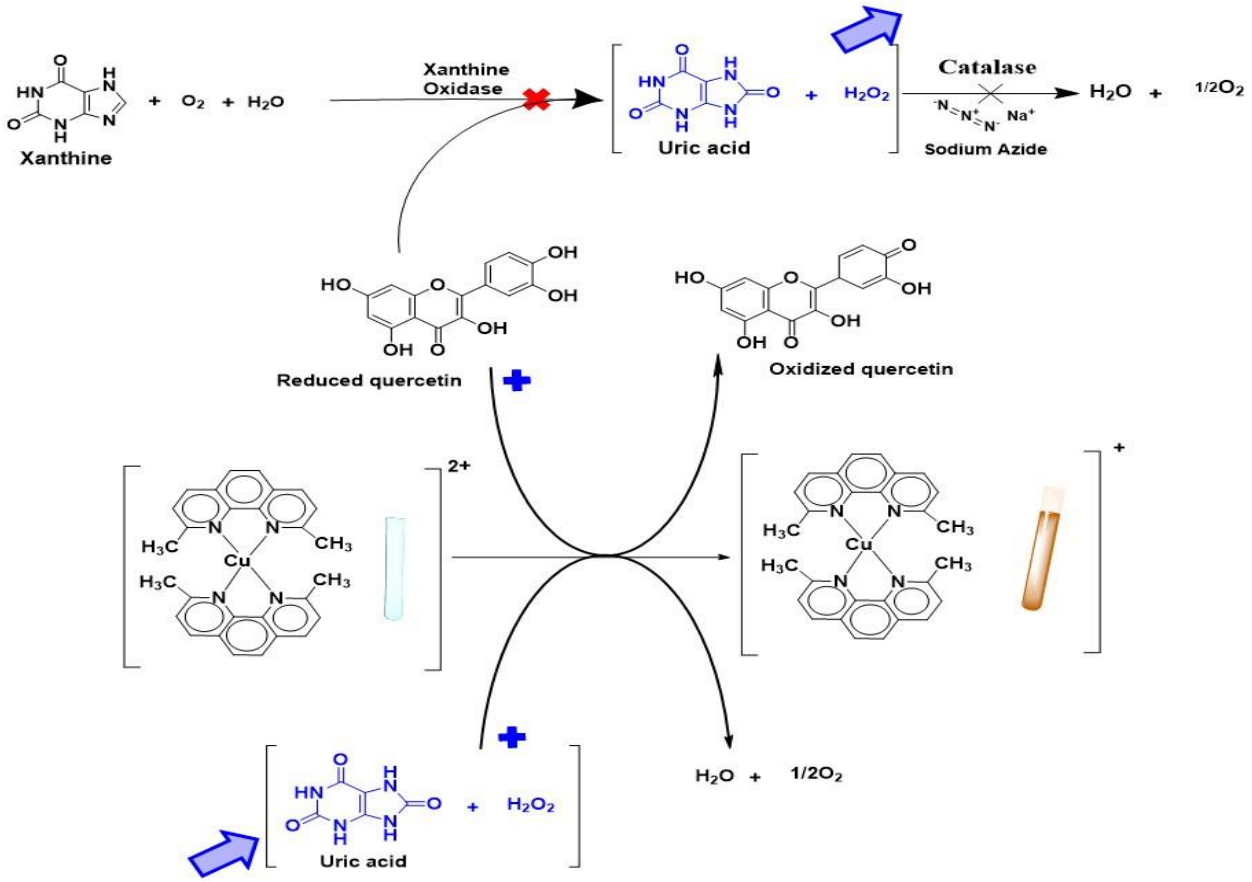

Figure 3-2: Scheme Cu(I)-neocuproine chelate (λmax = 450 nm) is formed by the interaction of Cu(II)-neocuproine complex with uric acid and hydrogen peroxide.

✚ Refers to compounds that cause an increase in absorbance.

✖ Refers to compounds that cause a decrease in absorbance.

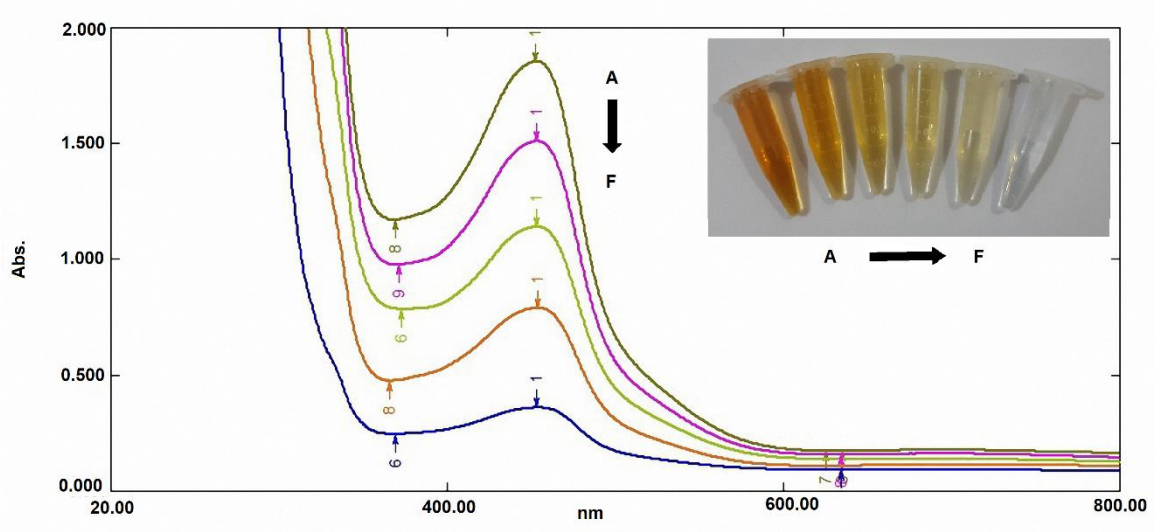

Figure 3-3: Spectrophotometric characteristics of the resulting Cu(I)-neocuproine complex ($Cu(Nc)_2^+$) were shown to be associated with XO enzyme activity. Absorption spectra were obtained by reducing ($Cu(Nc)_2^{2+}$) to a brightly colored Cu(I)-neocuproine complex ($Cu(Nc)_2^+$) as a result of the formation of hydrogen peroxide and uric acid from the XO enzyme reaction. The resulting complex was measured by spectrophotometer at 450 nm: (a to f) represent (100, 80, 60, 40, 20) µM uric acid and hydrogen peroxide, respectively.

The method is originally described by Özyürek *et al*. [153] to assess XOIs. The modified protocol considers two types of interference; the first is caused by the presence of the catalase enzyme, which breaks down hydrogen peroxide resulting from XO activity. After studying the key role of catalase in the resulting CUPRAC color, Özyürek et al. [153] concluded that the presence of catalase disrupted the absorbance signal as a result of Cu(I)–Nc. With high catalase activity, the CUPRAC peak produced by the presence of hydrogen peroxide may be totally suppressed. Özyürek et al. [152] reported that the CUPRAC method may be used to evaluate a possible XOI by assessing the CUPRAC absorbance of the xanthine-xanthine oxidase (X–XO) conversion products without hydrogen peroxide degradation. Despite the conclusions reached in the study, the interference of catalase present in fresh plant samples remained, and was used to assess XO inhibition activity. The current method avoided catalase interference by using sodium azide as a selective

inhibitor, as shown in **Figure 3-2**. Sodium azide was used effectively to prevent catalase interference in XO assessment [154].

The second interference is attributed to natural products such as polyphenols used to examine inhibition of the XO enzyme. Antioxidants such as polyphenols react with the CUPRAC reagent to produce the same color that results from reaction with the products of XO enzyme activity (uric acid and hydrogen peroxide).

Antioxidant interference that occurs with the XOI–CUPRAC method is easily prevented. Two test tubes are used: one with an enzymatic reaction time equal to 0 min (t_0), and the other with an enzymatic reaction time equal to 30 min (t_{30}). The use of a correction test tube (t_0) is necessary to eliminate interference caused by the presence of antioxidants in the sample. In the protocol, the test tube absorbance (t_{30}) is related to two types of compounds: products of XO enzymatic activity, hydrogen peroxide and uric acid, and antioxidants used to inhibit XO activity. The absorbance of the correction test tube (t_0) in the protocol was attributable only to antioxidants used to examine XO inhibition activity. We prevented interference of any substance that would change the CUPRAC reagent absorbance by subtracting the absorbance of the correction test tube (t_0) from the absorbance of the other test tube (t_{30}). This suggests that the residual absorbance is due to products of XO enzymatic activity, hydrogen peroxide and uric acid.

3.7.1 Validation and reproducibility

The modified CUPRAC procedure was validated by comparing the XO-inhibitory activity of herbal extracts as IC50 values in the X–XO reaction solution with matched samples using both suggested and reference methods. Five plant extracts rich in polyphenols were prepared

using a home blender. Fresh leaves (50 g) were mixed with buffer phosphate solution (950 ml, pH 7.8), and the final volume was adjusted to 1 L. The total polyphenol concentration was estimated using a spectrophotometric method. A series of concentrations were prepared for each extract depending on their polyphenol concentration. All plant extracts exhibited a positive result for the catalase enzyme; activity was measured using the aniline–hydroquinone method [79]. The ability of fresh plant extracts to inhibit XO enzyme was tested.

Table (3-7) indicates that the results of the proposed protocol were strongly associated with the results of the UV protocol [155]. The t-test analysis results confirmed that the current method is similar to the reference method. With the same quantities of plant extracts, the XO activity determined using the CUPRAC protocol was almost equal to that reported using the UV protocol.

Table (3-7) The XOI activity using the CUPRAC protocol (as IC50 values in g.mL^{-1}) was compared with the values obtained using the UV method on the same samples.

Type of extract	XOI activity (IC50 µg mL^{-1}) for herbal samples	
	Modified CUPRAC method	UV method
	Mean ± SD (RSD%)	Mean ± SD (RSD%)
Trigonella spp.	12.07 ± 0.57	11.25 ± 1.25
Portulaca grandiflora	13.71 ± 1.25	11.55 ± 1.4
Myrtus communis	14.35 ± 0.95	15.55 ± 1.35
Passiflora caerulea	14.75 ± 0.75	15.8 ± 1.25
Hibiscus sabdariffa	11.25 ± 0.65	11.77 ± 1.35
Trigonella spp.	12.55 ± 0.75	13.25± 1.25

3.7.2 Validation

The Bland–Altman analysis [156] is used to compare the XOI–CUPRAC method and the UV method. For mathematical studies, the QiMacros application (Know Ware International, Denver, USA) is used

with Microsoft Excel 2016. Series dilutions of fresh extract of roselle leaves *(Hibiscus sabdariffa L.)* are used to apply the Bland–Altman analysis. Polyphenol concentration varied from 0.5–20 µg gallic acid equivalent per ml. The Bland–Altman plot shows comparative differences between the XOI–CUPRAC and UV methods, and indicates the mean relative bias **Figure 3-4**. The correlation coefficient between the two protocols was 0.9935. Thus, the XOI–CUPRAC method is nearly as accurate as the reference procedure. Passing–Bablok similarity analysis revealed a strong association between the XOI-CUPRAC method and the UV protocol **Figure 3-5**.

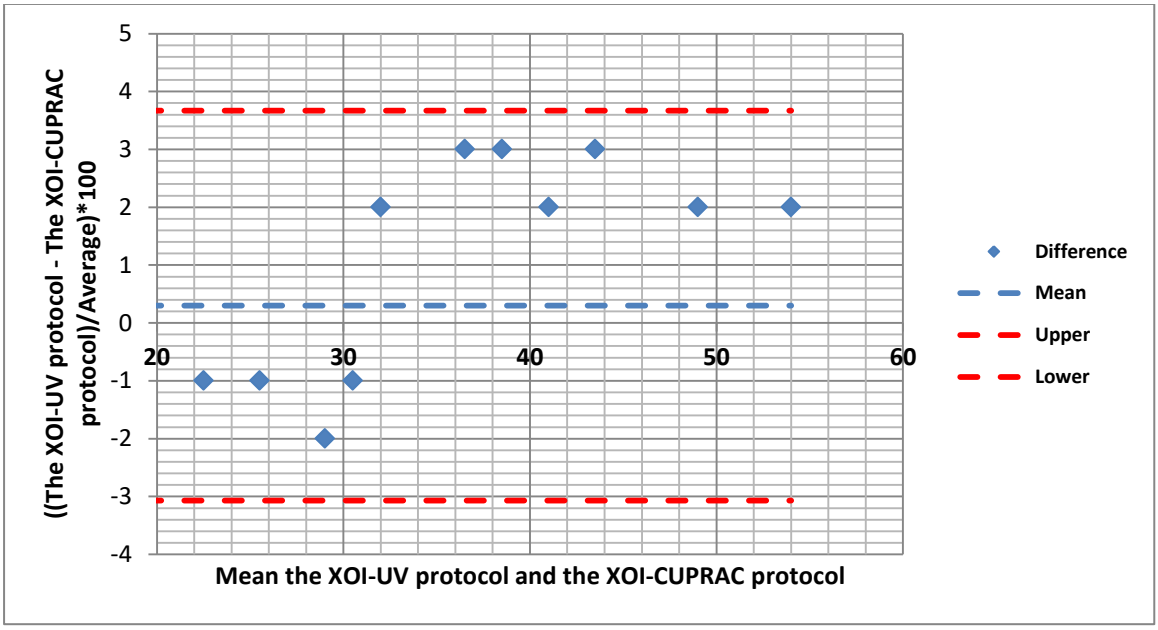

Figure 3-4: The Bland–Altman plot represents the relative differences in the XOI–CUPRAC method and UV protocol, as well as the mean relative bias.

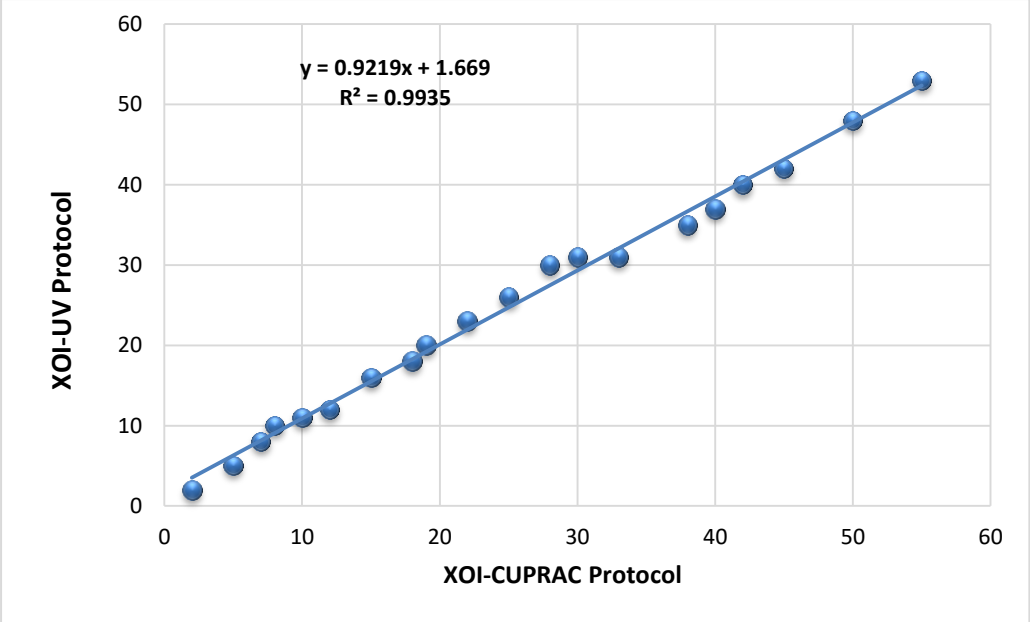

Figure 3-5: XOI activities were assessed using the XOI-CUPRAC method and UV protocol over a series of fresh extract dilutions of roselle leaves *(Hibiscus sabdariffa L.)* as an XOI.

From the results shown in **Figure 3-5**, the linearity of the XOI–CUPRAC method was compatible with that of the UV protocol. The LOQ 1% XOI and LOD 3% XOI results confirmed the high sensitivity of the modified XOI–CUPRAC method. The linearity of the XOI–CUPRAC method was comparable with that of the UV protocol. The XOI–CUPRAC method has many advantages over the UV protocol.

3. 8. Glutathione peroxidase 4 concentrations

Table (3-8) shows that the GPX4 activity rate for β- thalassemia major patients was significantly lower than the GPX4 activity rate for the control group. Glutathione peroxidase 4 (GPX4) is one of just a few enzymes that can decrease lipid peroxidation products in biological membranes in vivo [157]. Lipoxygenases at certain places cause lipid peroxidation enzymatically, whereas non-enzymatic processes, generally Fe^{2+}-driven Fenton chemistry, do it unselectively [158]. Lipoxygenases

are dioxygenases that catalyze the incorporation of molecular oxygen into polyunsaturated fatty acids (PUFA), resulting in the formation of hydroxyperoxides.Low quantities of peroxides (the so-called "peroxide tone") activate lipoxygenases by oxidizing Fe^{2+} to Fe^{3+} at the catalytic site [159]. GPX4 regulates the peroxide tone and the activity of lipoxygenases. 12/15-Lipoxygenase and GPX4 are antagonistic in terms of substrate oxidation (lipoxygenases) and reduction (GPX4), as well as cell death and survival induction.

In murine fibroblasts, 12/15-lipoxygenase causes cell death, but GPX4 protects cells against lipoxygenase-induced cell death [160]. In additional cases, lipoxygenases and GPX4 collaborate biochemically: Lipoxygenases create unsaturated fatty acid peroxidation products (P-O-O-H), which are highly reactive and prone to uncontrolled lipid membrane peroxidation. GPX4 reduces these peroxides to stable hydroxyl-derivatives (P-O-H) [161-162]. As a consequence, 15-lipoxygenase in humans and 12/15-lipoxygenase in mice, as well as GPX4, create a pair of enzymes with very similar functions[160-162]. Vitamin E's role in the interaction between lipoxygenases and GPX4 must also be investigated.

Table (3-8): Glutathione peroxidase 4 (ng/mL) in sera of patients with beta-thalassemia major and healthy control subjects.

Group	*n.*	Mean	Std. Deviation	Std. Error	Sign.
Control	150	7.7827	5.16735	.42191	---
Patients	150	5.7375	3.39288	.27703	0.01*

*: in comparison to group I (Healthy donors).

3.9. A simple chemical sensor for quantifying xanthine oxidase inhibition activity

3.9.1. The TMB method for assessment of XOI

This paper describes a simple chemical sensor for measuring XOI activity that uses a TMB-H_2O_2 system catalyzed by Cu^{2+}. The color intensity and absorbance were correlated with the amount of H_2O_2 formed by XO activity **Figure 3-6**. One unit of XO enzyme is defined as the number of micromoles of H_2O_2 produced per unit of time. As illustrated in **Figure 3-7**, the present method used sodium azide to prevent catalase enzyme interference. Cu^{2+} has been shown to catalyze TMB oxidation by H_2O_2 [163]. TMB oxidation by H_2O_2 forms a charge transfer complex with a maximum absorbance at 652 nm. As illustrated in **Figure 3-7**, sulfuric acid was used to convert the color to a bright yellow end product with strong absorbance at 450 nm.

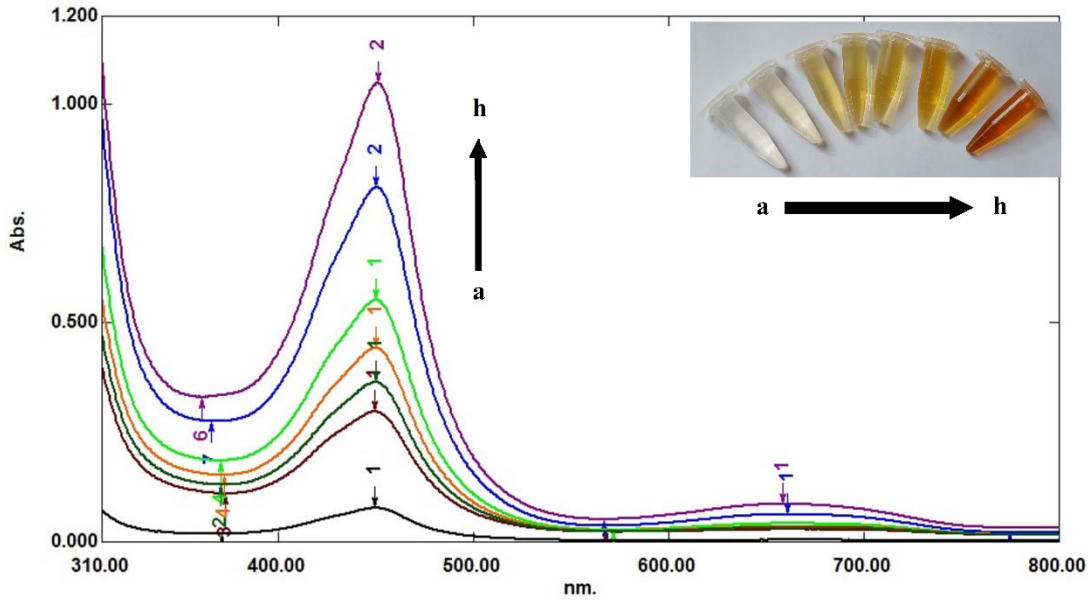

Figure 3-6: The spectrophotometric properties of the resulting diimine (dicatione) yellow product were correlated with XO activity. The color absorbance was correlated with the concentration of H_2O_2 produced by XO activity. The resulting complex was measured spectrophotometrically at 450 nm: (a-g) represent 60, 50, 40, 35, 30, 25, and 5 U/L of XO enzyme activity, respectively.

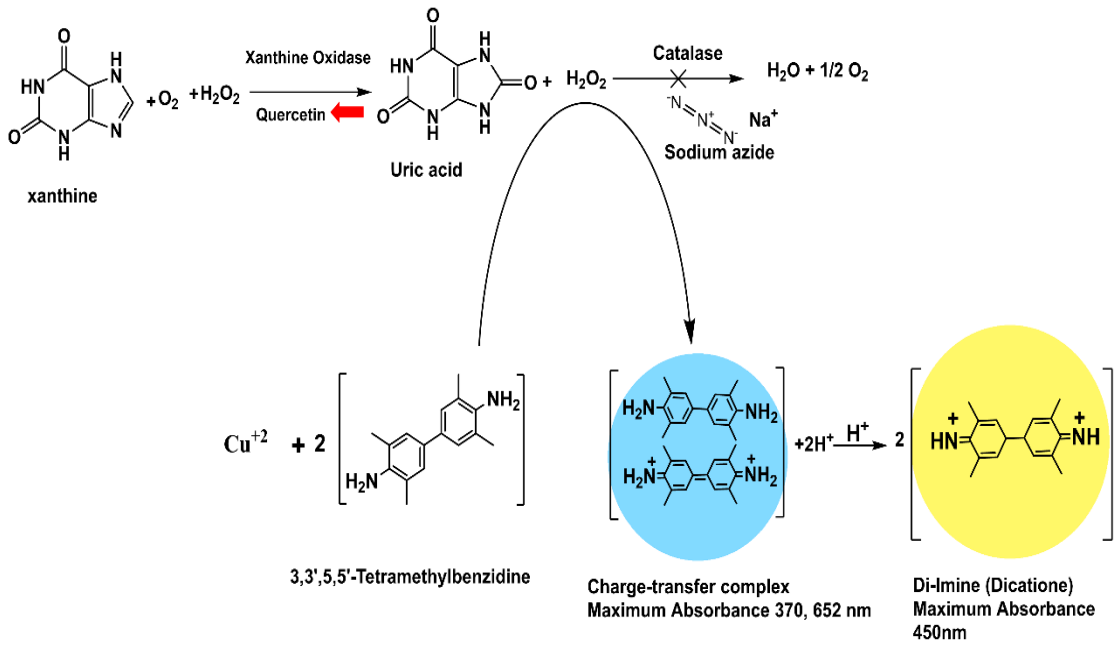

Figure 3-7:Scheme TMB oxidation by H_2O_2 produces a charge transfer complex with a maximum absorbance at 652 nm. Its color was converted to a brilliant yellow final product with strong absorption at 450 nm using sulfuric acid. H_2O_2 forms as a consequence of XO activity. Sodium azide was used to inhibit the catalase enzyme and prevent H_2O_2 consumption.

3.9.2. Optimization of the TMB-XO assay

Statistical applications were used for the BBD [164] to optimize reagent concentrations. According to the TMB-XO assay, the BBD is an excellent evaluating instrument to adjust the TMB and Cu^{2+} concentrations and incubation time to achieve optimal XO activity. **Table (3-9)** illustrates the regression model for the TMB-XO assay derived from the RSM's analysis of variance (ANOVA). The resulting F-value (9.92) indicates that the model was significant. However, the F-value for lack-of-fitness (11.03) showed that it was not significant. These findings indicate that the suggested model relationships were significant (p = 0.0032). The coefficient for the practical experiment's predicted response (predicted R^2 = 0.9237) was in reasonable agreement with the adjusted

response (adjusted R^2 = 0.9975). An ANOVA of the TMB-XO assay showed the actual association between the three independent variables of the proposed model. The associations were extremely significant and acceptable for this application. Contour graphs and three-dimensional (3D) BBD were used to examine the relationship between the three independent variables. The development of the graphs at their midpoint depended on the combination of two components when the third component was constant. The response plot in **Figure 3-8** shows the interactions between the parameters (TMB and Cu^{2+} concentrations and incubation time; **Figure 3-8(a-f)**. All of the graphs show considerable curvature.

The highest XO activity of 50 ± 2 $U.L^{-1}$ was obtained at optimum experimental conditions of 10 mmol L^{-1} Cu^{+2}, 6 mmol L^{-1} TMB, and a 30-minute incubation time. The obtained results aligned well with the expected XO activity, indicating that the RSM investigation was suitable and matched significantly with laboratory requirements.

Table (3-9): ANOVA results for the TMB-XO assay's experimental variables.

	Sum of squares	Degree of freedom	**Mean square**	**F-value**	**p-value**
Regression	243.6	9	27.0067	9.92	0.0032
Residual	19.057	7	2.7224		
Lack-of-fit	397.9751	5	3.6781	11.03	0.0852
Pure error	0.67	2	0.333		
Total	262.12	16			
R^2	0.9237				
Explainable R^2	0.9975				

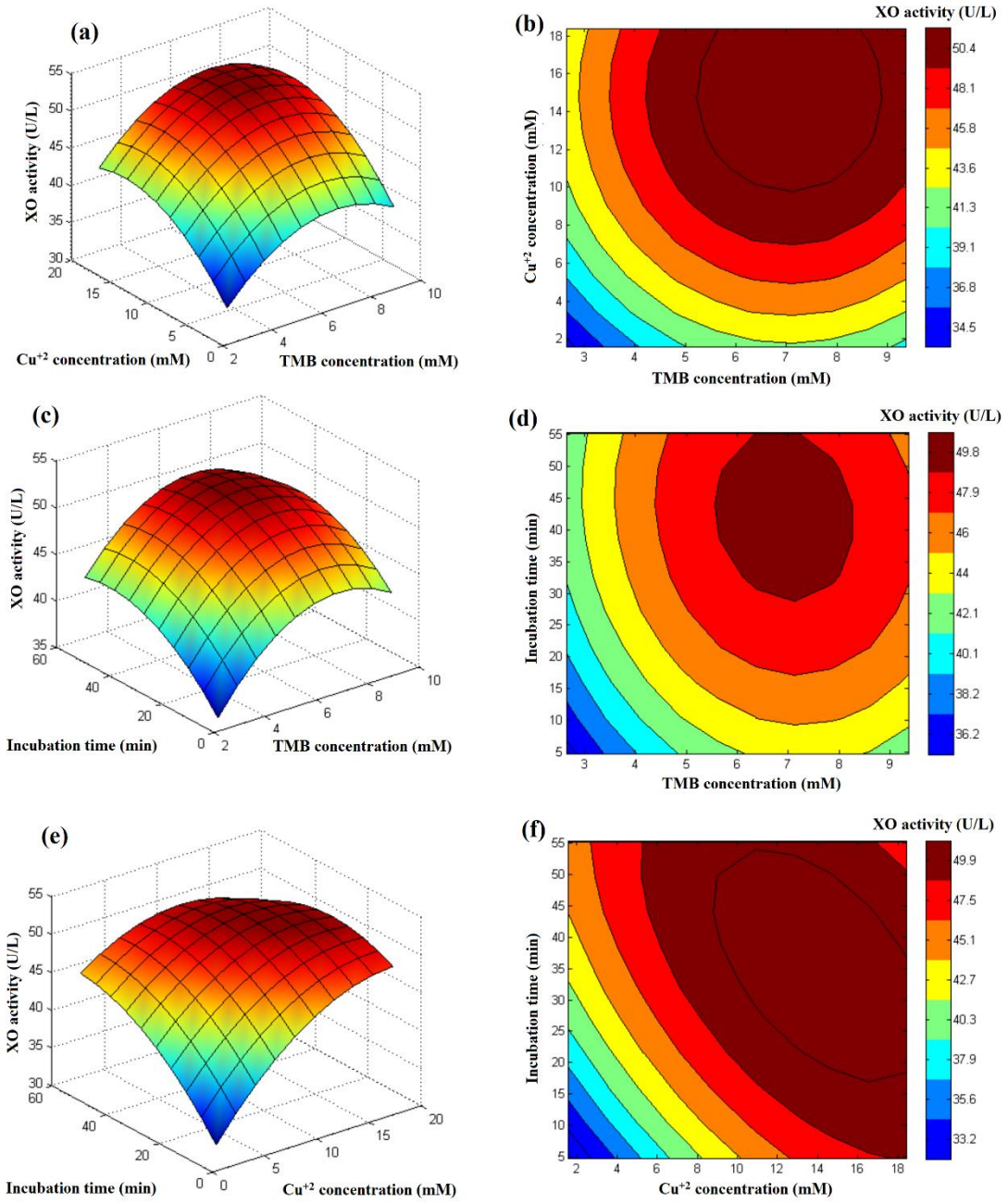

Figure 3-8: Graphs of 3D surface plots and contours showing the relationships between TMB concentration, Cu^{2+} concentration, and incubation time.

3.9.3. Signal stability

This study's observations of the colored compound indicated that it is remarkably stable at 25°C. Our measurements show that the diimine (dicatione) absorbance at 450 nm was remarkably constant for one day.

However, the absorbance decreased by 5% on the second day and 20% on the third day.

3.9.4. Sensitivity and linearity

The TMB-XO assay was linear across the range of 0.1–60 U L^{-1} of XO enzyme activity (Pearson's r = 0.998; **Figure 3-9**. The low values obtained for LOQ (0.1 U L^{-1}) and LOD (0.24 U L^{-1}) indicated the remarkable sensitivity of the TMB-XO assay. This assay's linearity was evaluated compared to the ABTS assay [79].

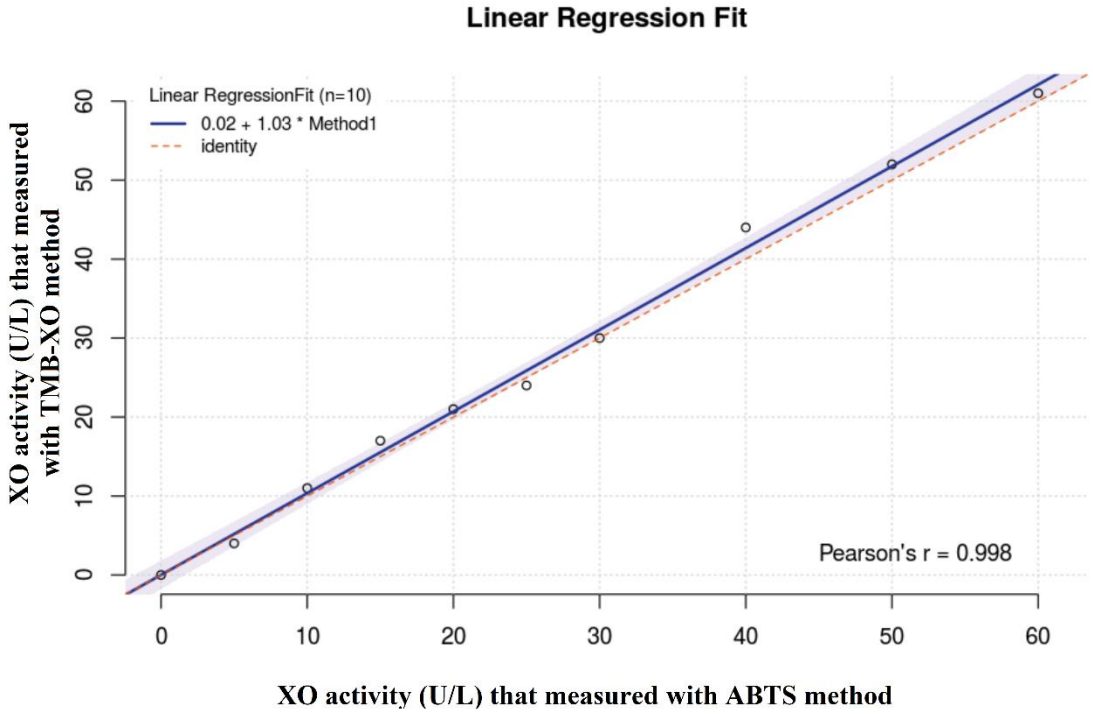

Figure 3-9: **The linearity of the investigated protocol was confirmed by drawing a straight line through the TMB-XO and ABTS assay results for various XO activity dilutions.**

3.9.5. Accuracy, reproducibility, and selectivity of the TMB-XO assay

Table (3-10) indicates the recovery values for each potentially interfering biochemical combination, showing that the proposed TMB-XO assay is suitable for measuring XO activity in the presence of interfering chemicals. In this procedure, 1 mL of 50 U L^{-1} XO was mixed with 1 mL aliquots of potentially interfering biochemical solutions. The

total XO activity was adjusted to 25 U L^{-1} using the UV method [112]. **Table (3-10)** shows the relationship between interfering biomolecules and relative percentage errors.

Table (3-10): Relationship between relative percentage errors and interfering biomolecules while measuring XO activity using the TMB-XO assay.

	Added XO U/l	Found XO U/l	Relative error (%)
Flask#1	25	25	0.00
Flask#2	25	24.5	-2.0
Flask#3	25	25.3	1.2
Flask#4	25	24.7	-1.2

3.9.6. Validation and reproducibility

The new TMB-XO assay was confirmed to be accurate by comparing the XOI activity of herbal extracts as half maximal inhibitory concentration (IC_{50}) values in the xanthine-XO reaction solution with matched samples using both suggested and reference methods. The catalase enzyme was present in all plant extracts, and its activity was assessed using the pyrogallol red protocol [165]. Fresh plant extracts were examined for their capacity to inhibit the XO enzyme. **Table (3-11)** shows that the proposed protocol's results aligned well with those of the UV method [112]. A t-test analysis indicated that the suggested chemical sensor and the reference method are compatible. The XOI activities quantified by the TMB-XO assay and the UV method were practically identical when similar concentrations of plant extracts were used.

Table (3-11): XOI activity levels with the TMB-XO assay and UV method with the same materials.

Type of extract	XOI activity (IC50 µg mL^{-1}) for herbal samples	
	The TMB-XO method	UV method
	Mean ± SD (RSD%)	Mean ± SD (RSD%)
Acacia iraqensis Rech.f.	13.25 ± 0.5	13.25 ± 1.02
Olea europaea L.	14.22 ± 0.7	14.75 ± 0.75
Lolium rigidum	15.25 ± 0.75	15.8 ± 1.03
Malva parvifLora	14.11 ± 0.8	15.2 ± 0.85
Medicago hispida	12.35 ± 0.55	12.5 ± 0.75
Trifolium resupinatum	13.05 ± 0.6	13.8 ± 0.5
Catechin *	2.15 ± 0.15	2.18 ± 0.19
Quercetin *	2.5 ± 0.15	2.65 ± 0.17

* IC_{50} values are presented in µg.mL^{-1}.

3.9.7. Method comparison

The TMB-XO assay and the UV method were compared using the Bland-Altman approach [128] performed using series dilutions of fresh extract of *roselle (Mentha pulegium L.) leaves*. Polyphenol concentrations ranged between 0.5 and 20 µg gallic acid equivalent per mL. The Bland-Altman graph illustrates the mean relative bias and the relative differences between the TMB-XO and UV methods **Figure 3-10**. The correlation between the two methods was 99.35%. This finding suggests that the TMB-XO assay is almost as accurate as the reference standard. The Passing-Bablok similarity analysis also indicated a strong relationship between the TMB-XO assay and the UV method **Figure 3-11**.

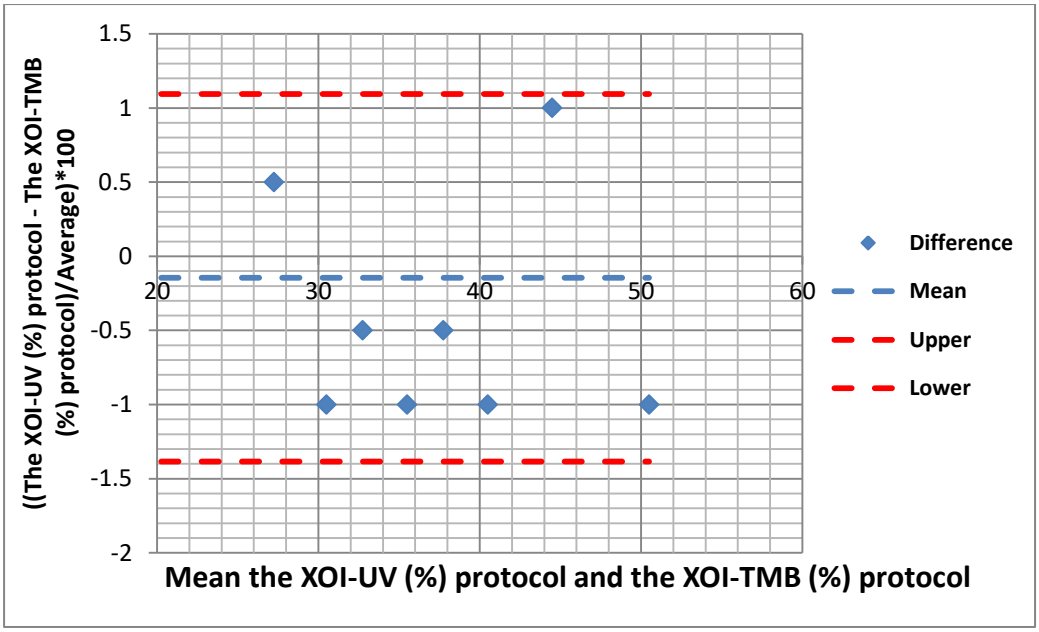

Figure 3-10: A Bland-Altman plot showing the mean relative bias and relative differences of XOI (%) determined with the TMB-XO assay and UV method.

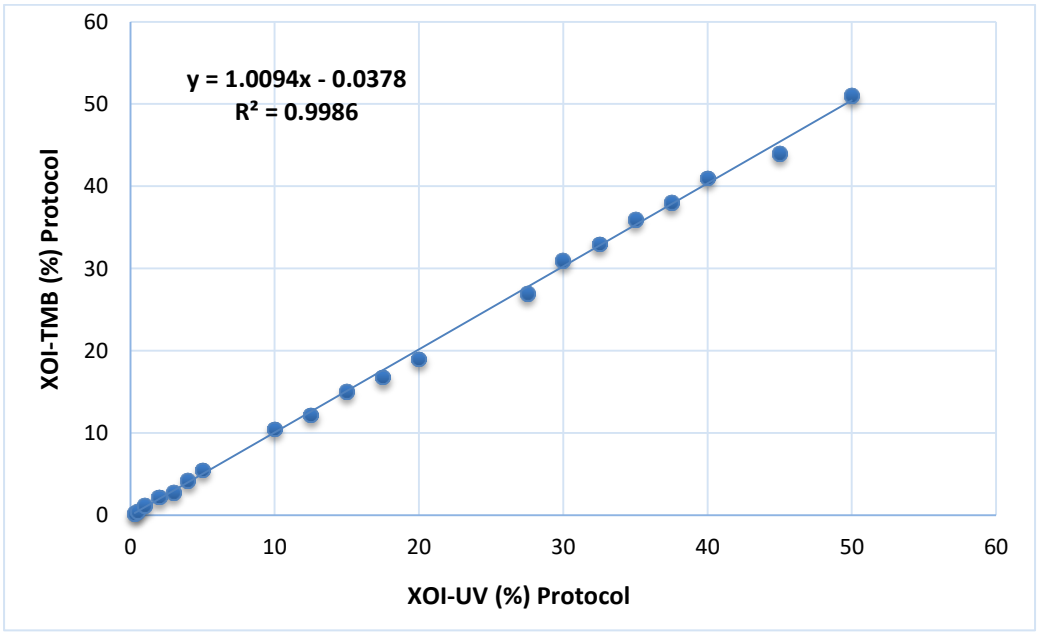

Figure 3-11: The TMB-XO assay and UV method were used to evaluate the XOI activity of *roselle leaves (Hibiscus sabdariffa L.)* over a series of fresh extract dilutions.

The new TMB-XO method has multiple advantages that distinguish it from earlier methods. The current sensor can be used for measurements in spectrophotometric cuvettes or 96 microplates. TMB is used as an effective sensor to quantify XO enzymatic activity. TMB

showed the greatest sensitivity [166-167], with more brilliant colored products and higher oxidation product stability than existing benzidine substrates used in peroxidase-based assays, reflecting its reputation as the preferred chemical probe in spectrophotometric protocols. Furthermore, TMB and its oxidation products are typically more stable than others, allowing their use in quantitative and semiquantitative (naked eye) spectrophotometric experiments. Therefore, the selected TMB substrate correlates with its molecular characteristics, analytical performance, and low toxicity [167].

Conclusions

It is concluded that : -

1- This study highlights a simple method for evaluating XOI activity using only a few steps. This procedure may be used to evaluate XOI activity in different types of biological samples with high concentrations of interfering chemicals.

2- Beta –Thalassemia major complications are associated with increment reactive oxygen species concentration and decrement total antioxidant levels.

3- The complications of β- thalassemia major are associated with an increase in lipid peroxide concentration in patients compared to healthy controls.

4- The xanthine oxidase activity level is studied, and the results of the study indicated to significant increase ($p < 0.05$) in xanthine oxidase activity concentration in all group of study patients with β-thalassemia major and comparable to healthy control persons [3.8811 U\ L] in patients with β- thalassemia major increased significantly to be [4.7115 U\ L]. This would be an important link between β-thalassemia major and vascular disease and other diseases.

5- This study proposed a simple chemical sensor for monitoring XO activity in a few simple steps. This method can assess XOI activity in various biological samples containing high concentrations of interfering substances.

Recommendations

The study recommends the following: -

1- Studies related to the enzyme xanthine oxidase in general are large and because it is one of the most important enzymes that produce free radicals, we recommend intensifying the study to know the important roles of this enzyme more broadly.

2- In the current study, the focus was on the relationship of the enzyme xanthine oxidase with patients with beta- thalassemia, so it is important to focus on studying the effect of other sources of free radicals on the work of the enzyme.

3- We recommend that beta- thalassemia patients take vitamin E as well as eat more vegetables and fruits that are antioxidants to balance or get rid of reactive oxygen species.

4- Stay away from external sources that cause an increase in reactive oxygen species such as pollution, smoking, radiation and others.

References

References

1. Lai K, Huang G, Su L, He Y. The prevalence of thalassemia in mainland China: evidence from epidemiological surveys. Scientific reports. 2017 Apr 19;7(1):1-1.

2. Neuman MG. Hepatotoxicity: mechanisms of liver injury. InLiver Diseases 2020 (pp. 75-84). Springer, Cham.

3. Adav SS, Wei J, Qian J, Gan NY, Yip LW, Sze SK. Aqueous humor protein dysregulation in primary angle-closure glaucoma. International Ophthalmology. 2019 Apr;39(4):861-71.

4. Belhoul KM, Bakir ML, Saned MS, Kadhim A, Musallam KM, Taher AT. Serum ferritin levels and endocrinopathy in medically treated patients with β thalassemia major. Annals of hematology. 2012 Jul;91(7):1107-14.

5. Abdul-RedhaIsmaiel M. Relationship between Oxidative Stress and the Blood Iron Concentration and Antioxidant Status in Major ß-thalassemia in Iraq. Archives of Razi Institute. 2022 Feb;77(1):187.

6. Jayachandran A, Shrestha R, Bridle KR, Crawford DH. Association between hereditary hemochromatosis and hepatocellular carcinoma: A comprehensive review. Hepatoma Research. 2020 Mar 6;6:8.

7. Fibach E, Dana M. Oxidative stress in β-thalassemia. Molecular diagnosis & therapy. 2019 Apr;23(2):245-61.

8. Kremastinos DT, Farmakis D, Aessopos A, Hahalis G, Hamodraka E, Tsiapras D, Keren A. β-thalassemia cardiomyopathy: history, present considerations, and future perspectives. Circulation: Heart Failure. 2010 May;3(3):451-8.

9. Kumfu S, Fucharoen S, Chattipakorn SC, Chattipakorn N. Cardiac complications in beta-thalassemia: From mice to men. Experimental Biology and Medicine. 2017 Jun;242(11):1126-35.

10. Thein SL. Genetic basis and genetic modifiers of β-thalassemia and sickle cell disease. Gene and Cell Therapies for Beta-Globinopathies. 2017:27-57.

11. Mettananda S, Higgs DR. Molecular basis and genetic modifiers of thalassemia. Hematology/Oncology Clinics. 2018 Apr 1;32(2):177-91.

12. Zhang J, Peng J, Gao P, Huang H, Cao Y, Zheng L, Miao D. Relationship between meaning in life and death anxiety in the elderly: Self-esteem as a mediator. BMC geriatrics. 2019 Dec;19(1):1-8.

13. Aju BY, Rajalakshmi R, Mini S. Protective role of Moringa oleifera leaf extract on cardiac antioxidant status and lipid peroxidation in streptozotocin induced diabetic rats. Heliyon. 2019 Dec 1;5(12):e02935.

14. Petruk G, Del Giudice R, Rigano MM, Monti DM. Antioxidants from plants protect against skin photoaging. Oxidative medicine and cellular longevity. 2018 Aug 2;2018.

15. Udem GC, Dahiru D, Etteh CC. In vitro Antioxidant Activities of Aqueous and Ethanol Extracts of Mangifera indica Leaf, Stem-Bark and Root-Bark. Pharmacognosy Communications. 2018 Jul 1;8(3).

16. Pedro NF, Biselli JM, Maniglia JV, de Santi-Neto D, Pavarino ÉC, Goloni-Bertollo EM, Biselli-Chicote PM. Candidate biomarkers for oral squamous cell carcinoma: differential expression of oxidative stress-related genes. Asian Pacific journal of cancer prevention: APJCP. 2018;19(5):1343.

17. Saio V, Syiem D, Sharma R, Dkhar J. Amelioration of age-dependent increase in oxidative stress markers in male mice by extract of Potentilla fulgens. Redox Report. 2016 May 3;21(3):130-8.

18. Breininger SP, Malcomson FC, Afshar S, Turnbull DM, Greaves L, Mathers JC. Effects of obesity and weight loss on mitochondrial structure and function and implications for colorectal cancer risk. Proceedings of the Nutrition Society. 2019 Aug;78(3):426-37.

19. Chakraborty I, Sen IK, Mondal S, Rout D, Bhanja SK, Maity GN, Maity P. Bioactive polysaccharides from natural sources: A review on the antitumor and immunomodulating activities. Biocatalysis and Agricultural Biotechnology. 2019 Nov 1;22:101425.

20. Cuijpers I, Simmonds SJ, van Bilsen M, Czarnowska E, González Miqueo A, Heymans S, Kuhn AR, Mulder P, Ratajska A, Jones EA, Brakenhielm E. Microvascular and lymphatic dysfunction in HFpEF and its associated comorbidities. Basic Research in Cardiology. 2020 Jul;115(4):1-5.

21. Soltani S, Arablou T, Jayedi A, Salehi-Abargouei A. Adherence to the dietary approaches to stop hypertension (DASH) diet in relation to all-cause and cause-specific mortality: a systematic review and dose-response meta-analysis of prospective cohort studies. Nutrition journal. 2020 Dec;19(1):1-3.

22. Singh R. Current Alzheimer's management with berries fruits therapy. J pub health catalog. 2018; 1 (2): 17-24. J pub health catalog 2018 Volume 1 Issue. 2018;2.

23. Chen YM, Lucas PW, Wellburn AR. Relationship between foliar injury and changes in antioxidant levels in red and Norway spruce exposed to acidic mists. Environmental Pollution. 1991 Jan 1;69(1):1-5.

24. Shastri A, Srivastava R, Jyoti B, Gupta M. The antioxidants-scavengers of free radicals for immunity boosting and human health/overall well being. International Journal of Contemporary Medical Research. 2016;3(10):2918-23.

25. Govindan N, Maniam GP, Rahim MH, Sulaiman AZ, Ajit A. Biological macromolecules from algae and their antimicrobial applications. InBiological Macromolecules 2022 Jan 1 (pp. 203-217). Academic Press.

26. Navel V, Sapin V, Henrioux F, Blanchon L, Labbé A, Chiambaretta F, Baudouin C, Dutheil F. Oxidative and antioxidative stress markers in dry eye disease: A systematic review and meta-analysis. Acta Ophthalmologica. 2022 Feb;100(1):45-57.

27. Evans HC, Dinh TT, Hardcastle ML, Gilmore AA, Ugur MR, Hitit M, Jousan FD, Nicodemus MC, Memili E. Advancing semen evaluation using lipidomics. Frontiers in Veterinary Science. 2021 Apr 16;8:601794.

28. Kumar H, Rajpoot D, Kumar A, Sharma S, Kumar A. Solid Lipid Nanoparticles: A Strategy to Improve Oral Delivery of the Biopharmaceutics classification system (BCS) Class II Drugs. International Journal of Pharmaceutical & Biological Archives. 2018;9(4):204-15.

29. Wear D, Vegh C, Sandhu JK, Sikorska M, Cohen J, Pandey S. Ubisol-Q10, a Nanomicellar and Water-Dispersible Formulation of

Coenzyme-Q10 as a Potential Treatment for Alzheimer's and Parkinson's Disease. Antioxidants. 2021 May;10(5):764.

30. Kand'ár R, Žáková P, Mužáková V. Monitoring of antioxidant properties of uric acid in humans for a consideration measuring of levels of allantoin in plasma by liquid chromatography. Clinica Chimica Acta. 2006 Mar 1;365(1-2):249-56.

31. Steenvoorden DP, van Henegouwen GM. The use of endogenous antioxidants to improve photoprotection. Journal of Photochemistry and Photobiology B: Biology. 1997 Nov 1;41(1-2):1-0.

32. Röllin HB, Channa K, Olutola B, Nogueira C, Odland JØ. In utero exposure to aluminium and other neurotoxic elements in urban coastal south african women at delivery: An emerging concern. International Journal of Environmental Research and Public Health. 2020 Mar;17(5):1724.

33. Ferreira SS, Alves AJ, Filipe-Ribeiro L, Cosme F, Nunes FM. Holistic and sustainable approach for recycling and valorization of polyvinylpolypyrrolidone used in wine fining. ACS Sustainable Chemistry & Engineering. 2018 Sep 11;6(11):14599-606.

34. Alta'ee AH, Majeed HA, Hadwan MH. The levels of vitamin E in seminal fluids and their association with male infertility: Short review. Research Journal of Pharmacy and Technology. 2018;11(5):2152-6.

35. Pazyar N, Houshmand G, Yaghoobi R, Hemmati AA, Zeineli Z, Ghorbanzadeh B. Wound healing effects of topical Vitamin K: A randomized controlled trial. Indian journal of pharmacology. 2019 Mar;51(2):88.

36. Gogola D. Phytochemical Screening, Antioxidant and Gastro-Protective Activity Studies on the Fruit Peels of Selected Varieties of Banana. Herbal Medicines Journal (Herb Med J). 2020 Aug 26;5(2):45-59.

37. David AV, Arulmoli R, Parasuraman S. Overviews of biological importance of quercetin: A bioactive flavonoid. Pharmacognosy reviews. 2016 Jul;10(20):84.

38. Krimmel B, Swoboda F, Solar S, Reznicek G. OH-radical induced degradation of hydroxybenzoic-and hydroxycinnamic acids and formation of aromatic products—A gamma radiolysis study. Radiation Physics and Chemistry. 2010 Dec 1;79(12):1247-54.

39. YABALAK E. Radical scavenging activity and chemical composition of methanolic extract from Arum dioscoridis Sm. var. dioscoridis and determination of its mineral and trace elements. Journal of the Turkish Chemical Society Section A: Chemistry. 2018;5(1):205-18.

40. Jayedi A, Soltani S, Zargar MS, Khan TA, Shab-Bidar S. Central fatness and risk of all cause mortality: systematic review and dose-response meta-analysis of 72 prospective cohort studies. bmj. 2020 Sep 23;370.

41. Sotler R, Poljšak B, Dahmane R, Jukić T, Pavan Jukić D, Rotim C, Trebše P, Starc A. Prooxidant activities of antioxidants and their impact on health. Acta clinica Croatica. 2019 Dec 1;58(4.):726-36.

42. Challa HJ, Ameer MA, Uppaluri KR. DASH diet to stop hypertension. InStatPearls [Internet] 2021 May 19. StatPearls Publishing.

43. Detzel MS, Schmalohr BF, Steinbock F, Hopp MT, Ramoji A, George AA, Neugebauer U, Imhof D. Revisiting the interaction of heme with hemopexin. Biological Chemistry. 2021 May 1;402(6):675-91.

44. Vijayan V, Wagener FA, Immenschuh S. The macrophage heme-heme oxygenase-1 system and its role in inflammation. Biochemical pharmacology. 2018 Jul 1;153:159-67.

45. Schmidt HM, Kelley EE, Straub AC. The impact of xanthine oxidase (XO) on hemolytic diseases. Redox biology. 2019 Feb 1;21:101072.

46. Gbotosho OT, Kapetanaki MG, Kato GJ. The worst things in life are free: The role of free heme in sickle cell disease. Frontiers in Immunology. 2021 Jan 27;11:561917.

47. Tatipamula VB, Kukavica B. Protective effects of extracts of lichen Dirinaria consimilis (Stirton) DD Awasthi in bifenthrin-and diazinon-induced oxidative stress in rat erythrocytes in vitro. Drug and Chemical Toxicology. 2022 Mar 4;45(2):680-7.

48. Belcher JD, Chen C, Nguyen J, Abdulla F, Zhang P, Nguyen H, Nguyen P, Killeen T, Miescher SM, Brinkman N, Nath KA. Haptoglobin and hemopexin inhibit vaso-occlusion and inflammation in murine sickle cell disease: Role of heme oxygenase-1 induction. PloS one. 2018 Apr 25;13(4):e0196455.

49. Pinheiro AK, Pereira DA, Dos Santos JL, Calmasini FB, Alexandre EC, Reis LO, Burnett AL, Costa FF, Silva FH. Resveratrol-nitric oxide donor hybrid effect on priapism in sickle cell and nitric oxide-deficient mouse. PloS one. 2022 Jun 2;17(6):e0269310.

50. Wang Y, Zhao M, Xu B, Bahriz SM, Zhu C, Jovanovic A, Ni H, Jacobi A, Kaludercic N, Di Lisa F, Hell JW. Monoamine oxidase A and

organic cation transporter 3 coordinate intracellular β1AR signaling to calibrate cardiac contractile function. Basic research in cardiology. 2022 Dec;117(1):1-20.

51. Nokkaew N, Mongkolpathumrat P, Junsiri R, Jindaluang S, Tualamun N, Manphatthanakan N, Saleesee N, Intasang M, Sanit J, Adulyaritthikul P, Kongpol K. p38 MAPK inhibitor (SB203580) and metformin reduces aortic protein carbonyl and inflammation in non-obese type 2 diabetic rats. Indian Journal of Clinical Biochemistry. 2021 Apr;36(2):228-34.

52. Jang T, Poplawska M, Cimpeanu E, Mo G, Dutta D, Lim SH. Vaso-occlusive crisis in sickle cell disease: a vicious cycle of secondary events. Journal of Translational Medicine. 2021 Dec;19(1):1-1.

53. Ohshima H, Bartsch H. Chronic infections and inflammatory processes as cancer risk factors: possible role of nitric oxide in carcinogenesis. Mutation Research/Fundamental and Molecular Mechanisms of Mutagenesis. 1994 Mar 1;305(2):253-64.

54. McCarthy MK, Reynoso GV, Winkler ES, Mack M, Diamond MS, Hickman HD, Morrison TE. MyD88-dependent influx of monocytes and neutrophils impairs lymph node B cell responses to chikungunya virus infection via Irf5, Nos2 and Nox2. PLoS pathogens. 2020 Jan 30;16(1):e1008292.

55. Day RO, Kannangara DR, Stocker SL, Carland JE, Williams KM, Graham GG. Allopurinol: insights from studies of dose–response relationships. Expert opinion on drug metabolism & toxicology. 2017 Apr 3;13(4):449-62.

56. Yan Y, Ren Y, Li X, Zhang X, Guo H, Han Y, Hu J. A polysaccharide from green tea (Camellia sinensis L.) protects human retinal endothelial cells against hydrogen peroxide-induced oxidative injury and apoptosis. International journal of biological macromolecules. 2018 Aug 1;115:600-7.

57. B. Halliwell and J. M. C. Gutteridge, “Free radicals, ageing and disease,” in Free Radicals in Biology and Medicine, pp. 422–437, Clarendron Press, Oxford, UK, 1989.

58. Sugier P, Sugier D, Sozinov O, Kołos A, Wołkowycki D, Plak A, Budnyk O. Characteristics of plant communities, population features, and edaphic conditions of Arnica montana L. populations in pine forests of mid-Eastern Europe. Acta Societatis Botanicorum Poloniae. 2019 Dec 1;88(4).

59. Elsheery NI, Helaly MN, Omar SA, John SV, Zabochnicka-Swiątek M, Kalaji HM, Rastogi A. Physiological and molecular mechanisms of salinity tolerance in grafted cucumber. South African Journal of Botany. 2020 May 1;130:90-102.

60. G.-R. Zhao, Z.-J. Xiang, T.-X. Ye, Y.-J. Yuan, and Z.-X. Guo, “Antioxidant activities of Salviamiltiorrhiza and Panax notoginseng,” Food Chemistry, vol. 99, no. 4, pp. 767–774, 2006.

61. M. Valko, M. Izakovic, M. Mazur, C. J. Rhodes, and J. Telser, “Role of oxygen radicals inDNA damage and cancer incidence,” Molecular and Cellular Biochemistry, vol. 266, no. 1-2, pp. 37–56,2004.

62. Oktyabrsky ON, Bezmaternykh KV, Smirnova GV, Tyulenev AV. Effect of resveratrol and quercetin on the susceptibility of Escherichia coli to antibiotics. World Journal of Microbiology and Biotechnology. 2020 Nov;36(11):1-4.

63. Naik RR, Shakya AK, Oriquat GA, Katekhaye S, Paradkar A, Fearnley H, Fearnley J. Fatty acid analysis, chemical constituents, biological activity and pesticide residues screening in Jordanian propolis. Molecules. 2021 Aug 21;26(16):5076.

64. Martorell M, Lucas X, Alarcón-Zapata P, Capó X, Quetglas-Llabrés MM, Tejada S, Sureda A. Targeting xanthine oxidase by natural products as a therapeutic approach for mental disorders. Current Pharmaceutical Design. 2021 Jan 1;27(3):367-82.

65. Kaur G, Singh JV, Gupta MK, Bhagat K, Gulati HK, Singh A, Bedi PM, Singh H, Sharma S. Thiazole-5-carboxylic acid derivatives as potent xanthine oxidase inhibitors: design, synthesis, in vitro evaluation, and molecular modeling studies. Medicinal Chemistry Research. 2020 Jan;29(1):83-93.

66. Borghi C, Palazzuoli A, Landolfo M, Cosentino E. Hyperuricemia: a novel old disorder—relationship and potential mechanisms in heart failure. Heart failure reviews. 2020 Jan;25(1):43-51.

67. Reina-Couto M, Pereira-Terra P, Quelhas-Santos J, Silva-Pereira C, Albino-Teixeira A, Sousa T. Inflammation in human heart failure: major mediators and therapeutic targets. Frontiers in Physiology. 2021;12.

68. Uduagbamen PK, Ogunkoya JO, AdebolaYusuf AO, Oyelese AT, Nwogbe CI, Ofoh CJ, Anyaele C. Hyperuricemia in Hypertension and Chronic Kidney Disease: Risk Factors, Prevalence and Clinical Correlates: A Descriptive Comparative Study. International Journal of Clinical Medicine. 2021 Sep 9;12(9):386-401.

69. Thengchaisri N, Hein TW, Ren Y, Kuo L. Activation of coronary arteriolar PKCβ2 impairs endothelial NO-mediated vasodilation: role of

JNK/Rho kinase signaling and xanthine oxidase activation. International journal of molecular sciences. 2021 Sep 9;22(18):9763.

70. Bredemeier M, Lopes LM, Eisenreich MA, Hickmann S, Bongiorno GK, d'Avila R, Morsch AL, da Silva Stein F, Campos GG. Xanthine oxidase inhibitors for prevention of cardiovascular events: a systematic review and meta-analysis of randomized controlled trials. BMC cardiovascular disorders. 2018 Dec;18(1):1-1.

71. Wang L, Wang X, Shi Z, Shen L, Zhang J, Zhang J. Bovine milk exosomes attenuate the alteration of purine metabolism and energy status in IEC-6 cells induced by hydrogen peroxide. Food Chemistry. 2021 Jul 15;350:129142.

72. Abu Bakar FI, Abu Bakar MF, Abdullah N, Endrini S, Fatmawati S. Optimization of extraction conditions of phytochemical compounds and anti-gout activity of Euphorbia hirta L.(Ara Tanah) using response surface methodology and liquid chromatography-mass spectrometry (LC-MS) Analysis. Evidence-Based Complementary and Alternative Medicine. 2020 Oct;2020.

73. M. T. T. Nguyen, S. Awale, Y. Tezuka, Q. Le Tran, and S. Kadota, "Xanthine oxidase inhibitors from the heartwood of Vietnamese *Caesalpinia sappan*," *Chemical and Pharmaceutical Bulletin*, vol. 53, no. 8, pp. 984–988, 2005.

74. P.Higgins, L.D. Ferguson, and M. R.Walters, "Xanthine oxidase inhibition for the treatment of stroke disease: a novel therapeutic approach," *Expert Review of Cardiovascular Therapy*, vol. 9, no. 4, pp. 399–401, 2011.

75. Dew TP, Day AJ, Morgan MR. Xanthine oxidase activity in vitro: effects of food extracts and components. Journal of Agricultural and Food Chemistry. 2005 Aug 10;53(16):6510-5.

76. F. Heinz, S. Reckel, in: H.-U. Bergmeyer (Ed.), Methods of Enzymatic Analysis, vol. 3, Wiley, New York, 1983, p. 210.

77. Cerbulis J, Farrell Jr HM. Xanthine oxidase activity in dairy products. Journal of Dairy Science. 1977 Feb 1;60(2):170-6.

78. Atlante A, Valenti D, Latina V, Amadoro G. Role of Oxygen Radicals in Alzheimer's Disease: Focus on Tau Protein. Oxygen. 2021 Nov 27;1(2):96-120.

79. Majkić-Singh N, Bogavac L, Kalimanovska V, Jelić Z, Spasić S. Spectrophotometric assay of xanthine oxidase with 2, 2'-azino-di (3-ethylbenzthiazoline-6-sulphonate)(ABTS) as chromogen. Clinica chimica acta. 1987 Jan 15;162(1):29-36.

80. Kusharto CM, Madanijah S. The Effect of Moringa Capsule and Moringa Tea Consumption on the Elderly's Uric Acid Level. Indian Journal of Public Health Research & Development. 2019 Mar 1;10(3).

81. Liu F, Yu R, Wei H, Wu J, He N, Liu X. Construction of a novel electrochemical sensing platform to investigate the effect of temperature on superoxide anions from cells and superoxide dismutase enzyme activity. Analytica Chimica Acta. 2022 Mar 15;1198:339561.

82. Çekiç SD, Avan AN, Uzunboy S, Apak R. A colourimetric sensor for the simultaneous determination of oxidative status and antioxidant activity on the same membrane: N, N-Dimethyl-p-phenylene diamine (DMPD) on Nafion. Analytica Chimica Acta. 2015 Mar 20;865:60-70.

83. Zhang LX, Lv Y, Xu A, Wang HZ. The prognostic significance of serum gamma-glutamyltransferase levels and AST/ALT in primary hepatic carcinoma. Bmc Cancer. 2019 Dec;19(1):1-9.

84. Thongtan T, Deb A, Vutthikraivit W, Laoveeravat P, Mingbunjerdsuk T, Islam S, Islam E. Antiplatelet therapy associated with lower prevalence of advanced liver fibrosis in non-alcoholic fatty liver disease: A systematic review and meta-analysis. Indian Journal of Gastroenterology. 2022 Mar 22:1-8.

85. Silva FA, Brito BB, Santos ML, Marques HS, Silva Júnior RT, Carvalho LS, Vieira ES, Oliveira MV, Melo FF. COVID-19 gastrointestinal manifestations: a systematic review. Revista da Sociedade Brasileira de Medicina Tropical. 2020 Nov 25;53.

86. Mihm S. Danger-associated molecular patterns (DAMPs): molecular triggers for sterile inflammation in the liver. International journal of molecular sciences. 2018 Oct;19(10):3104.

87. Podrini C, Borghesan M, Greco A, Pazienza V, Mazzoccoli G, Vinciguerra M. Redox homeostasis and epigenetics in non-alcoholic fatty liver disease (NAFLD). Current pharmaceutical design. 2013 May 1;19(15):2737-46.

88. Mbah NE, Lyssiotis CA. Metabolic regulation of ferroptosis in the tumor microenvironment. Journal of Biological Chemistry. 2022 Mar 1;298(3).

89. Bebber CM, Müller F, Prieto Clemente L, Weber J, von Karstedt S. Ferroptosis in cancer cell biology. Cancers. 2020 Jan;12(1):164.

90. Angeli JP, Proneth B, Hammond VJ, Tyurina YY, Tyurin VA, ODonnell VB, Kagan VE, Conrad M. Inactivation of the Ferroptosis

Regulator Gpx4 Triggers Acute Renal Failure in a Therapeutically Relevant Mechanism. Free Radical Biology and Medicine. 2014(76):S77-8.91. Mehta KJ, Farnaud SJ, Sharp PA. Iron and liver fibrosis: Mechanistic and clinical aspects. World journal of gastroenterology. 2019 Feb 7;25(5):521.

92. Jang EJ, Kim SC, Lee JH, Lee JR, Kim IK, Baek SY, Kim YW. Fucoxanthin, the constituent of Laminaria japonica, triggers AMPK-mediated cytoprotection and autophagy in hepatocytes under oxidative stress. BMC complementary and alternative medicine. 2018 Dec;18(1):1-1.

93. Martinez-Cayuela M. Oxygen free radicals and human disease. Biochimie 1995;77:147-61.

94. Dormandy TL. An approach to free radicals. Lancet 1983;2:1010-4.

95. Cheng HY, Lin TC, Yu KH, Yang CM, Lin CC. Antioxidant and free radical scavenging activities of *Terminalia chebula*. Biol Pharm Bull 2003;26:1331-5.

96. Cos P, Ying L, Calomme M, Hu JP, Cimanga K, Van PB, *et al*.Structure-activity relationship and classification of flavonoids as inhibitors of xanthine oxidase and superoxide scavengers. J Nat Prod 1998;61:71-6.

97. Liu N, Xu H, Sun Q, Yu X, Chen W, Wei H, Jiang J, Xu Y, Lu W. The role of oxidative stress in hyperuricemia and xanthine oxidoreductase (XOR) inhibitors. Oxidative Medicine and Cellular Longevity. 2021 Mar 26;2021.

98. Valko M, Leibfritz D, Moncol J, Cronin MT, Mazur M, Telser J.Free radicals and antioxidants in normal physiological functions and human disease. Int J Biochem Cell Biol 2007;39:44-84.

99. Forbes JM, Coughlan MT, Cooper ME. Oxidative stress as a major culprit in kidney disease in diabetes. Diabetes 2008;57:1446-54.

100. Watanabe S, Kanellis J, Nakagawa T, Han L, Ohashi R, Lan H,*et al*. Reducing uric acid as a means to prevent cardiovascular and renal disease. Expert Opin Ther Pat 2002;12:193-9.

101. Vazquez-Mellado J, Alvarez-Hernandez E, Burgos-Vargas R. Primary prevention in rheumatology: The importance of hyperuricemia. Best Pract Res Clin Rheumatol 2004;18:111-24.

102. Terkeltaub R. Gout. Novel therapies for treatment of gout and hyperuricemia. Arthritis Res Ther 2009;11:236.

103. Schlesinger N, Dalbeth N, Perez-Ruiz F. Gout - what are the treatment options? Expert Opin Pharmacother 2009;10:1319-28.

104. Hoey BM, Butler J, Halliwell B. On the specificity of allopurinol and oxypurinol as inhibitors of xanthine oxidase. A pulse radiolysis determination of rate constants for reaction of allopurinol and oxypurinol with hydroxyl radicals. Free Radic Res Commun 1988;4:259-63.

105. Nakamura M. Allopurinol-insensitive oxygen radical formation by milk xanthine oxidase systems. J Biochem 1991;110:450-6.

106. Fagugli RM, Gentile G, Ferrara G, Brugnano R. Acute renal and hepatic failure associated with allopurinol treatment. Clin Nephrol 2008;70:523-6.

107. Gullo VP, McAlpine J, Lam KS, Baker D, Petersen F. Drug discovery from natural products. J Ind Microbiol Biotechnol 2006;33:523-31.

108. Newman DJ, Cragg GM. Natural products as sources of new drugs over the last 25 years. J Nat Prod 2007;70:461-77.

109. Bustanji Y, Hudaib M, Tawaha K, Mohammad M, Almasri I,Hamed S, *et al*. *In vitro* xanthine oxidase inhibition by selected Jordanian medicinal plants. Jordan J Pharm Sci 2010. [In press].

110. Mohammad MK, Almasri IM, Tawaha K, Al-Nadaf A, Hudaib M, Al-Khatib HS, *et al*. Antioxidant, antihyperuricemic and xanthine oxidase inhibitory activities of Hyoscyamus reticulatus. Pharm Biol 2010;48:1376-83.

111. Hudaib MM, Tawaha KA, Mohammad MK, Assaf AM, Issa AY, Alali FQ, Aburjai TA, Bustanji YK. Xanthine oxidase inhibitory activity of the methanolic extracts of selected Jordanian medicinal plants. Pharmacognosy Magazine. 2011 Oct;7(28):320.

112. Cos P, Ying L, Calomme M, Hu JP, Cimanga K, Van Poel B, Pieters L, Vlietinck AJ, Berghe DV. Structure− activity relationship and classification of flavonoids as inhibitors of xanthine oxidase and superoxide scavengers. Journal of natural products. 1998 Jan 23;61(1):71-6.

113. Atlante A, Valenti D, Gagliardi S, Passarella S. A sensitive method to assay the xanthine oxidase activity in primary cultures of cerebellar granule cells. Brain Research Protocols. 2000 Nov 1;6(1-2):1-5.

114. Fried R. Colorimetric determination of xanthine dehydrogenase by tetrazolium reduction. Anal Biochem 1966;16:427–32.

115. Naoghare PK, Kwon HT, Song JM. On-chip assay for determining the inhibitory effects and modes of action of drugs against xanthine oxidase. Journal of pharmaceutical and biomedical analysis. 2010 Jan 5;51(1):1-6.

116. Liu S, Xing J, Zheng Z, Song F, Liu Z, Liu S. Ultrahigh performance liquid chromatography–triple quadrupole mass spectrometry inhibitors fishing assay: A novel method for simultaneously screening of xanthine oxidase inhibitor and superoxide anion scavenger in a single analysis. Analytica chimica acta. 2012 Feb 17;715:64-70.

117. Özyürek M, Bektaşoğlu B, Güçlü K, Apak R. Measurement of xanthine oxidase inhibition activity of phenolics and flavonoids with a

modified cupric reducing antioxidant capacity (CUPRAC) method. Analytica Chimica Acta. 2009 Mar 16;636(1):42-50.

118. Wu ZY, Zhang H, Li F, Yang FQ. Evaluation of xanthine oxidase inhibitory activity of flavonoids by an online capillary electrophoresis-based immobilized enzyme microreactor. Electrophoresis. 2020 Aug;41(15):1326-32.

119. Rubio CP, Cerón JJ. Spectrophotometric assays for evaluation of Reactive Oxygen Species (ROS) in serum: General concepts and applications in dogs and humans. BMC Veterinary Research. 2021 Dec;17(1):1-3.

120. Ortiz R, Antilén M, Speisky H, Aliaga ME, López-Alarcón C, Baugh S. Application of a microplate-based ORAC-pyrogallol red assay for the estimation of antioxidant capacity: first action 2012.03. Journal of AOAC International. 2012 Nov 1;95(6):1558-61.

121. Giera M, Kloos DP, Raaphorst A, Mayboroda OA, Deelder AM, Lingeman H, Niessen WM. Mild and selective labeling of malondialdehyde with 2-aminoacridone: assessment of urinary malondialdehyde levels. Analyst. 2011;136(13):2763-9.

122. Quaife ML, Dju MY. Chemical estimation of vitamin E in tissue and the tocopherol content of some normal human tissues. J Biol Chem. 1949 Aug 1;180(1):263-72.

123. Tipple TE, Rogers LK. Methods for the determination of plasma or tissue glutathione levels. InDevelopmental Toxicology 2012 (pp. 315-324). Humana Press, Totowa, NJ.

124. Nunes CA, Freitas MP, Pinheiro ACM, Bastos SC (2012) Chemoface: a novel free user-friendly interface for chemometrics, Journal of the Brazilian Chemical Society, 23: 2003-2010.

125. Bahar B, Tuncel AF, Holmes EW, Holmes DT (2017) An interactive website for analytical method comparison and bias estimation, Clinical Biochemistry, 50:1025-1029.
126. Shrivastava A, Gupta VB. Methods for the determination of limit of detection and limit of quantitation of the analytical methods. Chron. Young Sci. 2011 Jan 1;2(1):21-5.
127. Lamuela-Raventós RM. Folin–Ciocalteu method for the measurement of total phenolic content and antioxidant capacity. Measurement of Antioxidant Activity & Capacity: Recent Trends and Applications. 2018 Jan 11:107-15.
128. Gerke O. Reporting standards for a Bland–Altman agreement analysis: A review of methodological reviews. Diagnostics. 2020 May;10(5):334.
129. Aly SS, Fayed HM, Ismail AM, Abdel Hakeem GL. Assessment of peripheral blood lymphocyte subsets in children with iron deficiency anemia. BMC pediatrics. 2018 Dec;18(1):1-6.
130. Furuyama K, Kaneko K. Iron metabolism in erythroid cells and patients with congenital sideroblastic anemia. International Journal of Hematology. 2018 Jan;107(1):44-54.
131. Langer AL, Ginzburg YZ. Role of hepcidin-ferroportin axis in the pathophysiology, diagnosis, and treatment of anemia of chronic inflammation. Hemodialysis International. 2017 Apr;21:S37-46.
132. Hirsch RE, Sibmooh N, Fucharoen S, Friedman JM. HbE/β-thalassemia and oxidative stress: the key to pathophysiological mechanisms and novel therapeutics. Antioxidants & redox signaling. 2017 May 10;26(14):794-813.

133. Bruder G, Heid HW, Jarasch ED, Mather IH. Immunological identification and determination of xanthine oxidase in cells and tissues. Differentiation. 1982 Dec 1;23(1-3):218-25.

134. Xu RX, Wu YJ. Lipid-Modifying Drugs: Pharmacology and Perspectives. Coronary Artery Disease: Therapeutics and Drug Discovery. 2020:133-48.

135. Azimi V, Farnsworth CW, Roper SM. Comparison of the Friedewald Equation with Martin and Sampson Equations for Estimating LDL Cholesterol in Hypertriglyceridemic Adults. Clinical Biochemistry. 2022 Jul 26.

136. Cighetti G, Duca L, Bortone L, Sala S, Nava I, Fiorelli G, Cappellini MD. Oxidative status and malondialdehyde in β-thalassaemia patients. European journal of clinical investigation. 2002 Mar;32:55-60.

137. Nasseri E, Mohammadi E, Tamaddoni A, Qujeq D, Zayeri F, Zand H. Benefits of curcumin supplementation on antioxidant status in β-Thalassemia major patients: A double-blind randomized controlled clinical trial. Annals of Nutrition and Metabolism. 2017;71(3-4):136-44.

138. Bergasa NV. Hemochromatosis. InClinical Cases in Hepatology 2022 (pp. 341-370). Springer, London.

139. Ondei LD, Estevao ID, Rocha MI, Percário S, Souza DR, Pinhel MA, Bonini-Domingos CR. Oxidative stress and antioxidant status in beta-thalassemia heterozygotes. Revista brasileira de hematologia e hemoterapia. 2013;35:409-13.

140. Kuhn V, Diederich L, Keller IV TS, Kramer CM, Lückstädt W, Panknin C, Suvorava T, Isakson BE, Kelm M, Cortese-Krott MM. Red blood cell function and dysfunction: redox regulation, nitric oxide metabolism, anemia. Antioxidants & redox signaling. 2017 May 1;26(13):718-42..

141. Shehryar M, Aslam M, Sohail N, Qadeer S, Tariq T. Assessment of Dietary Behavior of Children Aged between 3-12 Years Suffering from Thalassemia Visiting Tertiary Care Hospitals, Lahore: Dietary behavior of Thalassemia children. Pakistan BioMedical Journal. 2019 Dec 31;2(2).
142. Rismayanti L, Yulistiani Y, Andarsini MR, Qibtiyah M. ANALYSIS OF DL-α-TOCOPHEROL AS ANTIOXIDANT ON MALONDIALDEHYDE LEVEL IN PEDIATRIC PATIENTS WITHβ-THALASSEMIA MAJOR. Folia Medica Indonesiana. 2017 Aug 15;53(1):49-55.
143. Sovira N, Lubis M, Wahidiyat PA, Suyatna FD, Gatot D, Bardosono S, Sadikin M. Effects of α-tocopherol on hemolysis and oxidative stress markers on red blood cells in β-thalassemia major. Clinical and Experimental Pediatrics. 2020 Aug;63(8):314.
144. Van Sadelhoff JH, Wiertsema SP, Garssen J, Hogenkamp A. Free amino acids in human milk: A potential role for glutamine and glutamate in the protection against neonatal allergies and infections. Frontiers in Immunology. 2020 May 28;11:1007.
145. Xue X, Deng Y, Wang J, Zhou M, Liao L, Wang C, Peng C, Li Y. Hydroxysafflor yellow A, a natural compound from Carthamus tinctorius L with good effect of alleviating atherosclerosis. Phytomedicine. 2021 Oct 1;91:153694.
146. Banerjee A, Chattopadhyay A, Pal PK, Bandyopadhyay D. Melatonin is a potential therapeutic molecule for oxidative stress induced red blood cell (RBC) injury: A review. Melatonin Research. 2020 Mar 18;3(1):1-31.
147. Gozukara KH, Ozcan O, Ozgur T, Kaya YS, Tutuk O. Protective effects of colchicine on testicular torsion/detorsion-induced ischemia/reperfusion injury in

rats. Urology journal. 2020 May 16;17(3):294-300.

148. Aliakbarpour F, Mahjoub S, Masrour-Roudsari J, Seyedmajidi S, Ghasempour M. Evaluation of salivary thiobarbituric acid reactive substances, total protein, and pH in children with various degrees of early childhood caries: a case–control study. European Archives of Paediatric Dentistry. 2021 Dec;22(6):1095-9.

149. Farashi S, Najmabadi H. Diagnostic pitfalls of less well recognized HbH disease. Blood Cells, Molecules, and Diseases. 2015 Dec 1;55(4):387-95.

150. Odashiro K, Maruyama T, Yokoyama T, Nakamura H, Fukata M, Yasuda S, Saito K, Fujino T, Akashi K. Impaired erythrocyte deformability in patients with coronary risk factors: Significance of nonvalvular atrial fibrillation. Journal of Atrial Fibrillation. 2013 Oct;6(3).

151. Jain SK, Mohandas N, Clark MR, Shohet SB. The effect of malonyldialdehyde, a product of lipid peroxidation, on the deformability, dehydration and 51Cr-survival of erythrocytes. British Journal of Haematology. 1983 Feb;53(2):247-55.

152. Jóźwiak JJ, Kasperczyk S, Tomasik T, Osadnik T, Windak A, Studziński K, Mastej M, Catapano A, Ray KK, Mikhailidis DP, Toth PP. Design and rationale of a nationwide screening analysis from the LIPIDOGRAM2015 and LIPIDOGEN2015 studies. Archives of Medical Science: AMS. 2022;18(3):604.

153. White J, Moira L, Gao X, Tarasev M, Chakraborty S, Emanuele M, Hines PC. Can red blood cell function assays assess response to red cell-modifying therapies?. Clinical Hemorheology and Microcirculation. 2021 Jan 7(Preprint):1-2.

154. Çekiç SD, Avan AN, Uzunboy S, Apak R. A colourimetric sensor for the simultaneous determination of oxidative status and antioxidant activity on the same membrane: N, N-Dimethyl-p-phenylene diamine (DMPD) on Nafion. Analytica Chimica Acta. 2015 Mar 20;865:60-70.

155. Hamza TA, Hadwan MH. New spectrophotometric method for the assessment of catalase enzyme activity in biological tissues. Current Analytical Chemistry. 2020 Dec 1;16(8):1054-62.

156. Zhang C, Wang R, Zhang G, Gong D. Mechanistic insights into the inhibition of quercetin on xanthine oxidase. International journal of biological macromolecules. 2018 Jun 1;112:405-12.

157. Miotto G, Rossetto M, Di Paolo ML, Orian L, Venerando R, Roveri A, Vučković AM, Travain VB, Zaccarin M, Zennaro L, Maiorino M. Insight into the mechanism of ferroptosis inhibition by ferrostatin-1. Redox biology. 2020 Jan 1;28:101328.

158. Maiorino M, Conrad M, Ursini F. GPx4, lipid peroxidation, and cell death: discoveries, rediscoveries, and open issues. Antioxidants & redox signaling. 2018 Jul 1;29(1):61-74.

159. Matak P, Matak A, Moustafa S, Aryal DK, Benner EJ, Wetsel W, Andrews NC. Disrupted iron homeostasis causes dopaminergic neurodegeneration in mice. Proceedings of the National Academy of Sciences. 2016 Mar 29;113(13):3428-35.

160. Altamura S, Vegi NM, Hoppe PS, Schroeder T, Aichler M, Walch A, Okreglicka K, Hültner L, Schneider M, Ladinig C, Kuklik-Roos C. Glutathione peroxidase 4 and vitamin E control reticulocyte maturation, stress erythropoiesis and iron homeostasis. Haematologica. 2020 Apr;105(4):937.

161. Cardoso BR, Hare DJ, Bush AI, Roberts BR. Glutathione peroxidase 4: a new player in neurodegeneration?. Molecular Psychiatry. 2017 Mar;22(3):328-35.

162. Cozza G, Rossetto M, Bosello-Travain V, Maiorino M, Roveri A, Toppo S, Zaccarin M, Zennaro L, Ursini F. Glutathione peroxidase 4-catalyzed reduction of lipid hydroperoxides in membranes: the polar head of membrane phospholipids binds the enzyme and addresses the fatty acid hydroperoxide group toward the redox center. Free Radical Biology and Medicine. 2017 Nov 1;112:1-1.

163. Lu HF, Li JY, Zhang MM, Wu D, Zhang QL. A highly selective and sensitive colorimetric uric acid biosensor based on Cu (II)-catalyzed oxidation of 3, 3′, 5, 5′-tetramethylbenzidine. Sensors and Actuators B: Chemical. 2017 Jun 1;244:77-83.

164. Bezerra MA, Santelli RE, Oliveira EP, Villar LS, Escaleira LA. Response surface methodology (RSM) as a tool for optimization in analytical chemistry. Talanta. 2008 Sep 15;76(5):965-77.

165. Farman AA, Hadwan MH. Simple kinetic method for assessing catalase activity in biological samples. MethodsX. 2021 Jan 1;8:101434.

166. Li M, Su H, Tu Y, Shang Y, Liu Y, Peng C, Liu H. Development and Application of an Efficient Medium for Chromogenic Catalysis of Tetramethylbenzidine with Horseradish Peroxidase. ACS Omega. 2019 Mar 19;4(3):5459-70.

167. Zhang X, Yang Q, Lang Y, Jiang X, Wu P. Rationale of 3, 3′, 5, 5′-tetramethylbenzidine as the chromogenic substrate in colorimetric analysis. Analytical Chemistry. 2020 Aug 14;92(18):12400-6.

الخلاصة

يرتبط مرض الثلاسيميا بعدد من المشكلات الصحية الرئيسية، بما في ذلك السرطان وتشوهات العظام وتضخم الطحال وبطء معدلات النمو ومشاكل القلب. يحدث مرض الثلاسيميا بسبب طفرات في الحمض النووي للخلايا المسؤولة عن إنتاج الهيموغلوبين ، وهي مادة في خلايا الدم الحمراء تحمل الأوكسجين في جميع أنحاء الجسم. تنتقل الطفرات المرتبطة بالثلاسيميا من الآباء إلى الأطفال.

البيتا ثلاسيميا الكبرى هو الشكل الأكثر أهمية التي تحتاج إلى علاج طبي فوري. بسبب تكون الكريات الحمر غير الفعالة. ونتيجة لذلك، تصبح عمليات نقل الدم المتكررة حاسمة مدى الحياة.

تراكم الحديد هي نتيجة حتمية لعمليات نقل الدم المزمنة. يقترن الحديد عموما بالترانسفيرين وينقل إلى نخاع العظم والأنسجة ، حيث يتم استقباله عبر مستقبل الترانسفيرين وتخزينه على شكل فيريتين. يشبع الحديد الزائد قدرة ربط الترانسفيرين ويعمل الحديد غير المرتبط بالترانسفيرين كمحفز في توليد أنواع الأوكسجين التفاعلية.

الإفراط في إنتاج انواع الاوكسجين التفاعلية يسبب الإجهاد التأكسدي في الأفراد الذين يعانون من الثلاسيميا الكبرى، مما يؤدي إلى أكسدة البروتين وتلف الأنسجة من خلال بيروكسيد الدهون. تستخدم كربونيل البروتين لتقييم زيادة أكسدة البروتين ، في حين يستخدم مالونديالدهيد، و هو مؤشر حيوي حساس لتلف الانسجة ، لتقييم اكسدة الدهون المحسنة.

في عام 2021-2022 ، أجريت الدراسة في جامعة بابل. تم جمع عينات دم من مركز الثلاسيميا في مستشفى الأطفال في محافظة بابل. أجريت الدراسة الحالية على المجموعتين التاليتين:

المجموعة الأولى: 150 مجموعة الاصحاء.

المجموعة الثانية: 150 مجموعة المرضى.

تتناول هذه الدراسة: -

1- تم تقييم إجمالي حالة الاكسدة للأفراد و اجمالي مستويات الحالة المضادة للأكسدة، كان للثلاسيميا تركيزات مصلية أعلى بكثير من إجمالي أنواع المؤكسدات من الاصحاء. في حين أن قدرة المرضى على مضادات الأكسدة الإجمالية في المصل كانت أقل بكثير من قدرة الاصحاء حيث تشير هذه النتائج إلى الإجهاد التأكسدي وآلية الدفاع المؤكسد للمرضى التي تتعرض للخطر.

2- تم التحقيق في تركيز بيروكسيد الدهون في أمصال الاصحاء والمرضى. تظهر نتائج الدراسة الحالية ارتفاعا كبيرا في تركيز المالونديهايد في جميع المرضى التابعين لهذه الدراسة مقارنة بالاصحاء. تم العثور على العديد من الجذور الحرة وغيرها من المركبات شديدة التفاعل في المرضى. زيادة تركيزات هذه الجزيئات التفاعلية في الأنسجة من شأنها أن تسبب بيروكسيد الدهون ، مما يؤدي إلى إطلاق مركبات مثل المالونديهايد ، والتي تم اكتشافها كواحدة من منتجات أكسدة الدهون.

3- تصف الدراسة الحالية بروتوكولا طيفيا بسيطا لطريقة كبراك المعدلة لتقييم مثبطات الزانثين اوكسيديز وتوضح قابليتها للتكرار ودقتها. تشير نتيجة هذه الدراسة إلى انخفاض معنوي في تركيز مثبطات أوكسيديز الزانثين في جميع مجموعات الدراسة الذين يعانون من البيتا ثلاسيميا الرئيسية وقابلة للمقارنة مع الأشخاص الأصحاء.

4- تمت دراسة مستوى نشاط الزانثين أوكسيديز ، وتشير نتائج الدراسة إلى زيادة كبيرة في تركيز نشاط الزانثين أوكسيديز في جميع مجموعات مرضى الدراسة الذين يعانون من البيتا ثلاسيميا مقارنة بالاصحاء.

5-تم الوصول إلى مدى تأثير البيتا ثلاسيميا الكبرى على نشاط أوكسيديز الزانثين، وكذلك تطوير طريقة جديدة لقياس نشاط الإنزيم، ومقارنتها بالطرق المعتادة.

جمهورية العراق

وزارة التعليم العالي والبحث العلمي

جامعة بابل / كلية العلوم

قسم الكيمياء

الدور الكيموحيوي لانزيم الزانثين اوكسيديز على شدة التلف الخلوي بسبب الحديد في مرضى بيتا ثلاسيميا الكبرى في محافظة بابل

رسالة

مقدمة إلى مجلس كلية العلوم/ جامعة بابل

كجزء من متطلبات نيل درجة الماجستير في علوم الكيمياء

من قبل

أحلام ماجد عزيز مهدي

بكالوريوس علوم كيمياء – جامعة بابل

2009-2008

بإشراف

أ. د. محمود حسين هدوان

1444 هـ 2022 م